

BRCA1 loss-of-function triggers metabolic vulnerability to glutamine deprivation

Marc-Olivier Turgeon

Thesis submitted to The Institute of Cancer Research in partial fulfilment of the requirements of the degree of Doctor of Philosophy (PhD).

Division of Cancer Biology
The Institute of Cancer Research
London, United Kingdom

October 2020

© 2020
Marc-Olivier Turgeon
ALL RIGHTS RESERVED

Dedicated to

My parents, Dominique and Jean-François, who have always supported me, and provided me with the right environment and solid foundations to allow me to go on crazy adventures like pursuing a PhD.

Author contributions

LC-MS instruments were maintained and metabolite samples were processed by Dr. Michel Wagner, Dr. Clément Regnault, and Dr. Gérald Larrouy-Maumus from the ICR Core Facility, Glasgow Polyomics, and Imperial College London respectively. Data analysis for samples submitted to the Glasgow Polyomics were performed by Dr. Clément Regnault.

Overexpression of HA-tagged BRCA1 and knockdown of *BRCA1* in MCF7 cells were generated with the help of Alessandra Totti. Dr. Leonor Puchades Carrasco contributed to the results presented in this thesis through her work which includes, but is not limited to, data analysis of Figure 4.5 and contributions to Figure 3.4, 4.2, 4.3, and 5.1.

All other experiments, and the writing of this thesis, were conducted by the author, Marc-Olivier Turgeon, under the supervision of Dr. George Poulgiannis.

Marc-Olivier Turgeon

Abstract

Germline and somatic mutations of *BRCA1* are associated with cancer initiation and progression. Although the role of *BRCA1* is clearly defined in DNA-repair pathways, alternative functions of *BRCA1* still remain obscure. Here, we examined the dependency of isogenic *BRCA1* mutant cells to the main metabolic substrates and showed that *BRCA1* loss-of-function renders cells more sensitive to glutamine deprivation. Consistently, glutamine deprivation led to more pronounced cell cycle arrest and apoptosis in *BRCA1* mutant cells, which also displayed increased glutamine consumption. Incorporation of carbon and nitrogen stable-isotope labelled glutamine indicated an alternative processing of glutamine through the GABA shunt which allows more efficient nitrogen processing. Interestingly, we observed higher glutamate decarboxylase 1 (*GAD1*) protein levels in *BRCA1* mutant cells and an increased sensitivity to *GAD1* silencing. This metabolic rewiring also led to increased production of aspartate while other non-essential amino acids were reduced. In line with this, *BRCA1* mutant cells displayed lower intracellular nucleotide levels, combined with increased intake and reduced secretion of nucleotide derivatives. Interestingly, the enhanced sensitivity of these cells to glutamine deprivation could be rescued by purine supplementation. Together, these data highlight the role of *BRCA1* mutations in driving increased liability to glutamine deprivation and suggest that targeting the GABA shunt may be a novel therapeutic strategy to treat breast cancer patients harbouring *BRCA1* mutations.

Acknowledgements

First and foremost, I would like to thank my supervisor Dr. George Poulgiannis for the opportunity to pursue my PhD in his lab and for his support over the last 4 years. Even when the project did not look very promising George always believed in me and gave me the resources to keep going.

I would also like to thank Dr. Gérald Larrouy-Maumus from Imperial College London. His expertise with LC-MS and the collaboration that we built has been instrumental in generating some of the key results presented in this thesis.

A thank you also goes to my backup supervisor Prof. Chris Lord and his whole team for providing me with useful cell lines, reagents and advice. In particular, I would like to thank Dr. Inger Brandsma for her insightful comments at the beginning of my PhD, as well as Dr. Rachel Brough, Dr. Stephen Pettitt, and Dr. Feifei Song who have kept up with my numerous requests over the last 4 years.

A very special thank you goes to Dr. Leonor Puchades Carrasco who moved back in forth between London and Spain throughout the last 4 years. Not only did Leonor teach me how to slow down and listen, she also contributed enormously to this project through multiple experiments, but most importantly through countless discussions about every possible metabolic pathway.

I would also like to thank every past and present member of the Poulgiannis lab for creating such a good lab dynamic and a stimulating environment to work in. In

particular, Dr. Nicholas Perry for being literally at my side from the beginning of this adventure and for great discussions on the terrace over many espressos, Dr. Nikos Koundouros for being an inspiration to always do great science and work harder, Aurélien Tripp for being the most altruistic and diligent lab mate, Dr. Evi Karali for keeping up with me and being instrumental to the good functioning of the lab, Dr. David Magee for great discussions and just being a nice person, and Thanasis Tsalikis for always being ready to help with any experiments.

I would also like to acknowledge Dr. Michel Wagner and Dr. Jyoti Choudhary from the LC-MS ICR core facility, Radhika Patel and Fredrik Wallberg from the ICR flow cytometry core facility, Mohie Galal for keeping up with my multiple media recipe requests, Dr. Clément Regnault from the Glasgow Polyomics Facility, and all the students, staff, and faculty at the ICR who have helped shape this adventure.

Finally, I would like to thank Cancer Research UK and its donors for trusting me to do something useful with their precious funding and give me the opportunity to pursue this project.

Table of Contents

1	Introduction.....	21
1.1	Breast cancer classification and clinical relevance.....	22
1.2	Clinical relevance and DNA-related functions of BRCA1 and BRCA2	24
1.2.1	Relevance of BRCA1/2 mutation status in clinical evaluation of cancer.....	24
1.2.2	BRCA1/2 functions in DNA repair.....	26
1.2.3	Stalled replication fork protection.....	30
1.2.4	BRCAness and synthetic lethality.....	31
1.3	Alternative functions of BRCA1 in cell biology.....	32
1.3.1	DNA damage response and cell cycle regulation	33
1.3.2	Cancer progression.....	34
1.3.3	Epithelial to mesenchymal transition.....	35
1.3.4	Stem cell regulation	36
1.3.5	Other functions and conclusion.....	36
1.4	Key pathways in cancer metabolism	38
1.4.1	Glycolysis.....	40
1.4.2	TCA cycle.....	41
1.4.3	Mitochondrial respiration.....	43
1.4.4	Pentose phosphate pathway.....	44
1.5	Glutamine in cancer metabolism	45
1.5.1	Glutamine transport	46
1.5.2	Glutaminolysis.....	47

1.5.3	Glutamine synthetase	48
1.5.4	Downstream use of glutamine and derivatives	49
1.5.4.1	NEAA synthesis	49
1.5.4.2	GSH synthesis	50
1.5.4.3	GABA synthesis	51
1.5.4.4	Nucleotide synthesis	52
1.6	Rationale of thesis	55
1.6.1	BRCA1 and cancer metabolism	56
1.6.2	Rationale and aims	58
2	Materials and Methods	60
2.1	Materials	60
2.1.1	Reagents.....	60
2.1.2	Media	61
2.1.3	Compounds.....	63
2.1.4	Consumables	64
2.1.5	Antibodies	64
2.1.6	Primers.....	65
2.1.7	Plasmids	66
2.1.8	siRNA.....	66
2.1.9	Cell lines	67
2.2	Cell culture and treatment.....	67
2.2.1	Dose Response Curves	68

2.2.2	Proliferation assay	68
2.2.3	Colony formation assay	69
2.2.4	Generation of shRNA knockdown.....	70
2.2.5	siRNA knockdown.....	70
2.2.6	Overexpression BRCA1	71
2.2.7	IncuCyte® scratch assay	71
2.3	Cell extract analysis.....	72
2.3.1	Reverse transcription quantitative PCR.....	72
2.3.2	Western blot.....	73
2.3.3	GSH measurement	74
2.3.4	GDH1 activity measurement.....	75
2.3.5	Ammonia measurement.....	75
2.4	Flow cytometry.....	75
2.4.1	ROS measurements	76
2.4.2	Annexin V assay	76
2.4.3	Cell cycle assay	77
2.5	Metabolic analyses	77
2.5.1	Seahorse Glyco and Mito Stress analysis	78
2.5.2	Mito Fuel Flex Analysis	78
2.5.3	Metabolite profiling.....	79
2.5.3.1	LC-MS ICR core facility	79
2.5.3.2	LC-MS Glasgow Polyomics.....	80

2.5.3.3	LC-MS Imperial College London	82
2.6	Statistical Analysis	84
3	Identification and characterisation of metabolic vulnerabilities in <i>BRCA1</i> mutant breast cancer	85
3.1	Glycolytic capacity as well as glutamine and fatty acid dependencies are increased in <i>BRCA1</i> -mutant cells	85
3.2	<i>BRCA1</i> -mutant cells have increased sensitivity to glutamine but not glucose deprivation	88
3.3	<i>BRCA1</i> -mutant cells exhibit increased sensitivity to glutamine inhibitors.....	91
3.4	Cell proliferation and clonogenic potential is increased in <i>BRCA1</i> -mutant cells and altered by glutamine withdrawal	93
3.5	Glutamine deprivation-induced cell cycle arrest and cell death are more pronounced in <i>BRCA1</i> -mutant cells.....	95
3.6	Chapter discussion	96
4	Exploration of the roles of glutamine in breast cancer and their importance in <i>BRCA1</i> mutant cells.....	100
4.1	Glutaminolysis is similar between <i>BRCA1</i> -mutant and -restored cells	100
4.2	<i>BRCA1</i> -mutant cells display increased glutamine-derived TCA cycle intermediates	102
4.3	GSH levels and sensitivity to oxidative stress are equivalent in <i>BRCA1</i> -mutant and -restored cells	103
4.4	Glutamine synthetase regulation is independent of <i>BRCA1</i>	107
4.5	<i>BRCA1</i> -mutant cells process glutamine through the GABA shunt to produce aspartate more efficiently.....	109
4.6	Chapter discussion	114
5	Mechanistic investigation of the links between <i>BRCA1</i> mutation and increased glutamine consumption	117

5.1	Sensitivity to glutamine deprivation is independent of HR DNA repair potential	117
5.2	High <i>TWIST1</i> mRNA expression does not drive the increased glutamine deprivation sensitivity phenotype	120
5.3	<i>BRCA1</i> mutation leads to a purine conserving phenotype	122
5.4	<i>BRCA1</i> loss-of-function increases GAD1 protein, but not mRNA levels.	124
5.5	Chapter discussion	126
6	Discussion.....	128
6.1	Microenvironment influences metabolic rewiring and homeostasis.....	128
6.2	Glutamine is essential for various cell functions	131
6.3	Role of aspartate and glutamine in nucleotide synthesis.....	134
6.4	<i>BRCA1</i> in metabolic rewiring and tumour progression	136
6.5	The importance of cancer metabolism in clinical treatment.....	139
6.6	Conclusion	142
7	References	144

List of figures

Figure 1.1 - BRCA1 and BRCA2 are essential for homologous recombination	27
Figure 1.2 - BRCA1 is important for multiple cell biology functions.....	33
Figure 1.3 - Key metabolic pathways and glutamine usage are affected in cancer cells	41
Figure 3.1 - BRCA1-mutant cells have increased glycolytic capacity as well as increased glutamine and fatty acid dependencies	87
Figure 3.2 - BRCA1-mutant cells have increased sensitivity to glutamine, but not glucose deprivation	90
Figure 3.3 - BRCA1-mutant cells exhibit increased sensitivity to glutamine inhibitors	92
Figure 3.4 - Cell proliferation and clonogenic potential is increased in BRCA1-mutant cells and altered by glutamine withdrawal.....	94
Figure 3.5 - Glutamine deprivation-induced cell cycle arrest is more pronounced in BRCA1-mutant cells	97
Figure 3.6 - Glutamine deprivation-induced apoptosis is more pronounced in BRCA1-mutant cells	98
Figure 4.1 - Glutaminolysis is equivalent between BRCA1-mutant and restored cells	101
Figure 4.2 - TCA cycle intermediates are increased in BRCA1-mutant cells	104
Figure 4.3 - GSH levels and sensitivity to oxidative stress are equivalent in BRCA1-mutant and -restored cells.....	106
Figure 4.4 - Glutamine synthetase regulation is independent of BRCA1	108
Figure 4.5 - BRCA1-mutant cells show enrichment of changes in nitrogen-related pathways	110
Figure 4.6 - BRCA1-mutant cells process glutamine through the GABA shunt to maintain high intracellular aspartate	112

Figure 4.7 - BRCA1 loss-of-function leads to consistent increase in aspartate and GABA across different cell lines.....	115
Figure 5.1 - Sensitivity to glutamine deprivation is independent of HR DNA repair potential.....	119
Figure 5.2 - High TWIST1 mRNA expression does not drive the increased glutamine deprivation sensitivity phenotype.....	121
Figure 5.3 - <i>BRCA1</i> mutation leads to a purine conserving phenotype.	123
Figure 5.4 - BRCA1 loss-of-function increases GAD1 protein, but not mRNA levels.	125

List of tables

Table 1.1 - Nucleotide structure and nomenclature54

Table 2.1 - Special Ham's F12 formulation 61

Table 2.2 - qPCR primers..... 65

Table 2.3 - shRNA constructs 66

List of abbreviations

α KG: α -ketoglutarate.

2-DG: 2-deoxy-D-glucose.

53BP1: p53-binding protein 1.

ABAT: 4-aminobutyrate aminotransferase.

ADP: adenosine diphosphate.

ALDH5A1: aldehyde dehydrogenase 5 family member A1.

ALT: alanine transaminase.

AMP: adenosine monophosphate.

ANOVA: analysis of variance.

ASNS: asparagine synthetase.

ATM: ataxia-telangiectasia mutated.

ATP: adenosine triphosphate.

ATR: ATM and Rad3-related.

BARD1: BRCA1-associated RING domain protein 1.

BenSer: O-Benzyl-L-serine.

BPTES: Bis-2-(5-phenylacetamido-1,3,4-thiadiazol-2-yl) ethyl sulfide.

BRCA1: breast cancer associated gene 1.

BRCA2: breast cancer associated gene 2.

BRCT: BRCA1 C-terminus.

BSA: bovine serum albumin.

Chk1: checkpoint kinase 1.

Chk2: checkpoint kinase 2.

CtIP: CtBP-interacting protein.

CTP: cytidine triphosphate.

CVD: cardiovascular disease.

DDR: DNA-damage response.

DMEM: Dulbecco's Modified Eagle Medium.

DON: 6-Diazo-5-oxo-L-norleucine.

DSB: double strand break.

dTMP: thymidine monophosphate.

dUMP: deoxy UMP.

ECAR: extracellular acidification rate.

EGCG: Epigallocatechin gallate.

EMT: epithelial-to-mesenchymal transition.

ER: oestrogen receptor.

ETC: electron transport chain.

F6P: fructose 6-phosphate.

FADH₂: flavin adenine dinucleotide.

FOXC1: forkhead box C1.

G3P: glyceraldehyde 3-phosphate.

G6P: glucose 6-phosphate.

G6PD: G6P dehydrogenase.

GABA: γ -aminobutyrate.

GABA-T: GABA transaminase.

GAD: glutamate decarboxylase.

GCLC: glutamate-cysteine ligase catalytic subunit.

GDH1: glutamate dehydrogenase 1.

GLS1: glutaminase 1.

GLS2: glutaminase 2.

GLUT1: glucose transporter 1.

GMP: guanosine monophosphate.

GOT1: glutamic-oxaloacetic transaminase 1.

GOT2: glutamic-oxaloacetic transaminase 2.

GPX1: GSH peroxidase 1.

GS: glutamine synthetase.

GSH: glutathione.

GSR: GSH reductase.

GSS: GSH synthetase.

GSSG: oxidized GSH dimer.

HDAC: histones deacetylase.

HER2: human epidermal growth factor receptor 2.

HK: hexokinase.

HR: homologous recombination.

IDH: isocitrate dehydrogenase.

IHC: immunohistochemistry.

IMP: inosine monophosphate.

IMPDH: IMP dehydrogenase.

IR: ionising radiation.

JAG1: jagged canonical notch ligand 1.

JAK: janus kinase.

L-BSO: L-Buthionine-sulfoximine.

LC-MS: liquid chromatography mass spectrometry.

MET: mesenchymal-to-epithelial transition.

MRN: MRE11A-RAD50-NBS1.

NADH: nicotinamide dinucleotide.

NADPH: nicotinamide adenine dinucleotide phosphate.

NEAA: non-essential amino acid.

NH_4^+ : ammonium.

NHEJ: non-homologous end-joining.

NRF2: nuclear factor erythroid 2-related factor 2.

OAA: oxaloacetate.

OCR: oxygen consumption rate.

PALB2: partner and localizer of BRCA2.

PARP: poly ADP-ribose polymerase.

PBS: phosphate buffered saline.

PFK: phosphofructokinase.

PHGDH: phosphoglycerate dehydrogenase.

PPP: pentose-phosphate pathway.

PR: progesterone receptor.

PRPP: phosphoribosyl pyrophosphate.

R5P: ribose-5-phosphate.

RAD51: RAD51 recombinase.

RING: really interesting new gene.

RIPA: radioimmunoprecipitation assay.

ROS: reactive oxygen species.

RPA: replication protein A.

SARS-CoV-2: severe acute respiratory syndrome coronavirus 2.

SLC: solute carrier type transporters.

SSB: single strand break.

ssDNA: single-stranded DNA.

SSP: serine synthesis pathway.

STAT1: signal transducer and activator of transcription 1.

STAT3: signal transducer and activator of transcription 3.

TBHP: tert-Butyl hydroperoxide.

TBS: Tris-buffered saline.

TCA: tricarboxylic acid.

TNBC: triple negative breast cancer.

UMP: uridine monophosphate.

UTP: uridine triphosphate.

UV: ultraviolet.

xCT: cystine-glutamate antiporter.

XMP: xanthosine monophosphate.

ZBRK1: zinc finger protein 350.

ZNF350: zinc finger protein 350.

1 Introduction

Diseases that have decimated or have the potential to decimate large proportions of the human population have always captured our imagination. Whether it is a highly transmissible virus that leads to a global pandemic such as severe acute respiratory syndrome coronavirus 2 (SARS-CoV-2), or complex diseases that are inherent to our biology such as cancer, they have caused a high burden on society in the short or long-term. Interestingly, a less explored common point between these two seemingly unrelated conditions, is the fear of the unknown associated with them. On one end, the SARS-CoV-2 is a novel virus which is still poorly characterised, while on the other, cancer is a complex process that is still not fully understood. In both cases, the fear associated with this lack of knowledge often amplifies the distress and anxiety for afflicted individuals and relatives.

As of 2017 statistics, cancer was still the second most common health-related cause of death behind cardiovascular disease (CVD) worldwide¹. However, recent epidemiological studies have shown that it has overtaken CVD in certain high-income countries to become the first health-related cause of death^{2,3}. Despite vast improvements in the treatment and diagnosis of cancer and CVD, both lead to a large number of deaths worldwide, however, society in general has developed a particular fear of cancer⁴. This fear is often driven by a poor understanding of cancer biology which leads to practitioners and patients having a core view of cancer as a “vicious, unpredictable, and indestructible enemy.”⁴ Arguably, at a molecular level, cancer is a more complex disease than CVD. In fact, many argue that cancer is not one disease but multiple different ones characterised by the

tissue of origin, the development stage, the microenvironment, and many other factors. Research conducted in the last decades also shows intra-tumour heterogeneity, suggesting that each individual cancer cell is uniquely shaped by internal and external factors. Together, these observations explain the high level of variation found in cancer. Therefore, the complexity of cancer biology leaves medical oncologists with the very difficult task of translating incomplete and challenging scientific knowledge into bits of information that can provide a simple understanding to afflicted patients and their relatives. However, our current understanding of cancer is often not enough to satisfy human curiosity, and it is certainly not enough to develop treatments that are consistently efficient. Why do normal cells become cancerous? What makes them grow? Why do tumours metastasise? How can we stop it? These are all questions that cancer biologists try to understand to improve the current treatment modalities and patient prognosis. Accordingly, the work presented in this thesis aims to address some minuscule parts of these very complex questions, with a particular focus on breast cancer and metabolism.

1.1 Breast cancer classification and clinical relevance

Although there have been important advances in the treatment and diagnosis of breast cancer in the last decades, it still remains, based on the 2018 statistics, the cancer type with the highest incidence and mortality rate in female (incidence: 24.2%, mortality: 15.0%)⁵. Overall, combining male and female data, breast cancer incidence and mortality rate is second behind only lung cancer⁵.

While the clinical management of breast cancer is driven by general medical guidelines, it is also a complex decision-making process that takes place between patients and oncologists and is beyond the scope of this thesis. Briefly, to inform better clinical care, breast cancer is classified using two different approaches. The first one uses cell surface markers identified by immunohistochemistry (IHC) including oestrogen receptor (ER), progesterone receptor (PR), and human epidermal growth factor receptor 2 (HER2)⁶. Out of the different subtypes classified with this approach, the ER/PR-, HER2-, also known as triple negative breast cancer (TNBC) has the worst overall and disease-free survival⁶. The second classification approach uses molecular markers to separate breast cancers into four different subtypes: luminal A, luminal B, HER2-enriched, and basal-like^{7,8}. The most aggressive of the four subtypes, basal-like cancer, can be characterised by the expression of 50 predictor genes labelled as PAM50 which provide accurate prediction of the patient outcome and response to chemotherapy⁹. It has been argued that the basal-like subtype is so dramatically different to the other three, that it should be classified as a different cancer on its own¹⁰. The basal-like subtype also makes up around 85% of the TNBC histological subtype⁸. While there are clear differences between the subtypes generated using both approaches, the overlap between them also reinforces the argument that these classifications are not perfect and each cancer is unique. Yet, these classification approaches help medical oncologists tailor the treatments to a certain extent.

In general, removal of primary tumours through surgery is still one of the first-line treatments considered for patients with breast cancer. Additionally,

depending on multiple factors, different courses of adjuvant therapy can also be prescribed following surgery^{11,12}. Tumours expressing ER and PR can be treated with aromatase inhibitors which inhibit the synthesis of oestrogen and limit the activation of those hormone receptors on cancer cells, or with tamoxifen which blocks the binding of oestrogen to ER^{13,14}. From a different point of view, cancers expressing HER2 respond well to trastuzumab, a monoclonal antibody against HER2¹². While these examples demonstrate that tumour classification can help inform treatment, this is not so simple in the context of the most aggressive TNBC and basal-like subtypes where chemotherapy is still the main adjuvant therapy. Additionally, even “targeted” treatments described above are still often combined with chemotherapy^{11,12}. Unfortunately, the drugs used as part of chemotherapy treatments, including anthracyclines, taxanes, and alkylating agents, have not changed much since their introduction in the 1940s, and our understanding of their molecular mechanism of action is often limited or incomplete. Therefore, investigating cancer biology mechanisms could lead to improved treatment modalities, particularly in the context of the TNBC and basal-like subtypes where treatments are not informed by clear molecular mechanisms.

1.2 Clinical relevance and DNA-related functions of BRCA1 and BRCA2

1.2.1 Relevance of BRCA1/2 mutation status in clinical evaluation of cancer

One common feature of TNBC and basal-like cancers is the enrichment of somatic mutations of the breast cancer associated genes 1 and 2 (*BRCA1/BRCA2*)^{15,16}. Additionally, *BRCA1/2* germline mutations have been shown to lead to increased cancer risk^{17,18}. Although the exact roles of *BRCA1/2* in cancer

progression is still unclear, there is no doubt that *BRCA1/2* are key players in breast cancer pathogenesis. *BRCA1* was first discovered to be associated to early-onset breast cancer and assigned to chromosome 17 by Marie-Claire King and her group back in 1990, and was then cloned 4 years later by Mark Skolnick and his colleagues^{19,20}. This started the hunt for other genes associated with breast cancer and led to the discovery and cloning of *BRCA2* in 1994 and 1995 respectively^{21,22}. Since then, our understanding of the role of *BRCA1* and *BRCA2* in cell biology and their role in breast cancer is continually advancing.

The incidence of germline *BRCA1/2* mutations is estimated to be 1 in 250 women in the general population, however, the penetrance of the phenotype, which is estimated at around 80%, includes large variation in different studies²³. This could be due to different mutations of *BRCA1/2* or to other factors that might affect tumour development. Yet, patients with a familial history of breast cancer are often screened for *BRCA1/2* mutations which can indicate that those patients are at higher risk of developing breast and ovarian cancer²⁴. However, controversial studies have shown that germline *BRCA1/2* mutation status only partly explains familial breast cancer clustering²⁵. Additionally, given the high incidence of sporadic breast cancer (i.e. not driven by germline *BRCA1/2* mutations), it is likely that members of the same family could be affected as a result of simple coincidence, further complicating the prediction of breast cancer susceptibility.

Interestingly, as mentioned above, somatic *BRCA1/2* mutations also arise in sporadic breast cancer as well as other types of cancer including colorectal and

pancreatic cancers²⁶⁻²⁸. More specifically, they are enriched in TNBC and basal-like subtypes of breast cancer. Overall, these observations suggest that mutations of these genes can lead to a survival advantage for cancer cells. Importantly, although BRCA1 and BRCA2 share common functions (explored later), they are independent and can support the development and progression of breast cancer through different mechanisms. From a clinical point of view, *BRCA1* and *BRCA2* germline mutations have a similar relevance to inform patient risk and treatment course. This is most likely as a result of BRCA1 and BRCA2 sharing important functions in DNA repair (Figure 1.1). However, the role of BRCA1 in cell biology and cancer progression expands beyond DNA repair and will be explored more extensively in subsequent sections.

1.2.2 BRCA1/2 functions in DNA repair

DNA damage occurs naturally in replicating cells, arising from external insults [e.g. ultraviolet (UV), ionising radiation (IR), carcinogenic chemicals] or from errors during the DNA replication process. Therefore, cells have evolved multiple DNA repair mechanisms to cope with this damage and maintain the integrity of the DNA. One particularly detrimental type of DNA damage is double strand breaks (DSBs) which can arise from chromosome breakage, dysfunctional replication fork processing, or telomere deprotection²⁹. DSBs can be repaired through multiple mechanisms influenced by a number of other factors²⁹. The two most well-described repair mechanisms are: homologous recombination (HR), and non-

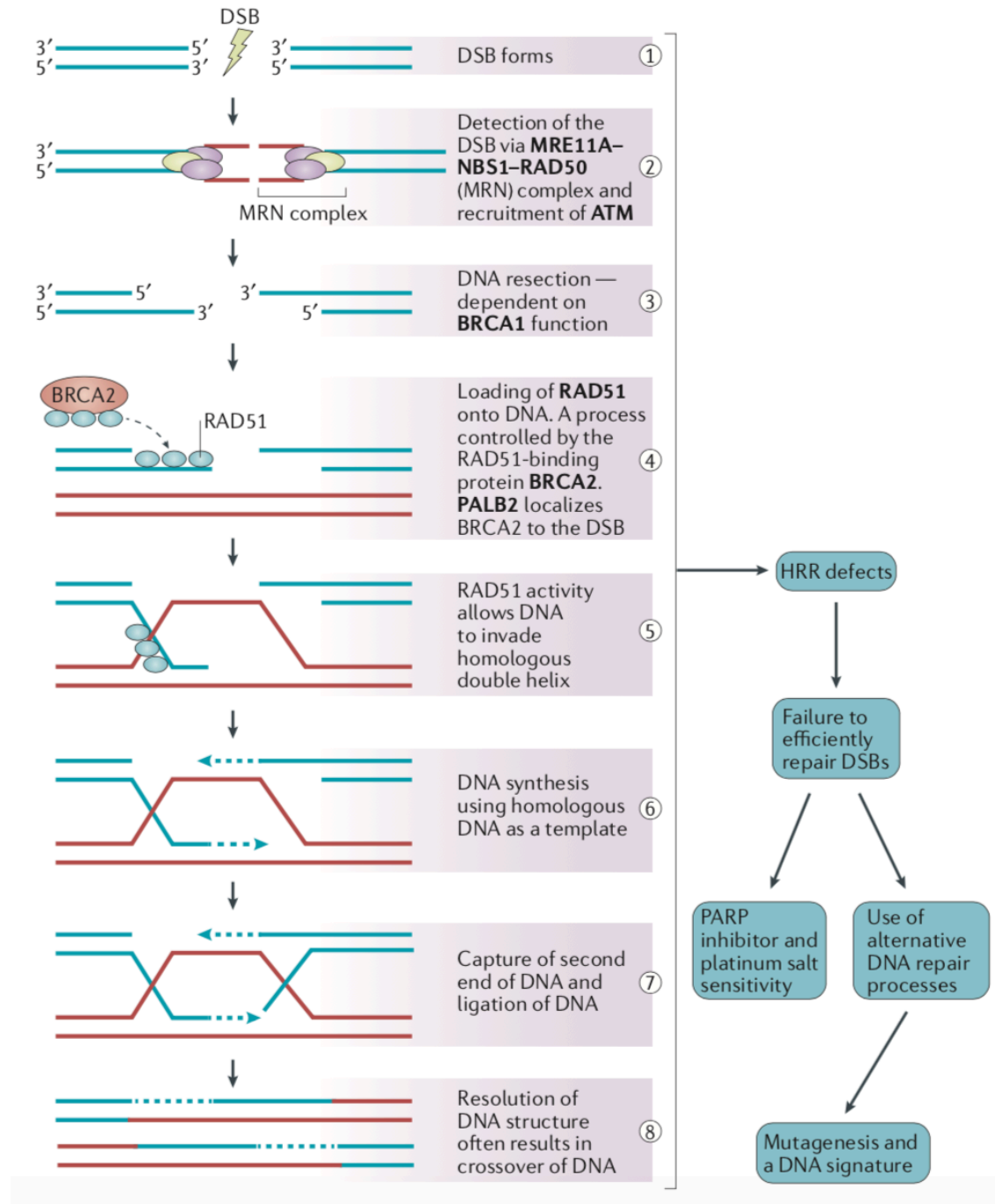


Figure 1.1 - BRCA1 and BRCA2 are essential for homologous recombination

Schematic representation of the steps of double strand break (DSB) repair through homologous recombination (HR) and the role of breast cancer associated genes 1 and 2 (BRCA1/2) in the process. For simplicity, multiple protein complexes involved in the process are not represented. (Adapted from Lord & Ashworth, 2016)

homologous end-joining (NHEJ)²⁹⁻³¹. Briefly, HR occurs during S/G2 phase of the cell cycle and uses complementary sister chromatin strand of DNA as a template, resulting in error-free DNA repair³². Conversely, NHEJ occurs throughout the cell cycle and is a rapid, high-capacity mechanism through which damaged DNA ends are ligated together with minimal reference to DNA sequence^{33,34}. Therefore, NHEJ is more prone to potential loss of nucleotides and introduction of deletion mutations than HR since DNA ends can partially degrade before repair³³.

As mentioned above, both BRCA1 and BRCA2 are involved in DNA repair, more specifically in HR (Figure 1.1)^{35,36}. The *BRCA2* gene encodes the 384 kDa BRCA2 protein which contains eight central BRC repeats and a C-terminal domain that interacts with RAD51 recombinase (RAD51). Additionally, BRCA2 contains a partner and localizer of BRCA2 (PALB2) binding domain at the N-terminus and an OB domain which interacts with single-stranded DNA (ssDNA) towards the C-terminus. While multiple factors dictate whether NHEJ or HR is used to repair DSBs, a key determinant that leads to the commitment to HR is the resection of one strand of DNA initiated by the MRE11A-RAD50-NBS1 (MRN) complex recruited to sites of DSBs. Following resection, the ssDNA is coated with replication protein A (RPA) which protects the ssDNA from degradation. The main role of BRCA2 is to subsequently recruit RAD51 to RPA-coated ssDNA sites and enable the formation of RAD51 nucleoprotein filaments that displace RPA³⁷⁻³⁹. RAD51 subsequently supports homologous strand crossover which is required for error-free repair associated with HR (Figure 1.1)⁴⁰. BRCA2 has also been shown to

potentially act as a scaffold for other important complexes in stalled replication fork protection and DNA-damage response (DDR)⁴¹.

While BRCA1 is also important for HR and DDR, there are many reports suggesting that it has a broader role in cell biology by acting as a scaffold for important complexes, but also through transcriptional regulation and ubiquitin ligase activity. The 220 kDa BRCA1 protein encoded by the *BRCA1* gene is formed of three main domains often mutated in cancer: 1) the RING (really interesting new gene) domain that is found near the N-terminus, provides the E3 ubiquitin ligase activity of BRCA1 and is essential for its interaction with BRCA1-associated RING domain protein 1 (BARD1) which also contains a RING domain; 2) the domain spanning exon 11-13, which is essential for the interaction with RAD50, RAD51, and PALB2, among other proteins; and 3) the BRCA1 C-terminus (BRCT) domains found near the C-terminus, which are essential for interactions with BACH1, CtBP-interacting protein (CtIP), and Abraxas^{42,43}. In DNA-repair, different domains/functions of BRCA1 are needed to support and modulate HR. For example, BRCA1 modulates CtIP and the MRN complex at sites of DSBs to initiate resection, both as a scaffold and through its ubiquitin activity (Figure 1.1)^{44,45}. Importantly, BRCA1, through its competition with p53-binding protein 1 (53BP1), is also essential to determine which repair pathway will be used to repair the break⁴⁶. Briefly, NHEJ is believed to be the default pathway for DSBs repair where 53BP1 and its associated Shieldin complex block DNA end resection while joining broken DNA ends closer together⁴⁰. Interestingly, although the mechanism is still unclear, 53BP1 can be inhibited by BRCA1 leading to its displacement from sites of DSBs

and promotion of DNA resection⁴⁷. Additionally, chromatin marks have also been shown to modulate the binding of 53BP1 or BRCA1 to DSB sites⁴⁸.

1.2.3 Stalled replication fork protection

Another important function of BRCA1/2 that is also related to DNA repair and genome stability is the protection of stalled replication forks^{49,50}. During DNA replication, DNA is unwound to allow the replication machinery to access the DNA strands, the resulting complexes are termed replication forks. Replication forks travelling along the template DNA can be challenged or slowed by the encounter of DNA lesions⁵¹, DNA regions that are difficult to replicate⁵², or collision with the transcriptional machinery⁵³. If not handled properly, these compromised or stalled replication forks can lead to fork breakage/collapse which results in genomic instability. Interestingly, similar proteins are involved in DSB repair and in protection and/or repair of stalled replication fork, however, the complexes that they form do not necessarily operate through the same biochemical mechanisms in both situations^{49,50}.

Briefly, there are two key steps in stalled replication fork protection: 1) stabilisation, and 2) reversal. Stabilisation involves protecting the exposed ssDNA that is present at stalled forks by coating the ssDNA with RPA, while reversal allows remodelling of the fork and resection of DNA to promote HR-mediated fork restart or branch migration⁴⁹. Similarly to HR, stalled fork protection requires BRCA1/2 and RAD51 recruitment, however, there is evidence to suggest that they do not necessarily act through the same mechanisms^{54,55}. For example, while the

role of BRCA2 in stimulating the formation of RAD51 nucleofilaments to stalled fork is essential, its role in recruiting RAD51 is not⁵⁴. The formation of RAD51 filaments prevents the excessive nucleolytic cleavage of DNA and the resulting fork collapse/breakage⁵⁴. Additionally, BRCA1/2 has been shown to modulate the MRN complex through other mechanisms which also prevent excessive nucleolytic cleavage⁵⁶.

1.2.4 BRCAness and synthetic lethality

Because of the roles of BRCA1 and BRCA2 in HR and stalled replication fork protection, loss-of-function mutations in *BRCA1/2* can lead to increased DNA damage and chromosomal instability. Interestingly, mutations and/or reduced expression of other genes involved in HR or related pathways also result in a similar phenotype coined BRCAness⁵⁷. Tumours with a BRCAness phenotype also share other common features such as sensitivity to DNA damaging agents including platinum salts and mitomycin C⁵⁷. Additionally, these tumours are sensitive to agents that lead to stalled replication fork and subsequent DSBs such as the topoisomerase poison camptothecin and poly ADP-ribose polymerase (PARP) inhibitors such as olaparib. PARP1 is important for single strand breaks (SSBs) repair, however, the synthetic lethality of PARP inhibitors in HR-deficient cancer appears to originate mostly from PARP trapping at sites of SSBs^{58,59}. The trapped PARP leads to aberrant processing of replication fork, subsequent fork collapse, and DSBs. This increase in DSBs, coupled with deficient HR process leads to increased DNA damage accumulation, or repair through NHEJ which leads to potential incorporation of mutations or chromosomal instability. In line with

this, mutations in genes involved in stalled replication fork protection, including *BRCA1/2*, can also explain, at least in part, the synthetic lethality observed with PARP inhibitors⁶⁰. In the clinic, a few PARP inhibitors are now approved for the treatment of specific types of cancer to take advantage of this synthetic lethality effect⁶¹. Unfortunately, resistance to treatment with PARP inhibitors or other agents that are synthetic lethal in an HR-deficient context still arise⁶². Additionally, resistance to chemotherapy in *BRCA1/2* deficient cancers can arise by promoting fork stability through *BRCA1/2*-independent mechanisms^{60,63}. Therefore, understanding more about the biological changes caused by mutations in *BRCA1* and/or *BRCA2* could help the identification of alternative therapies.

1.3 Alternative functions of BRCA1 in cell biology.

While both *BRCA1* and *BRCA2* are interesting in relation to DNA repair, due to its wider role in cell biology, I will focus on *BRCA1* for the remainder of this thesis. Historically, DNA repair and replication has always been a popular field of cancer biology, therefore, research on *BRCA1* has generally been more focused on these cellular processes. However, it is becoming increasingly clear that *BRCA1* has a broader role that extends beyond DNA repair and into other important cell functions (Figure 1.2)⁶⁴⁻⁶⁶. Interestingly, these alternative functions of *BRCA1* are independent or only partly associated with the DSB repair machinery. In the following sections, I will describe the key alternative functions that have been attributed to *BRCA1*.

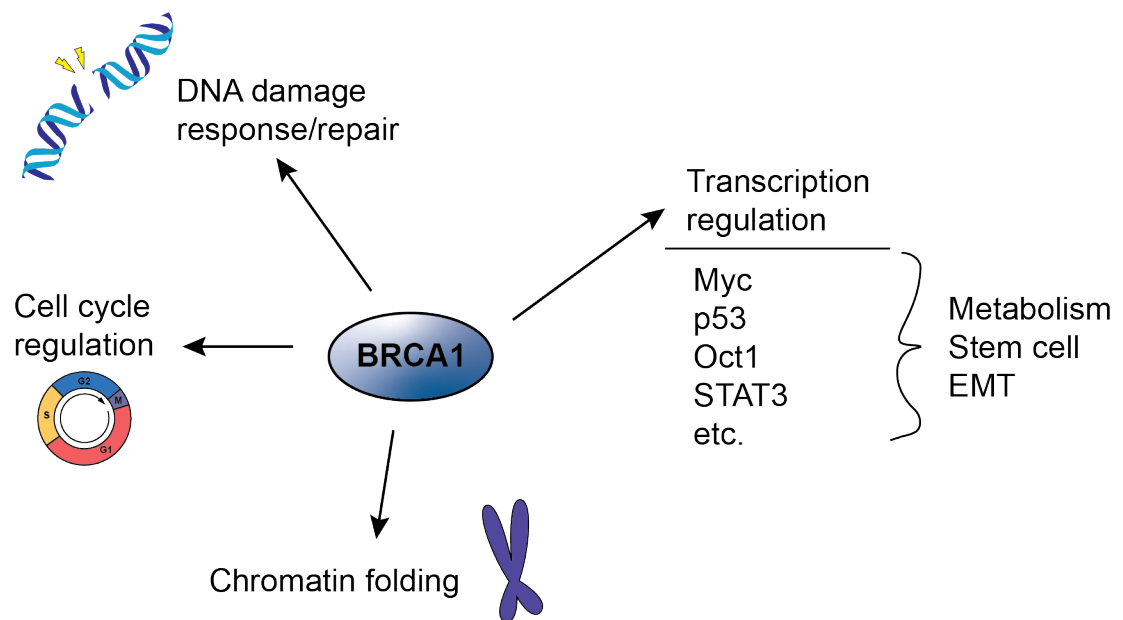


Figure 1.2 - BRCA1 is important for multiple cell biology functions

Schematic representation providing an overview of the different described functions of BRCA1 including but not limited to: DNA damage response/repair, cell cycle regulation, chromatin folding, and transcriptional regulation of known transcription factors. Epithelial-to-mesenchymal transition (EMT).

1.3.1 DNA damage response and cell cycle regulation

In addition to the DNA repair mechanisms that protect against DNA damage, cells have evolved the DDR which coordinates a number of cell functions to protect cells and organisms from genomic instability caused by extensive DNA damage⁶⁷. DDR is activated following DNA damage to allow cells to repair the damage, or to trigger apoptosis or other defence mechanisms if the damage is too substantial. Therefore, the DDR is closely related to DNA repair and it is no surprise that BRCA1 is a key player in coordinating both processes^{66,68}.

Importantly, both DNA repair and DDR are closely linked with cell cycle regulation for two main reasons: 1) replication of DNA happening during S phase is a major source of DNA damage, and 2) undergoing replication with mutated or damaged

DNA can either lead to transmission of the defective DNA or cause genomic instability. In line with this, cell cycle replication checkpoints are closely coupled with mechanisms that sense damaged DNA, a process that involves BRCA1⁶⁹.

Upon DNA damage, cell cycle checkpoints can halt cell cycle to allow time to repair the defect before cell replication is resumed⁷⁰. The main regulators of DDR are ataxia-telangiectasia mutated (ATM) and ATM and Rad3-related (ATR) kinases which get activated in response to DNA damage and phosphorylate a number of downstream targets important for DDR⁷¹. Among those targets, phosphorylation of checkpoint kinase 1 and 2 (Chk1/Chk2) is important to halt the cell cycle⁶⁶. Interestingly, BRCA1 has been involved in modulating the kinase activity of Chk1 which affects both G1/S and G2/M checkpoints^{72,73}. Additionally, BRCA1 can be phosphorylated by ATM at two distinct sites depending on the checkpoint activated⁶⁶. Overall, loss-of-function of BRCA1 abrogates the G2/M checkpoint⁷³. Although the role of BRCA1 in cell cycle regulation and DDR is still not fully understood, it is clear that it plays an essential part in the fine tuning of these important cellular functions.

1.3.2 Cancer progression

On a more general level, BRCA1 has been suggested as an important factor in cancer development since it leads to breast and ovarian cancer predisposition^{17,18}. Broadly speaking, cancer progression is a complex process that involves both cell intrinsic and extrinsic factors. While many tumour suppressors and oncogenes are involved in cancer progression, it is widely accepted that

BRCA1 is a key player in this process⁷⁴. The effect of BRCA1 mutations on cancer progression are often attributed to its role in DNA repair as loss of HR can lead to an increased mutation rate that could contribute to cancer progression. However, BRCA1 also plays a role in transcriptional and epigenetic regulation of important factors involved in cell differentiation and stem cell maintenance⁷⁵.

1.3.3 Epithelial to mesenchymal transition

In luminal breast cancer cells, *BRCA1* mRNA downregulation leads to cell dedifferentiation and a luminal-to-basal switch. Mechanistically, BRCA1 binds to the *TWIST1* promoter, an important transcription factor in epithelial-to-mesenchymal transition (EMT), to inhibit its activity, therefore supporting a more epithelial phenotype⁷⁶. Therefore, loss-of-function of BRCA1 leads to higher TWIST expression and a more basal phenotype. Additionally, BRCA1 represses the expression of forkhead box C1 (FOXC1), another important transcription factor in EMT⁷⁷. In normal conditions, EMT is a complex process essential for embryonic development through which polarised epithelial cells associated with a basement membrane undergo molecular changes to become mesenchymal⁷⁸. The resulting mesenchymal cells can migrate into other tissues where they can give rise to important organs. In cancer, although it has not been mechanistically proven yet, there are widely accepted theories that EMT plays an essential role in cancer progression and metastasis. Epithelial-like tumour cells can undergo EMT to migrate out of the primary tumour site and invade other tissues where they then potentially undergo mesenchymal-to-epithelial transition (MET) in order to establish into a new site. Importantly, EMT and MET are not all-or-nothing switches and

there are varying degrees of progression between the mesenchymal and epithelial phenotypes⁷⁸. Interestingly, what most likely supports cancer progression is an ability to switch between the two phenotypes more readily.

1.3.4 Stem cell regulation

Not only does BRCA1 modulate EMT, it also plays a role in cell differentiation. In fact, downregulation of *BRCA1* mRNA leads to increased stem/progenitor cell pools and replicative potential^{79,80}. One potential mechanism that can explain this phenotype is the regulation of Notch signalling by BRCA1-induced jagged canonical notch ligand 1 (JAG1) expression which is important to maintain stem/progenitor cells in the breast⁸¹. In fact, downregulation of Notch1 and JAG1 phenocopies BRCA1 loss⁸¹.

1.3.5 Other functions and conclusion

Most of the BRCA1 functions described above combine a few important mechanisms of BRCA1 including formation or recruitment of important complexes, ubiquitination, and/or transcriptional regulation⁸². More specifically, the transcriptional regulation activity of BRCA1 appears to be important in modulating many different cell functions in different context⁷⁵. For example, in some reports, BRCA1 has been shown to interact with major transcription factor c-Myc to repress its transcriptional activity⁸³, and interacts with p53 to stimulate its activity⁸⁴. BRCA1 has also been shown to regulate ER- α ⁸⁵, signal transducer and activator of transcription 1 (STAT1) and JAK-STAT3 signalling^{86,87}, as well as regulating

miRNA-155⁸⁸. Additionally, BRCA1 induces changes in chromatin folding through its interaction with COBRA1⁸⁹, or through regulation of histones deacetylases (HDACs)⁹⁰. Overall, although the alternative functions of BRCA1 appear disjointed, and although some of them might be an artefact of the experimental models used, it is clear that BRCA1 plays a key role in regulating cell biology. Interestingly, it is still unclear why *BRCA1* mutations are enriched in certain types of cancer only, and why *BRCA1* germline mutations lead to increased cancer risk in breast and ovaries specifically. Understanding the tissue-specific extrinsic factors that might be involved would provide a more sophisticated framework to understand the role of BRCA1 in cell biology.

In line with the renewed interest in cancer metabolism and microenvironment, investigations about the potential role of BRCA1 in cancer metabolism have started to emerge⁹¹⁻⁹³, the exact nature of which will be explored in more detail in a further section. These studies provide a good starting point to evaluate the role of BRCA1 in cell metabolism. However, more mechanistic studies are needed to determine the exact role of BRCA1 in cancer metabolism. More particularly, it would be interesting to explore if BRCA1 regulates metabolism directly. As discussed above, BRCA1 regulates a multitude of cell functions that are closely intertwined with metabolic pathways, as such, metabolic rewiring triggered by BRCA1 loss-of-function is somewhat expected. However, it is unclear to which extent BRCA1 regulates metabolism directly, and/or whether changes in metabolism can affect BRCA1 expression or function.

1.4 Key pathways in cancer metabolism

The fundamental concept that cell metabolism is affected in cancer dates back to the initial observations of Otto Warburg in the 1920s. At the time, Warburg observed that, even in the presence of normal levels of oxygen, cancer cells use more glucose and produce more lactate by fermentation than normal cells, a phenotype that is known as the Warburg effect⁹⁴⁻⁹⁶. Warburg and scientists following in his steps hypothesised that this was a result of mitochondrial dysfunction, however, this was never tested or observed directly^{94,97}. When thinking about cell metabolism from a purely energy point of view, the Warburg effect is very puzzling. Indeed, using glucose for mitochondrial respiration is a much more efficient adenosine triphosphate (ATP) generating process than glycolysis alone. This is why early scientists studying cancer metabolism believed that there must be defects in mitochondrial functions. Since then, however, cancer metabolism research has evolved beyond those initial observations to look at metabolic needs of cells more holistically^{96,98,99}.

It is widely accepted that the main characterising feature of cancer cells is their uncontrolled increase in proliferation rate. Interestingly, this increase in proliferation rate does not lead to a dramatic increase in energy demand (in the form of ATP) compared to cells performing “normal” functions^{96,100}. On the contrary, actively proliferating cells are more likely limited by the synthesis of building blocks such as nucleotides, amino acids, and phospholipids that are essential to replicate and produce a new cell^{96,100}. In line with this, cancer cells change their metabolism in a number of different ways to accommodate this high

demand in building blocks. Pavlova and Thompson describe the main hallmarks of cancer metabolism, or the main categories of changes that can occur in cancer cells⁹⁹. These hallmarks include: 1) deregulated glucose and amino acid uptake, 2) opportunistic ways of acquiring nutrients, 3) use of metabolic intermediates for biomass and nicotinamide adenine dinucleotide phosphate (NADPH) synthesis, 4) increased demand for nitrogen, 5) alterations in metabolite-driven gene expression, and 6) alterations in metabolite interaction with the microenvironment⁹⁹. Before diving further in some examples of how cancer cells modify their metabolism, it is important to point that these hallmarks are not universal across all cancer cells. Although all cancer cells have a similar end-goal (i.e. replicating), the access to nutrients in their microenvironment and/or intrinsic molecular mechanisms dictate which metabolic changes are necessary to accomplish this desired outcome¹⁰⁰⁻¹⁰². It is becoming increasingly clear that the context of each tumour plays a major role in defining metabolic vulnerabilities in cancer cells¹⁰³. Unfortunately, many previous articles, including seminal work in cancer metabolism, have sometimes overlooked these important aspects and often made generalised simplifications about cancer metabolism across different tissues of origin, intrinsic molecular characteristics, and/or external factors. This leads to conflicting results describing metabolic dependencies in the literature. A few interesting examples include: 1) some tumours and cell lines with amplified serine synthesis enzyme phosphoglycerate dehydrogenase (PHGDH) are sensitive to PHGDH inhibition^{104,105}, however in some context PHGDH is dispensable¹⁰⁶; and 2) based on the cancer type, there is differential sensitivity to isocitrate dehydrogenase (IDH) inhibitors among tumours with mutated tricarboxylic acid (TCA) cycle enzyme IDH^{107,108}. Interestingly, these

examples provide starting points for the investigation of differential external and internal factors that can modulate the response to inhibition of particular metabolic pathways. Here, I will give a brief overview of the main metabolic pathways involved in our studies and how they can be modified in cancer (Figure 1.3).

1.4.1 Glycolysis

Since Warburg's initial observations, glycolysis has always been a main focus point in cancer metabolism research. Briefly, glycolysis encompasses all the enzymatic processes that occur during the initial steps of glucose degradation to result in the production of pyruvate or lactate. The first step of glycolysis is the irreversible phosphorylation of glucose into glucose 6-phosphate (G6P), which is catalysed by hexokinase (HK) and occurs as soon as glucose enters the cell through the glucose transporter 1 (GLUT1)¹⁰⁹. Subsequently, G6P can be directed into the pentose-phosphate pathway (PPP, explored later) through G6P dehydrogenase (G6PD), or further degraded to fructose 6-phosphate (F6P). Another key step in glycolysis is the rate-limiting production of fructose 1, 6-biphosphate through the enzyme phosphofructokinase (PFK). Further down the pathway, through other enzymatic reactions, two molecules of glyceraldehyde 3-phosphate (G3P) are produced, which can be diverted into the serine synthesis pathway (SSP), or further catabolised into pyruvate. The whole process consumes two molecules of ATP and produces four molecules of ATP and two molecules of nicotinamide dinucleotide (NADH)¹⁰⁹. The resulting pyruvate molecules can be further processed into acetyl-CoA and incorporated into the TCA cycle (explored later) or converted into lactate through the lactate dehydrogenase enzymatic

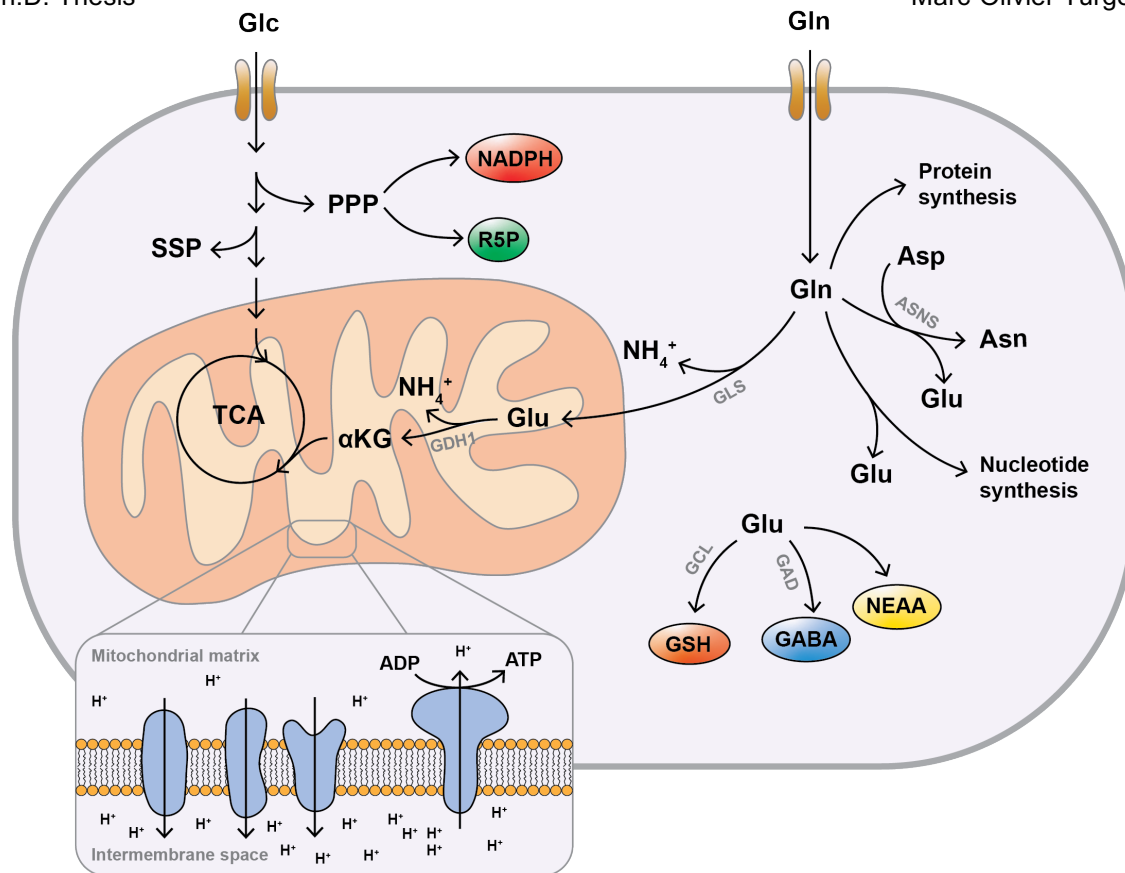


Figure 1.3 - Key metabolic pathways and glutamine usage are affected in cancer cells

Schematic representation of the key metabolic pathways affected in cancer cells including, glycolysis, pentose-phosphate pathway (PPP), tricarboxylic acid (TCA) cycle, and mitochondrial respiration, as well as glutamine usage and downstream derivatives. Serine synthesis pathway (SSP), glutamine (Gln), glucose (Glc), aspartate (Asp), asparagine (Asn), α -ketoglutarate (α KG), ribose 5-phosphate (R5P), glutathione (GSH), γ -aminobutyric acid (GABA), non-essential amino acid (NEAA), glutamate dehydrogenase (GDH1), glutaminase (GLS), asparagine synthetase (ASNS), glutamate-cysteine ligase (GCL), glutamate decarboxylase (GAD).

reaction which consumes one molecule of NADH^{109} . While there are numerous reports of increased glucose consumption and glycolysis in cancer^{110,111}, the exact factors fine tuning this process require further investigation.

1.4.2 TCA cycle

Another main point of focus in cancer metabolism is the TCA cycle which is

a central hub in cell metabolism occurring in the mitochondrial matrix. Through the TCA cycle, metabolites derived from the main fuel sources of cells are oxidised to produce NADH and flavin adenine dinucleotide (FADH_2), which can be used to synthesise ATP through mitochondrial respiration¹¹². In parallel, TCA cycle derivatives can be used as precursors to synthesise macromolecules that can be used as building blocks or play a role in cell signalling¹¹³. The main three sources of fuel for the TCA cycle are glucose, glutamine, and fatty acids. Importantly, depending on different factors, cells rely more or less on those three different substrates, which makes the TCA cycle a convergence point that modulates the consumption of the different fuel sources^{109,113}. Just like glucose, fatty acids are also degraded to acetyl-CoA through a process called β -oxidation before being integrated into the TCA cycle¹¹³. The resulting acetyl-CoA then reacts with oxaloacetate (OAA) to produce citrate which is then transformed to cis-aconitate, D-isocitrate, α -ketoglutarate (α KG), succinyl-CoA, succinate, fumarate, malate, and back to OAA through different biochemical reactions. Glutamine, on the other hand, enters the TCA cycle after being metabolised to α KG through a process called glutaminolysis (described later)¹¹³. For each molecule of acetyl-CoA being oxidised in the TCA cycle, the process generates three molecules of NADH, one molecule of FADH_2 , and two molecules of CO_2 . On the other hand, α KG oxidation leads to the production of two molecules of NADH, one molecule of FADH_2 , and one molecule of CO_2 . Overall, these processes are more efficient to generate ATP from NADH and FADH_2 through the electron transport chain as compared to glycolysis¹⁰⁹. However, as discussed earlier, although ATP is necessary for cell survival, the production of ATP is not a rate limiting step for cancer cell growth¹⁰⁰.

Indeed, many cancer cells shunt glucose into the PPP or SSP and use glutamine and fatty acids as alternative fuel sources to feed the TCA cycle to generate the necessary TCA cycle intermediates. Interestingly, in some context, α KG is reduced to citrate in the cytosol and sometimes further reduced to malate and fumarate in a process called reductive carboxylation¹¹⁴. One explanation for this process is that citrate is shuttled into the mitochondria to produce NADPH¹¹⁵. Another non-mutually exclusive explanation is that cells need to consume cytosolic NADH to maintain a high ratio of NAD^+/NADH to allow glycolysis to continue or to allow catabolic breakdown of TCA cycle intermediates^{114,116}. In line with this, the production of lactate from pyruvate also yields NAD^+ at the expense of NADH.

1.4.3 Mitochondrial respiration

As discussed above, the mitochondria play a major role in cell metabolism and have always been a focal point in research since their discovery in the 1890s¹¹⁷. The mitochondria are important for a number of different functions including energy production in the form of ATP, production of metabolite intermediates, reactive oxygen species (ROS) regulation, and cell death and signalling^{118,119}. In fact, most TCA cycle reactions described earlier occur in the mitochondrial matrix, and glycolysis is also closely linked to mitochondria. Therefore, it is difficult to study metabolism without holistically investigating these interrelated pathways.

Perhaps the most well-known function of mitochondria is their role in energy production which led to the nickname “powerhouses of the cell”. Energy production

or ATP replenishment happens through mitochondrial respiration. Briefly, electron donors NADH and FADH₂ donate electrons through a chain of different enzymatic reactions termed the electron transport chain (ETC)¹²⁰. The final electron acceptor is oxygen which is reduced to H₂O. The energy produced by this transfer of electrons is coupled with the transfer of protons into the intermembrane space which produces a proton gradient¹²¹. In the final step of oxidative phosphorylation, ATP synthase uses the energy from the proton gradient to transfer a phosphate group onto adenosine diphosphate (ADP) to replenish the pool of ATP^{120,122}.

Interestingly, since mitochondrial respiration consumes NADH and produces NAD⁺, it also plays an important role in regulating cell processes that rely on a high ratio of NAD⁺/NADH. Accordingly, as discussed above, since ATP levels are often not limiting in cancer cells, providing NAD⁺ for important catabolic reactions can be the main role of mitochondrial respiration in certain context in cancer biology^{122,123}. For example, aspartate is essential for synthesis of nucleotides, amino acids, and N-acetyl-aspartate. Since processing of TCA cycle substrates into OAA, the precursor of aspartate, requires NAD⁺, inhibition of mitochondrial respiration can prevent aspartate synthesis^{122,124}.

1.4.4 Pentose phosphate pathway

Another important pathway that is closely linked with glycolysis in cancer metabolism is the PPP through which intermediates of glycolysis can be diverted to generate reducing power in the form of NADPH. NADPH is subsequently used for anabolic reactions or to regenerate the pool of reduced glutathione (GSH)¹²⁵. The

PPP is also used to synthesise ribose-5-phosphate (R5P), the sugar moiety necessary for the production of nucleotides. Overall, the PPP is separated into two branches: the oxidative and non-oxidative branch. Through a few unidirectional biochemical reactions, the oxidative branch uses G6P from glycolysis to generate NADPH and R5P. On the other hand, the reactions occurring in the non-oxidative branch are mostly bidirectional and allow for fine tuning the products of the PPP¹²⁵. Indeed, in conditions where NADPH is more important than R5P, the R5P synthesised from the oxidative branch can be recycled back into F6P or G3P and fed back into glycolysis where it can be used to generate G6P and fuelled into the oxidative branch again, resulting in further production of NADPH^{125,126}. Alternatively, if R5P is more important for the cell, the non-oxidative branch is used to generate R5P from F6P and G3P, a process that does not produce NADPH^{127,128}. In cancer, the needs of the cells for both NADPH and R5P production are increased and therefore the regulation of the PPP is affected. Just like the other pathways described above, the exact conditions and mechanisms that modulate the changes observed in cancer need further investigation.

For this thesis, I have chosen to focus on the main metabolic pathways that have been extensively studied and form major regulatory hubs in cancer metabolism. However, cell metabolism involves a much more complex network of additional pathways that are outside the scope of this thesis.

1.5 Glutamine in cancer metabolism

While investigating metabolic pathways provides an interesting perspective

in cancer metabolism, it is also important to explore metabolism from the point of view of the substrates consumed. Since Warburg's first observations, glucose has always been at the centre stage of cancer metabolism research, however, more recently, glutamine has also been shown to be an important substrate for a number of metabolic pathways. Importantly, glutamine is the most concentrated amino acid in plasma with levels up to 0.7 mM¹²⁹, and, unlike many other metabolites, glutamine levels are equivalent between plasma and tumour interstitial fluid¹³⁰. Glutamine is a non-essential amino acid in normal cells but becomes conditionally essential in many different types of cancer cells⁹⁹. Overall, it provides an alternative carbon source to glucose and it is the main source of nitrogen for actively dividing cells. The downstream uses of glutamine are broad as it leads to many important derivatives. Generally, it can be used for the synthesis of proteins, nucleotides, fatty acid, other amino acids, GSH, and neurotransmitter γ -aminobutyrate (GABA), among others (Figure 1.3)¹³¹⁻¹³³. Therefore, glutamine plays a central role in cell metabolism.

1.5.1 Glutamine transport

The first step that regulates glutamine usage in cells is the transport from the extracellular environment. Glutamine is transported across the cell membrane using a variety of different transporters that are part of four different families of the solute carrier type transporters (SLC): SLC1, SCL6, SLC7, SLC38. While most of these transporters only support influx, some of them also support mono- or bidirectional efflux. Additionally, each family and/or transporter behaves slightly differently and also supports the transport of other substrates¹²⁹. For example,

SLC1A5 is the only member of SLC1 family that transports glutamine, however, it is thought to be the main transporter for glutamine in cancer cells including TNBC¹³⁴. Accordingly, its expression is regulated via c-Myc and/or Rb related mechanisms¹³⁵. SLC1A5 is a neutral transporter and exchanges Na⁺ and any of five neutral amino acids (serine, cysteine, alanine, glutamine, threonine) depending on the concentration levels across the membrane, therefore, glutamine cannot accumulate intracellularly without being processed. Interestingly, coupling of SLC1A5 with SLC7 family members SLC7A5 and SLC7A11 is thought to be essential for the increased proliferation of cancer cells with high expression of SLC1A5¹³⁶. SLC7A5 exchanges glutamine for leucine, while SLC7A11 exchanges glutamate for cystine¹³⁷. Other members of the SLC38, SLC6, and SLC7 families are expressed more or less in different organs and operate through different mechanisms. Overall, glutamine transport is a highly regulated process depending on multiple factors.

1.5.2 Glutaminolysis

Once inside the cell, glutamine can be used directly for protein, nucleotide, and/or asparagine synthesis. However, in order to produce other derivatives, it needs to be degraded through a process called glutaminolysis. Throughout this process, the amide group of glutamine is cleaved off by glutaminase 1 or 2 (GLS1/GLS2) to generate glutamate, which is further degraded to α KG by glutamate dehydrogenase 1 (GDH1), both reactions result in the release of ammonium (NH₄⁺) as a by-product. The final product of glutaminolysis, α KG, is then fed into the TCA cycle, a process called anaplerosis. Intermediates of this

process (i.e. glutamate and α KG) can be used for alternative purposes (explored later). Additionally, glutamate is formed as a “by-product” of usage of glutamine for nucleotide or asparagine synthesis, and α KG can be produced via transamination reactions which transfer the amino group of glutamate onto different keto-acids. These transamination reactions generate other amino acids such as alanine and aspartate in the process. Interestingly, GDH1 is allosterically regulated and, in the presence of low glutamate, can function in reverse to generate glutamate from α KG by recycling free intracellular NH_4^+ ¹³⁸. GLS1 mRNA expression is also regulated by c-myc¹³⁹.

1.5.3 Glutamine synthetase

While most cells degrade glutamine into downstream intermediates, in some context, *de novo* synthesis of glutamine is also important. This occurs through the glutamine synthetase (GS) reaction which uses glutamate and free NH_4^+ to form glutamine¹⁴⁰. At a systemic level, the change from glutamate to glutamine modulated by GS is essential to detoxify NH_4^+ and glutamate from certain tissues¹⁴¹. In line with this, different organs express different levels of GS. In cancer, GS is differentially expressed across cancer types and is thought to dictate the sensitivity of certain cancers to glutamine deprivation^{142,143}. More specifically, GS has a higher expression level in luminal subtypes of breast cancer which are resistant to glutamine deprivation while its expression is low in basal breast cancers which rely on glutamine for survival^{142,143}. Accordingly, GS has been considered as a potential biomarker to predict the prognosis of patients with breast cancer. However, it is still unclear whether low GS expression drives a more

aggressive phenotype in breast cancer or whether GS expression is reduced as a result of other changes linked with the more aggressive basal phenotype.

1.5.4 Downstream use of glutamine and derivatives

As described above, multiple enzymes and pathways coordinate the intake and processing of glutamine. Glutamine is tightly regulated as it is essential for multiple downstream processes either directly or indirectly through anaplerosis. Apart from mitochondrial respiration and protein synthesis, some of the key downstream uses of glutamine include synthesis of non-essential amino acid (NEAA), GSH, GABA, and nucleotides.

1.5.4.1 NEAA synthesis

As the main source of nitrogen in cancer cells and an important carbon source, glutamine is essential in the synthesis of NEAA. Firstly, the amide group of glutamine can be transferred onto aspartate to synthesise asparagine through the asparagine synthetase (ASNS) enzyme. This leads to the production of glutamate as a by-product and consumes one molecule of aspartate. Every other NEAA derived from glutamine originate from glutamate, the first downstream product of glutamine. Briefly, the amino group of glutamate is transferred onto OAA or pyruvate, resulting in the production of aspartate and alanine respectively¹⁴⁴. These transamination reactions are catalysed by the enzymes glutamic-oxaloacetic transaminase 1 and 2 (GOT1/GOT2) or alanine transaminase (ALT) respectively¹⁴⁴. Interestingly, these transamination reactions can also occur in reverse resulting in the synthesis of glutamate from alanine or aspartate¹⁴⁴. GOT2

is expressed in the mitochondrial matrix and promotes the synthesis of aspartate, while GOT1 is localised in the cytosol and mostly promotes the reverse reaction^{122,124}. Importantly, different enzymes can promote transamination between any amino acid and keto acid, a process which is also important for GABA regulation (explored later).

1.5.4.2 GSH synthesis

Glutamate can also be used to synthesise GSH, the main ROS scavenger. ROS is a general term used to describe molecules with unpaired electrons derived from partially reduced molecular oxygens. These comprise free radicals such as superoxide anion or non-radical such as hydrogen peroxide coming from the environment or constantly generated through internal cell functions¹⁴⁵. Although there has been plenty of research trying to tackle the role of ROS in cell biology and disease, it is still unclear exactly what levels of ROS are optimal for cell proliferation and under which context. However, it is now widely agreed that some ROS are required for cell signalling and that too much ROS can lead to oxidative damage of DNA, proteins, or lipids and can even result in cell death¹⁴⁵⁻¹⁴⁷. Consistently, cells have evolved different mechanisms to maintain ROS levels in check. One of the main ROS regulation mechanism is through GSH. GSH is present in cells in two forms: the reduced GSH form, as well as the oxidised GSH dimer (GSSG). As a mechanism to capture and stabilise the unpaired electrons originating from ROS, a number of enzymes catalyse the reduction of ROS which leads to the oxidation of GSH into GSSG. GSSG can stably support unpaired electrons as the charge is distributed across the whole molecule which prevents

oxidative damage. GSSG is then reduced back to GSH by the enzyme glutathione reductase using the reducing potential of NADPH and the cycle starts anew¹⁴⁵⁻¹⁴⁷. GSH is synthesised in the cytoplasm from glycine, cysteine, and glutamate¹⁴⁸. The rate-limiting reagent for the production of GSH is usually cysteine which can be produced from serine through the transsulfuration pathway¹⁴⁹, or imported into the cell as a cystine dimer in exchange for glutamate via the cystine-glutamate antiporter SLC7A11 also known as xCT¹⁵⁰. The synthesis of GSH is catalysed by two sequential enzymatic reactions: 1) cysteine and glutamate are linked using the rate-limiting enzyme glutamate-cysteine ligase catalytic subunit (GCLC), and 2) the resulting glutamyl-cysteine is further linked with glycine to form GSH¹⁴⁸. Although cysteine is usually the rate-limiting reagent in the synthesis of GSH, glutamate is also important and can therefore influence the ROS sensitivity of cells which is an important aspect of cancer metabolism¹⁵¹.

1.5.4.3 GABA synthesis

GABA is a four-carbon non-proteinogenic amino acid well-known for its role as the main inhibitory neurotransmitter of the brain¹⁵², but it has also been shown to play a role in regulating insulin-producing beta cells in the pancreas¹⁵³. Interestingly, GABA was first identified in plants in 1885 before its role as neurotransmitter was discovered in the 1950s. In plants, GABA is important to regulate the nitrogen pool and plays a role in regulating growth signalling^{154,155}. Recently, GABA synthesis enzymes have been shown to be expressed in cancer and GABA has been suggested as a potential oncometabolite¹⁵⁶⁻¹⁶⁰. Through the GABA shunt, GABA can be synthesised by α KG that is diverted out of the TCA

cycle to generate glutamate, or directly from glutamine-derived glutamate.

Glutamate is then decarboxylated by the glutamate decarboxylase (GAD) enzyme to produce GABA. Interestingly, GABA can be further processed to succinic semialdehyde through GABA transaminase (GABA-T), and subsequently oxidised to succinate which can feed back into the TCA cycle^{154,159,161}. The regulation of glutamine-glutamate-GABA is very important in the brain and takes place across different cell types and compartments.

1.5.4.4 Nucleotide synthesis

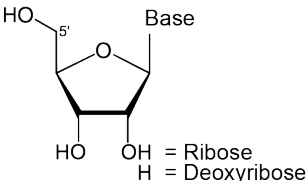
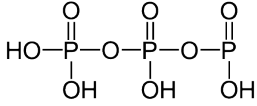
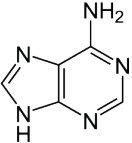
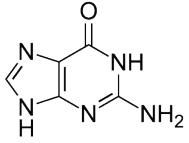
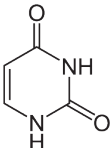
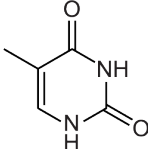
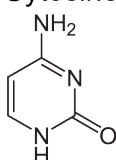
Glutamine is also used to synthesise nucleotides which are building blocks for DNA replication and RNA transcription as well as important signalling molecules. Nucleotides can be scavenged and recycled from degrading DNA and RNA or from the microenvironment, as well as synthesised *de novo* using mostly glucose, glutamine and CO₂ as substrates^{162,163}. In general, rapidly proliferating cells rely primarily on *de novo* synthesis as the demand for DNA replication and RNA synthesis is too high to maintain nucleotide pools through the salvage pathway only¹⁶³. Importantly, *de novo* nucleotide synthesis is energetically and metabolically costly and involves multiple feeder pathways such as glycolysis, PPP, SSP, one-carbon cycle, TCA cycle, and glutamine transamination among others¹⁶². Accordingly, nucleotide synthesis is highly regulated and relies on the coordination of many signalling pathways. Nucleotides are formed of one of five nucleic bases (adenine, guanine, cytosine, thymine, uracil) separated into two different categories (purines and pyrimidines), a five-sugar moiety (ribose or deoxyribose), and up to three phosphate groups. Nucleotides are named according

to the nucleic base they are made of (Table 1.1)¹⁰⁹. Glutamine is particularly important as a nitrogen source for nucleic bases which are nitrogen-rich compounds. Glutamine contributes between one and three nitrogen groups directly to different bases, and can indirectly contribute all five nitrogen atoms that form guanine, the most nitrogen-rich nucleic base¹⁶³.

Pyrimidine bases are formed of one nitrogen ring and include cytosine, thymine, and uracil. The *de novo* synthesis of pyrimidine bases occurs mostly in the cytoplasm except one step taking place in the mitochondrial matrix. It involves the combination of carbamoyl phosphate and aspartate to generate orotate which is linked to R5P coming from the PPP and yields the common pyrimidine precursor uridine monophosphate (UMP)¹⁶². Subsequently, UMP is transformed to uridine triphosphate (UTP) which is then turned into cytidine triphosphate (CTP) with the addition of one amide group from glutamine. In parallel, UMP can be modified to deoxy UMP (dUMP) and subsequently to thymidine monophosphate (dTMP). As part of the salvage pathway, cytosine can be transformed into uracil which means that supplementing with cytosine or cytidine can replenish both CTP and dTMP pools, while supplementation with thymine or thymidine can only replenish the dTMP pool.

Purine bases are made of two fused nitrogen rings and include adenine and guanine, as well as precursor hypoxanthine and xanthine, which form the nucleotides adenosine monophosphate (AMP), guanosine monophosphate (GMP), inosine monophosphate (IMP), and xanthosine monophosphate (XMP),

Table 1.1 - Nucleotide structure and nomenclature

		 +	Phosphate Groups  +
	Nucleic Base	Nucleosides	Nucleotides
Purines	Adenine 	Adenosine or Deoxyadenosine	AMP, ADP, ATP or dAMP, dADP, dATP
	Guanine 	Guanosine or Deoxyguanosine	GMP, GDP, GTP or dGMP, dGDP, dGTP
Pyrimidines	Uracil 	Uridine or Deoxyuridine	UMP, UDP, UTP or dUMP, dUDP, dUTP
	Thymine 	Thymidine*	dTMP, dTDP, dTTP
	Cytosine 	Cytidine or Deoxycytidine	CMP, CDP, CTP or dCMP, dCDP, dCTP

* Thymidine is always formed with a deoxyribose

respectively¹⁶². Unlike pyrimidine synthesis, purine synthesis only takes place in the cytoplasm and the purine nucleic base is built directly on an activated R5P molecule called phosphoribosyl pyrophosphate (PRPP) that is used as a scaffold. Synthesis of precursor IMP requires glutamine, aspartate and one-carbon cycle derivatives. Subsequently, AMP and GMP synthesis from IMP requires the addition of a nitrogen group from aspartate and glutamine respectively¹⁶². The synthesis of GMP is a two-step process including the formation of XMP by the IMP dehydrogenase (IMPDH) enzyme. As part of the purine salvage pathway, nucleic bases can be converted back to their respective nucleoside or nucleotide while nucleotides can be degraded into nucleic bases only. Additionally, adenosine can be converted back to inosine which itself can lead to IMP¹⁶². Therefore, adenine, adenosine, hypoxanthine, or inosine supplementation can support the synthesis of both GMP and AMP, while guanine or guanosine supplementation can only support the synthesis of GMP. Finally, as part of the degradation of nucleotides, hypoxanthine and guanine can be degraded into xanthine which is then further transformed into uric acid and gets excreted.

1.6 Rationale of thesis

While it is clear that metabolic pathways are altered in cancer, the exact intrinsic and extrinsic factors that lead to those changes still need to be more carefully explored⁹⁹. Unlike most cell signalling pathways which are mostly regulated through expression levels and activity of the proteins involved, metabolic pathways are also regulated through allosteric regulation of downstream metabolites. Indeed, many enzymatic reactions are bidirectional and are driven by

the abundance of products on either side of the reaction. This further complicates the analysis of metabolic flux and diminishes the importance of the concept of rate-limiting reactions. In line with this, recent cancer metabolism studies show that the tumour microenvironment and nutrient availabilities dictate the metabolic changes occurring in cancer cells^{101,130}. However, well known oncogenes and tumour suppressors such as Ras, c-Myc, PI3K, p53, and BRCA1 have also been shown to directly or indirectly regulate metabolic enzyme activity or expression levels⁹⁹. Interestingly, indirect regulation of metabolic pathways could be a result of metabolic pressures originating from a generally more aggressive oncogenic phenotype rather than direct oncogenic regulation of metabolic enzymes. Additionally, there are many metabolic enzymes that can get mutated in cancer cells and also lead to metabolic changes¹¹³. Particularly regarding glutamine, it has been shown that c-Myc activation leads to a metabolic reprogramming that increases glutaminolysis, as well as activates enzymes involved in the synthesis of nucleotides⁹⁹. However, other factors driving the need for particular substrates need further investigation.

1.6.1 BRCA1 and cancer metabolism

Cancer research has led to increased understanding of specific aspects of cancer biology. However, although communities of experts share knowledge within their respective sub-fields, there is often lack of cross-talk between less related fields. The rationale for the work presented in this thesis comes from a desire to connect aspects of cancer biology usually studied independently in order to inform better patient care and gain a better understanding of the disease. Here, we

hypothesise that there is a connection between BRCA1 loss-of-function and cancer metabolism, which is important for the pathogenesis and treatment response of tumours bearing *BRCA1* mutations. Accordingly, in the last few years, there have been studies suggesting that BRCA1 could impact metabolism in different context⁹¹⁻⁹³.

Among the first reports published, overexpression of wild-type BRCA1 was shown to enhance antioxidant capacity and resistance to hydrogen peroxide treatment in luminal breast and prostate cancer expressing endogenous levels of BRCA1¹⁶⁴. These initial findings were further supported by Gorrini et al. who showed that BRCA1 interacts with nuclear factor erythroid 2-related factor 2 (NRF2) and regulates its antioxidant capacity in mouse mammary epithelial cells and breast cancer cells, while also suggesting a role for oestrogen signalling⁹². Additionally, BRCA1 has also been shown to interact with acetyl-CoA carboxylase and regulate lipid synthesis in luminal breast cancer MCF7 cells and normal breast MCF10A cells¹⁶⁵.

In parallel, other studies showed that BRCA1 leads to metabolic reprogramming more broadly. For example, Privat et al. showed that stable expression of wild-type BRCA1 in breast cancer SUM1315 *BRCA1* mutant cells leads to a reduction in glycolysis-related metabolites and an increase in mitochondrial respiration and TCA cycle-related metabolites. Their results also supported the role of BRCA1 in regulating antioxidants and lipid synthesis⁹³. However, another study where one allele of *BRCA1* was mutated in normal

mammary MCF10A cells showed increases in mitochondrial respiration and TCA cycle activity associated with the *BRCA1* mutation⁹¹.

Recently, some more mechanistic work has started to emerge linking *BRCA1* transcriptional regulation with specific metabolic functions. For example, through its E3 ligase activity, *BRCA1* regulates the transcription factor Oct1 and carbohydrate metabolism¹⁶⁶. Additionally, *BRCA1* regulates aspartate metabolism by repressing *GOT2* mRNA expression through the formation of a repressor complex with ZBRK1 also known as zinc finger protein 350 (ZNF350)¹⁶⁷.

Together, all these studies clearly show that *BRCA1* has an impact on cell metabolism. However, there are discrepancies between studies based on the models used or the context, leading to a slightly disjointed literature. Importantly, most studies were done in normal breast (cell lines or fibroblasts) or luminal breast cancer cells, whereas mutations in *BRCA1* are most often found in TNBC. Further investigation into the mechanistic role of *BRCA1* in cancer metabolism could help clarify its function(s). Given the nature of *BRCA1*, it is likely that the multiple functions are not mutually exclusive.

1.6.2 Rationale and aims

The work presented in this PhD thesis explores the links between *BRCA1* function and metabolic changes in basal-like breast cancer, and seeks to identify potential metabolic vulnerabilities that could be exploited to improve treatment. Overall, I show that *BRCA1* mutant cells are more sensitive to glutamine

deprivation, and rewire their metabolism to more efficiently process glutamine through the GABA shunt and maintain high levels of aspartate. Additionally, I explore the possible links between these metabolic changes and BRCA1. As such, the results section of this thesis is separated into three chapters focusing on different aspects of the project: 1) Identification and characterisation of metabolic vulnerabilities in *BRCA1* mutant breast cancer; 2) exploration of the roles of glutamine in breast cancer and their importance in *BRCA1* mutant cells; and 3) mechanistic investigation of the link between BRCA1 and the observed phenotype.

2 Materials and Methods

2.1 Materials

2.1.1 Reagents

CellTiter 96® AQueous One Solution (G3581, Promega), Sulforhodamine B (SRB; S1402, Sigma-Aldrich), CyQUANT Cell Proliferation Assay (C7026, Thermo Fisher), Crystal Violet (C0775, Sigma-Aldrich), FuGENE® HD transfection reagent (E2311, Promega), Polybrene (TR-1003-G, Sigma-Aldrich), Lipofectamine RNAiMAX Transfection Reagent (13778075, Thermo Fisher), RNeasy Mini Kit (74106, Qiagen), QuantiTect Reverse Transcription Kit (205313, Qiagen), SYBR™ Select Master Mix (4472918, Thermo Fisher), leupeptin (L2884, Sigma-Aldrich), pepstatin A (P5318, Sigma-Aldrich), Na₃VO₄ (450243, Sigma-Aldrich), DL-Dithioereitol (646653, Sigma-Aldrich), Calyculin A (9902, Cell Signaling Technology), β-glycerolphosphate (G9422, Sigma-Aldrich), PMSF (8553, Cell Signaling Technology), Bio-Rad Protein Assay Dye Reagent Concentrate (5000006, Bio-Rad), NuPAGE™ 3-8% Tris-Acetate Mini Protein Gel (EA0375BOX, Thermo Fisher), 4-15% Mini-PROTEAN® TGX Stain-Free™ Protein Gels (4538083, Bio-Rad), Trans-Blot Turbo Mini 0.2 μm Nitrocellulose Transfer Packs (1704158, Bio-Rad), Clarity Max Western ECL Substrate (1705062, Bio-Rad), GSH-Glo™ Glutathione Assay (V6911, Promega), Glutamate Dehydrogenase Activity Assay Kit (ab102527, Abcam), Ammonia Assay Kit (ab83360, Abcam), CM-H2DCFDA probe (C6827, Thermo Fisher), NucBlue™ Fixed Cell ReadyProbes™ Reagent (DAPI; R37606, Thermo Fisher), Propidium iodide solution (P4864, Sigma-Aldrich), FITC Annexin V (556419, BD Biosciences), BrdU

(19-160, Sigma-Aldrich), Seahorse XF Cell Mito Stress Test Kit (103015-100, Agilent), Seahorse XF Cell Glycolysis Stress Test Kit (103020-100, Agilent), Seahorse XF Mito Fuel Flex Test Kit (103260-100, Agilent), Pierce™ BCA Protein Assay Kit (23225, Thermo Fisher).

2.1.2 Media

All experiments with SUM149 cells where glutamine or glucose levels were manipulated were performed with Ham's F12 media produced in-house hereafter referred as Special Ham's F12. The Special Ham's F12 was produced following the formulation of commercially available Ham's F12 except for glutamine, glutamate, glucose, sodium pyruvate, hypoxanthine, and thymidine which were removed (Table 2.1). Unless specified otherwise, missing components from the Special Ham's F12 were supplemented to the same level as the commercially available formulation. For experiments where glutamine levels were manipulated in Dulbecco's Modified Eagle Medium (DMEM), commercially available DMEM with high glucose and no glutamine was supplemented with the relevant amount of glutamine.

Table 2.1 - Special Ham's F12 formulation

Components	Molecular Weight	Concentration (mg/L)	mM
Amino Acids			
Glycine	75	7.5	0.1
L-Alanine	89	8.9	0.0999999994
L-Arginine hydrochloride	211	211	1
L-Asparagine-H ₂ O	150	15.01	0.10006667
L-Aspartic acid	133	13.3	0.1
L-Cysteine hydrochloride-H ₂ O	176	35.12	0.19954544

L-Histidine hydrochloride-H2O	210	21	0.1
L-Isoleucine	131	4	0.030534351
L-Leucine	131	13.1	0.1
L-Lysine hydrochloride	183	36.5	0.19945355
L-Methionine	149	4.5	0.030201342
L-Phenylalanine	165	5	0.030303031
L-Proline	115	34.5	0.3
L-Serine	105	10.5	0.1
L-Threonine	119	11.9	0.099999994
L-Tryptophan	204	2.04	0.01
L-Tyrosine disodium salt dihydrate	262	7.81	0.02980916
L-Valine	117	11.7	0.1
Vitamins			
Biotin	244	0.0073	2.99E-05
Choline chloride	140	14	0.1
D-Calcium pantothenate	477	0.5	0.001048218
Folic Acid	441	1.3	0.002947846
Niacinamide	122	0.036	2.95E-04
Pyridoxine hydrochloride	206	0.06	2.91E-04
Riboflavin	376	0.037	9.84E-05
Thiamine hydrochloride	337	0.3	8.90E-04
Vitamin B12	1355	1.4	0.00103321
i-Inositol	180	18	0.1
Inorganic Salts			
Calcium Chloride (CaCl ₂) (anhyd.)	111	33.22	0.2992793
Cupric sulfate (CuSO ₄ ·5H ₂ O)	250	0.0025	1.00E-05
Ferric sulfate (FeSO ₄ ·7H ₂ O)	278	0.834	0.003
Magnesium Chloride (anhydrous)	95	57.22	0.6023158
Potassium Chloride (KCl)	75	223.6	2.9813335
Sodium Bicarbonate (NaHCO ₃)	84	1176	14
Sodium Chloride (NaCl)	58	7599	131.01724
Sodium Phosphate dibasic (Na ₂ HPO ₄) anhydrous	142	142	1
Zinc sulfate (ZnSO ₄ ·7H ₂ O)	288	0.863	0.002996528
Other Components			
Linoleic Acid	280	0.084	3.00E-04
Lipoic Acid	206	0.21	0.001019417
Phenol Red	376.4	1.2	0.003188098
Putrescine 2HCl	161	0.161	0.001

Ham's F12 (21700018, Thermo Fisher), DMEM, high glucose, no glutamine (11960044, Thermo Fisher), DMEM, high glucose, pyruvate (11995065, Thermo Fisher), Roswell Park Memorial Institute (RPMI) 1640 medium (21875091, Thermo Fisher), DMEM/F12, HEPES (11330057, Thermo Fisher), Fetal Bovine Serum (FBS; 10270106, Thermo Fisher), hydrocortisone (H0888, Sigma-Aldrich), Insulin-Transferrin-Selenium (41400045, Thermo Fisher), benzylpenicillin sodium (Britannia Pharmaceutical Limited), streptomycin sulfate salt (S9137, Sigma-Aldrich), puromycin (ant-pr-1, InvivoGen), D-glucose (10117, VWR International), L-glutamine (G5792, Sigma-Aldrich), L-glutamic acid (G1251, Sigma-Aldrich), sodium pyruvate solution (S8638-100ML, Sigma-Aldrich), adenine (A2786, Sigma-Aldrich), guanine (G11950, Sigma-Aldrich), thymidine (T1895, Sigma-Aldrich), hypoxanthine (H9636, Sigma-Aldrich), Phosphate buffered saline, pH 7.4 (PBS, 10010023, Thermo Fisher), Hank's Balanced Salt Solution (HBSS, 14175095, Thermo Fisher), L-Glutamine (13C5, 99%, CLM-1822-H, Cambridge Isotope Laboratories), L-Glutamine (15N2, 98%, NLM-1328, Cambridge Isotope Laboratories).

2.1.3 Compounds

Epigallocatechin gallate (EGCG; E4143, Sigma-Aldrich), L-Buthionine-sulfoximine (L-BSO; B2515, Sigma-Aldrich), O-benzyl-L-serine (BenSer; 13900, Sigma-Aldrich), 6-diazo-5-oxo-L-norleucine (DON; D2141, Sigma-Aldrich), bis-2-(5-phenylacetamido-1,3,4-thiadiazol-2-yl) ethyl sulfide (BPTES; SML0601, Sigma-Aldrich) CB-839 (S7655, Selleckchem), Menadione (M5625, Sigma-Aldrich),

Luperox® TBH70X, *tert*-Butyl hydroperoxide (TBHP; 458139, Sigma-Aldrich), Sulfasalazine (S1576, Selleckchem).

2.1.4 Consumables

Nunc™ MicroWell™ 96-Well Microplate (167008, Thermo Fisher), Falcon® Clear Flat Bottom TC Treated 6-Well plate (353046, Corning), Corning® 100 mm TC Treated Culture Dish (430167, Corning), Falcon® 25 cm² Cell Culture Flask (353108), IncuCyte® ImageLock 96-well plate (4379, Essen Biosciences), Nunc™ F96 MicroWell™ White Cell Culture Plate (136101, Thermo Fisher), Falcon™ Round-Bottom Polypropylene Tubes (352053, Falcon), Nunc™ 96-well Round Bottom Microwell Plate (268152, Thermo Fisher), Seahorse XFe96 FluxPak (102416-100, Agilent), LC/MS V-shape vials (Agilent 5188-2788).

2.1.5 Antibodies

Vinculin XP® Rabbit mAb (1:1000, 13901, Cell Signalling Technologies), GLUL Rabbit mAb (1:1000, 80636, Cell Signalling Technologies), HA-tag Rabbit mAb (1:1000, 3724, Cell Signalling Technologies), phospho-Histone H2A.X (Ser139) Antibody (1:1000, 2577, Cell Signalling Technologies), Phospho-Chk1 (S345) Rabbit mAb (1:000, 2348, Cell Signalling Technologies), E-cadherin Rabbit mAb (1:10000, ab40772, Abcam), Vimentin Rabbit Antibody (1:10000, ab92547, Abcam), SNAIL/SLUG Rabbit Antibody (1:1000, ab85936, Abcam), GAPDH Rabbit mAb (1:5000, 2118S, Cell Signalling Technologies), BrdU-FITC Antibody (347583, BD Biosciences), goat anti-Rabbit IgG HRP conjugate (1:5000, 1706515, Bio-Rad), GAD1 Rabbit Antibody (1:1000, 5305, Cell Signalling Technologies).

2.1.6 Primers

Oligonucleotides used for qPCR reactions (Table 2.2) were purchased from Sigma-Aldrich.

Table 2.2 - qPCR primers

Gene	Sense	Antisense
<i>BRCA1</i>	5'-ACAGCTGTGTGGTGCTTCTGTG-3'	5'- CATTGTCCTCTGTCCAGGCATC-3'
<i>BRCA2</i>	5'-CTACACCACCCACCCTTAGT-3'	5'-CACTGTCTGTACAGAAGCG-3'
<i>GLS1</i>	5'-CTTCCAGCTGTGCTCCATTG-3'	5'-TTCGAACTGCTTCAGGGCTC-3'
<i>GDH1</i>	5'-GGTCATCGAAGGCTACCG-3'	5'-TCAGTGCTGTAACGGATACCTC-3'
<i>GCLC</i>	5'-GCACCCTCGCTTCAGTACCT-3'	5'-ATCCGGCTTAGAAGCCCTTG-3'
<i>GSS</i>	5'-GAAAGGCGAACTAGTGTTGGG-3'	5'-AGAGCGTGAATGGGGCATAG-3'
<i>GPX1</i>	5'-CCGGGACTACACCCAGATGA-3'	5'-TCTTGGCGTTCTCCTGATGC-3'
<i>GSR</i>	5'-CTGAAGTTCTCCAGGTCAAGG-3'	5'-GAGCAGGCAGTCAACATCTG-3'
<i>GLUL</i>	5'-AACCTGCCTGTTCGGACACC-3'	5'-AGGTGTTCCAGCCACAGAA-3'
<i>TWIST</i>	5'-CAAGAAGTCTGCGGGCTGTG-3'	5'-AATCGAGGTGGACTGGGAACCG-3'
<i>FOXC1</i>	5'-TAAGCCCATGAATCAGCCG-3'	5'-GCCGCACAGTCCCATCTCT-3'
<i>FOXC2</i>	5'-GCAACCCAACAGCAAACCTTTC-3'	5'-GACGGCGTAGCTCGATAGG-3'
<i>CAD</i>	5'-ACCACGACACCTGAAAGACC-3'	5'-CTCCTCAGCTGGCAAACCT-3'
<i>PPAT</i>	5'-TGGGGATCCGAGAGGAATGT-3'	5'-AGACCCATTCCCTTGTGTGA-3'
<i>ODC1</i>	5'-CTGGGCGCTCTGAGATTGTC-3'	5'-CATCGAGGAAGTGGCAGTCA-3'
<i>MYC</i>	5'-CCTACCCTCTCAACGACAGC-3'	5'-CTTGTTCTCCTCAGAGTCGC-3'
<i>RPL19</i>	5'-ATGTATCACAGCCTGTACCTG-3'	5'-TTCTTGGTCTCTTCTCCTTG-3'
<i>GAD1</i>	5'-GGGAACTAGCGAGAACGAGG-3'	5'-CAGAAACAGGCTCGGCTCT-3'
<i>ABAT</i>	5'-CCTTCTTGGTGGACGAGGTC-3'	5'-TGAAGATCCGGTAGGGAGCA-3'
<i>ALDH5A1</i>	5'-CAGTCATCACCCCGTGGAAT-3'	5'-ACCTGAAGGAATCCCAGCCT-3'

2.1.7 Plasmids

Plasmid overexpressing wild-type HA-tagged BRCA1, pBABEpuro HA BRCA1 was a gift from Stephen Elledge (14999, Addgene)¹⁶⁸. Empty vector control pBABE-puro was a gift from Hartmut Land, Jay Morgenstern, and Bob Weinberg (1764, Addgene)¹⁶⁹. TRC Lentiviral shRNA plasmids were purchased from Horizon Discovery (Table 2.3).

Table 2.3 - shRNA constructs

Name	The RNAi Consortium (TRC) ID
shBRCA1_1	TRCN0000039833
shBRCA1_5	TRCN0000039837
shGLUL_1	TRCN0000045628
shGLUL_5	TRCN0000045632
shBRCA2	TRCN0000040197
shTWIST1_1	TRCN0000020539
shTWIST1_4	TRCN0000020542

2.1.8 siRNA

AllStars Negative Control siRNA (1027280, Qiagen), Hs_BRCA1_13 FlexiTube siRNA (5'-CAGCAGTTTATTACTCACTAA-3', SI02654575, Qiagen), Hs_BRCA1_14 FlexiTube siRNA (5'-CAGGAAATGGCTGAACTAGAA-3', SI02664361, Qiagen), Hs_GAD1_5 FlexiTube siRNA (5'-ATGGCTGACATCAACGGCCAA-3', SI03051559, Qiagen), Hs_GAD1_7 FlexiTube siRNA (5'-TCGCCTTGTGAGTGCCTTCAA-3', SI03116505, Qiagen).

2.1.9 Cell lines

All cell lines were authenticated by short tandem repeat analysis (Eurofins Scientific) and were regularly tested for mycoplasma infection. SUM149 *BRCA1* restored (3 independently cultured clones), *BRCA1* mutant (3 independently cultured clones), *BRCA1* mutant *Rev7* KO, *BRCA1* mutant *53BP1* KO cell lines were obtained from Prof. Chris Lord's group at the ICR in London. SUM149 *BRCA1* restored sh*BRCA1*, sh*BRCA2*, sh*GLUL*, and sh*TWIST* were derived from one clone of SUM149 *BRCA1* restored cells as described in the shRNA knockdown section. SUM149 *BRCA1* mutant sh*TWIST* were derived from SUM149 *BRCA1* mutant parental cell line. Unless specified otherwise, all SUM149 cell lines were cultured in Ham's F12 media supplemented with 5% FBS, 0.5 µg/mL hydrocortisone, 10 µg/mL Insulin-Transferrin-Selenium, 100 U/mL penicillin, and 100 µg/mL streptomycin. All other breast cancer cell lines were purchased from the American Type Culture Collection (ATCC). MDA-MB-468 cells were cultured in DMEM/F12 supplemented with 5% FBS, 100 U/mL penicillin, and 100 µg/mL streptomycin. HEK293, MDA-MB-231, Hs578T, and MCF7 cells were cultured in DMEM supplemented with 10% FBS, 100 U/mL penicillin, and 100 µg/mL streptomycin. T47D cells were cultured in RPMI medium supplemented with 10% FBS, 100 U/mL penicillin, and 100 µg/mL streptomycin. Unless specified otherwise, all cells were grown at 37 °C in a humidified 5% CO₂ incubator.

2.2 Cell culture and treatment

2.2.1 Dose Response Curves

Cells were seeded at a confluency of 5,000/well for SUM149 or 1,000/well for MCF7, MDA-MB-231 and Hs578T in 100 μ L of appropriate media in a 96-well plate format. For glutamine or glucose dose-response curves, 24 hours after seeding, the media was aspirated and cells were washed with 100 μ L of phosphate buffered saline (PBS) before replacing with media containing the appropriate concentration of glutamine, glucose and/or other supplements indicated in the figure legends. Other treatments (e.g. ionising radiation) were performed immediately after replacing the media. For dose-response curves with small molecule inhibitors, a 6X concentrated stock of the final concentration for each dose was prepared in the appropriate media and 20 μ L was added to each well 24 hours after seeding the cells. Following 1-5 days of incubation, 20 μ L of CellTiter 96® AQueous One Solution was added to each well and the cells were incubated for 3 hours at 37 °C in a 5% CO₂ incubator. Subsequently, absorbance was measured at 490 nm using a SpectraMax M5 Microplate Reader (Molecular Devices). Alternatively, following 1-5 days of incubation, cells were fixed and stained for quantification using sulforhodamine B as described in Vichai et al., 2006¹⁷⁰.

2.2.2 Proliferation assay

SUM149 cells were seeded at a confluency of 5,000/well in 100 μ L of media in a 96-well plate. The next day, the media was aspirated and cells were washed with 100 μ L of PBS before replacing with media containing the appropriate

concentration of glutamine. The zero time point was collected directly after media replacement. Each time point was collected by removing the media, washing with 200 μ L of PBS and freezing the plate at -80 °C until all plates were collected or for a minimum of 24 hrs. Cells were quantified using the CyQuant® Cell Proliferation Assay following the manufacturer's instructions. Briefly, thawed cells were incubated with 200 μ L of CyQuant dye/lysis buffer mix for 5 mins protected from light prior to measuring the sample fluorescence using a SpectraMax M5 Microplate Reader (Molecular Devices) with filters set for ~480 nm excitation and ~520nm emission maxima.

2.2.3 Colony formation assay

SUM149 cells were seeded at a confluency of 1,000/well in 6-well plates. For BPTES treatments, 400 μ L of 6X concentrated drug or vehicle control diluted in complete culture media were added 24 hours after seeding the cells. For glutamine or glucose deprivation, cell culture media was aspirated and cells were washed with 1mL of PBS before the media was replaced by culture media with appropriate concentrations of glutamine or glucose. The cells were allowed to grow for 12 days and the colonies were stained using crystal violet according to Franken et al., 2006¹⁷¹. The number of colonies and total area were quantified using the GelCount (Oxford Optronix) instrument. For Figure 5.1D, the data is presented as percentage reduction from the 1 mM to the 0.1 mM glutamine condition.

2.2.4 Generation of shRNA knockdown

HEK293 cells were seeded on 100mm dish and cultured until a density of around 70%. Cells were then transfected with 0.4 μg v-SVG, 3.7 μg GAG/Pol, 3.7 μg Rev lentiviral packaging vectors, and 4.2 μg of relevant TRC Lentiviral shRNA plasmids (Table 2.3), using 24 μL of FuGENE® HD Transfection Reagent. Briefly, DNA and transfection reagent were mixed in 600 μL final volume of serum free media and incubated for 25 mins before being added dropwise to the cell plate in a total volume of 6 mL normal culture media. Cells were incubated for 6 hours and the media was changed to fresh normal culture media and left to grow for 48 hours. Two days prior to the infection, cells to be infected were seeded at a density of 150,000/well (SUM149) or 75,000/well (MCF7) in 2 mL of appropriate culture media in a 6-well plate. After 48 hours of transfection of the HEK293 cells, media was collected from the transfected HEK cells, filtered using a 0.45 μm filter, and supplemented with Polybrene (4 $\mu\text{g}/\text{mL}$). The media of the cells to be infected was removed and replaced with media containing the viral particles and incubated for 6 hours before being replaced by normal media. Selection was started 24 hours after with media containing 2 $\mu\text{g}/\text{mL}$ of puromycin. Cells were selected for 3 days and were maintained in media with 1 $\mu\text{g}/\text{mL}$ puromycin for further culturing.

2.2.5 siRNA knockdown

One day prior to transfection, cells were seeded into 25 cm^2 flask to a final density of around 70%. The next day, the cells were transfected with indicated siRNA duplexes at a final concentration of 20 nM using Lipofectamine RNAiMAX

Transfection Reagent following the manufacturer's instructions. The following day, cells were detached using trypsin and seeded for relevant experiments.

2.2.6 Overexpression BRCA1

One day prior to transfection, HEK293 cells seeded onto 100 mm dishes to a density of around 70%. The next day, HEK293 cells were transfected with 3 μg of plasmid of interest and 3 μg pCL-Ampho Retrovirus Packaging vector using 18 μL of FuGENE® HD Transfection Reagent as described above. Supernatant containing retroviral particles was then collected 48hrs and 72hrs post-transfection, filtered through a 0.45 μm filter and supplemented with 4 $\mu\text{g}/\text{ml}$ Polybrene. Cells to be infected were seeded at a density of 150,000/well in a 6-well plate 48 hours prior to infection. Cells to be infected were incubated with supernatant containing retroviral particles at 37°C for 12hrs, which was then replaced with normal growth medium. After 12hrs, cells were infected again with newly harvested retrovirus-containing supernatant as described above. Selection with 2 $\mu\text{g}/\text{mL}$ of puromycin was started 24 hours following the last infection. Cells were selected for 3 days and were maintained in 1 $\mu\text{g}/\text{mL}$ puromycin for further culturing.

2.2.7 IncuCyte® scratch assay

SUM149 cells were seeded at a density of 40,000/well in 100 μL of media in an IncuCyte® ImageLock 96-well plate. The next day, following one wash with PBS, the culture media was replaced by media with indicated concentrations of glutamine and incubated for 24hrs. A wound area was then created using the

Essen® 96-well WoundMaker™ according to the manufacturer's instructions. The cells were then washed 2 times with 200 µL PBS and the media with indicated concentrations of glutamine was replaced. Plates were incubated in the IncuCyte® S3 Live Cell Analysis System for 48 hrs with images collected every 2 hours using phase-contrast with 10X magnification. Images were analysed for wound density with the IncuCyte® Analysis Software.

2.3 Cell extract analysis

2.3.1 Reverse transcription quantitative PCR

Cells were seeded at a density of 75,000/well in 12-well plates in 1 mL of appropriate culture media 2 days prior to RNA extraction. On the day of extraction, the culture media was removed and cells were washed with 1 mL PBS before being placed on ice. RNA was extracted using the RNeasy Mini Kit following the manufacturer's instructions. The extracted RNA was quantified using a NanoDrop™ ND-1000 UV-Vis Spectrophotometer (Thermo Fisher) and 200 µg was reverse transcribed to cDNA using the QuantiTect Reverse Transcription Kit according to the manufacturer's instructions. The resulting cDNA was diluted to a final volume of 40 µL in RNase free H₂O and 1 µL of resulting cDNA was used to perform qPCR. The reactions were performed with SYBR™ Select Master Mix according to the manufacturer's instructions. Briefly, 4 pmol of relevant primers (Table 2.2) were mixed with 1X SYBR™ Select Master Mix and 1 µL cDNA to a final volume of 10 µL. Reactions were analysed using a QuantStudio 6 Flex Real-

Time PCR System (Thermo Fisher) and data were analysed using the $\Delta\Delta\text{CT}$ method with RPL19 as a housekeeping gene¹⁷².

2.3.2 Western blot

Cells were seeded at a density of 200,000/well (SUM149) or 100,000/well (MCF7) in 6-well plates; or 2,000,000/dish (SUM149) in 100 mm culture dish, 48 hrs prior to being harvested; or 150,000/well (SUM149) 72 hrs prior to being harvested. Cells seeded 72 hours prior to harvest were treated for 48hrs with indicated concentrations of glutamine as described in the colony formation assay section, or treated with 8 Gray of ionising radiation 24 hrs prior to being harvested. On the day of harvesting, cells were washed with ice cold PBS once. Lysates used to detect BRCA1 were produced by immediately adding 200 μL radioimmunoprecipitation assay (RIPA) buffer supplemented with protease and phosphatase inhibitors (4 μg leupeptin, 4 μg pepstatin A, 2 mM Na_3VO_4 , 1 mM DL-Dithioereitol, 10 μM Calyculin A, 250 μM beta-glycerolphosphate, 400 μM PMSF) to the cells. Cells used to produce lysates for immunoblotting of other proteins were flash frozen in liquid nitrogen prior to lysing the cells with 50 μL of the same lysis buffer. In both cases, cells were detached using cell scraper and lysates were collected into 1.5 mL microcentrifuge tubes. Lysates were incubated on ice for 15 mins, sonicated for 10 seconds with a microtip sonicator, and cleared by centrifugation for 20 mins at 13.5k rpm at 4 °C. The resulting supernatant was collected and protein levels were quantified using Bio-Rad Protein Assay Dye Reagent Concentrate according to the manufacturer's instructions. For detection of HA-tagged BRCA1, 50 μg of proteins was loaded onto a NuPAGE™

3-8% Tris-Acetate Mini Protein Gel and resolved at 120V in NuPAGE™ Tris-Acetate SDS Running Buffer before being transferred onto an activated PVDF membrane using a wet transfer system at 20V overnight at 4 °C. The resulting membrane was blocked for 1 hour with 5% milk in Tris-buffered saline (TBS) with 0.2% Tween®20 (TBST) at room temperature and subsequently incubated overnight at 4 °C with HA-tag antibody diluted (1:1000) in 5% bovine serum albumin (BSA) in TBST. For immunoblotting of other proteins, 20 µg of proteins was loaded onto 4-15% Mini-PROTEAN® TGX Stain-Free™ Protein Gels and resolved at 200V before being transferred with Trans-Blot Turbo Mini 0.2 µm Nitrocellulose Transfer Packs using the Trans-Blot Turbo Transfer System (Bio-Rad) according to the manufacturer's instructions. The resulting membrane was blocked as described above and incubated overnight at 4 °C with the appropriate antibody diluted in 5% BSA in TBST. Following primary antibody incubation, all membranes were washed three times for 10 mins in TBST before being incubated with the appropriate secondary antibody diluted in 5% milk in TBST for one hour at room temperature. Subsequently, membranes were washed as described above, incubated with Clarity Max Western ECL Substrate, and images were acquire using the Azure 400 Imaging System (Azure Biosystems).

2.3.3 GSH measurement

Total GSH levels were measured using the GSH-Glo™ Glutathione Assay detection kit from Promega according to the manufacturer's instructions. Briefly, on the day before the assay, SUM149 cells were seeded at a density of 15,000/well in 100 µL in white 96-well plate. Cell culture media was removed and cells were

washed with 100 μ L PBS at room temperature before adding the 1X GSH-Glo™ Reagent, Luciferin Detection Reagent, and measuring luminescence as described in the manufacturer's protocol.

2.3.4 GDH1 activity measurement

GDH1 activity measurements were performed using the Glutamate Dehydrogenase Activity Assay Kit following the manufacturer's instructions. Briefly, one day before the assay, SUM149 cells were seeded onto a 6-well plate at density of 300,000/well. The next day, cells were washed with cold PBS and harvested on ice by scraping cells with 100 μ L of Assay Buffer. A volume of 50 μ L of lysates was loaded onto a clear 96-well plate to perform the assay following the manufacturer's protocol.

2.3.5 Ammonia measurement

Ammonia measurements were performed using the Ammonia Assay Kit following the manufacturer's instructions. Briefly, cells were prepared as described in the GDH1 activity measurements and harvested using Assay Buffer. A volume of 25 μ L of lysates was used to perform the assay following the manufacturer's protocol.

2.4 Flow cytometry

2.4.1 ROS measurements

ROS levels were assessed with flow cytometry using the CM-H2DCFDA probe according to the manufacturer's instructions. Briefly, SUM149 cells were seeded at a confluency of 200,000/well onto a 6-well plate. The next day, cells were treated for 48 hours with indicated glutamine concentrations. Following treatment, cells were stained with 5 μ M of CM-H2DCFDA probe diluted in PBS for 30 mins at 37 °C. After incubation, excess probe was removed and the cells were washed with 1 mL of PBS before being trypsinised and resuspended in 1 mL of Hank's Balanced Salt Solution (HBSS) supplemented with NucBlue™ Fixed Cell ReadyProbes™ Reagent (DAPI) according to the manufacturers' instructions. Samples were transferred to Falcon™ Round-Bottom tubes and FITC signal was quantified on the BD LSR II Flow Cytometer (BD Biosciences) using the BD FACS Diva software.

2.4.2 Annexin V assay

SUM149 cells were seeded at a density of 15,000/well in 100 μ L of cell culture media in a 96-well plate. The next day, cell culture media was replaced for Special Ham's F12 media with indicated concentrations of glutamine as described in the Dose Response Curves section and cells were allowed to grow for 48 hrs. On the day of the assay, the culture media from each well was transferred to a round bottom 96-well plate. Subsequently, cells were detached using 50 μ L of trypsin, resuspended using the respective cell culture media from each well, and transferred to a round bottom plate. A volume of 100 μ L of 3 μ g/mL propidium

iodide (PI), 1:100 dilution FITC Annexin V (AV), and 7.5 mM calcium chloride diluted in cell culture media was added to each well. Cells were quantified for FITC and PE Texas Red with the BD LSR II Flow Cytometer (BD Biosciences) with the 96-well plate adapter, and analysed using the BD FACS Diva software.

2.4.3 Cell cycle assay

SUM149 cells were seeded onto 25 cm² flasks at a density of 1,000,000/flask. The next day, cell culture media was replaced for Special Ham's F12 with indicated glutamine concentration following one wash with 5 mL PBS and cells were allowed to grow for 48 hrs. Prior to harvesting, the cells were incubated with 5 µM BrdU in PBS for 30 mins. To harvest the cells, cells were trypsinised and washed with PBS before being resuspended in 300 µL of cold PBS. Cells were fixed by adding 700 µL of cold ethanol and incubated at 4 °C overnight. The next day, cells were washed in PBS and resuspended in 10 mL of 0.5 mg/mL pepsin in 100 mM HCl solution and incubated at room temperature for 20 mins. Cells were then washed with blocking solution (0.5% Tween, 0.1% BSA in PBS) and incubated in 2 M HCl solution at 37 °C for 12 mins before 100 mM borate buffer pH 8.5 was added. Cells were centrifuged and incubated in blocking solution with anti-BrdU-FITC antibody for 2 hrs on ice. Finally, cells were washed once with blocking solution and resuspended in 200 µL of 20 µg/mL PI and 10 ng/mL RNase A in PBS. Samples were quantified for FITC and PE Texas Red signals using a BD LSR II Flow Cytometer (BD Biosciences) using the BD FACS Diva software.

2.5 Metabolic analyses

2.5.1 Seahorse Glyco and Mito Stress analysis

The Seahorse Glyco and Mito Stress tests were performed according to the manufacturer's instructions. Briefly, SUM149 cells were seeded at a confluency of 20,000/well in a 96-well Seahorse cell culture microplate and incubated in a 5% CO₂ incubator at 37 °C overnight. The next morning, culture media was replaced with pH-adjusted (pH = 7.4 ± 0.1) bicarbonate-free DMEM supplemented with 10 mM glucose, 1 mM sodium pyruvate, and 2 mM L-Glutamine for the Mito test or 2 mM L-Glutamine for the Glyco test. The plate was then incubated at 37 °C for 1 hr in a non-CO₂ incubator before being transferred to the Seahorse XFe96 Analyzer along with the loaded cartridge. Extracellular acidification rate (ECAR) and oxygen consumption rate (OCR) were measured at regular time intervals while the relevant compounds were injected for both tests. The compounds were diluted to obtain final concentrations in the wells of 10 mM glucose, 1 μM oligomycin, 0.5 μM FCCP, 0.5 μM Rotenone/Antimycin A (R/A), and 50 mM 2-deoxy-D-glucose (2-DG).

2.5.2 Mito Fuel Flex Analysis

The Mito Fuel Flex assays were performed according to the manufacturer's instructions. Briefly, cells were prepared as for the Mito and Glyco analysis described above, and media was replaced with the same culture media as for the Mito test. Following transfer of the plate and loaded cartridge into the Seahorse XFe96 Analyzer, OCR was measured over regular time intervals between appropriate inhibitor injections. For all conditions, inhibitors were diluted to obtain final concentrations in the wells of 3 μM BPTES, 4 μM Etomoxir, and 2 μM

UK5099. Glutamine, glucose, and fatty acid dependency and capacity were calculated based on the changes in OCR recorded following subsequent injections of relevant inhibitors following the formulas: Dependency (% Δ OCR pmol/min) = $(\text{Baseline OCR} - \text{Target inhibitor OCR} / \text{Baseline OCR} - \text{All inhibitors OCR}) * 100$; Capacity (% Δ OCR pmol/min) = $(1 - (\text{Baseline OCR} - \text{Other 2 inhibitors OCR} / \text{Baseline OCR} - \text{All inhibitors OCR})) * 100$.

2.5.3 Metabolite profiling

Three different liquid chromatography mass spectrometry (LC-MS) approaches were used to measure total metabolite levels: 1) data presented in Figure 4.5 were generated using the ICR core facility approach; 2) data presented in Figure 5.3C and 5.3B (AMP, UMP, xanthine) were generated using the Glasgow Polyomics approach; and 3) all other experiments were performed in collaboration with Dr. Gérald Larrouy-Maumus from Imperial College London. Nitrogen and carbon glutamine tracing experiments were performed using the Imperial College approach.

2.5.3.1 LC-MS ICR core facility

Cells were seeded onto 6-well plates at a density of 200,000/well 48hrs prior to extraction. On the day of extraction, the plates were placed on ice and the media was removed carefully. The cells were washed two times with cold PBS before addition of 1 mL extraction buffer (methanol/H₂O 8:2 v/v at - 80 °C). Cells were scrapped and transferred to 1.5 mL Eppendorf tubes. After centrifugation for 10

mins at 13,000 rpm at 4 °C, supernatants were evaporated to dryness and stored at -80 °C until LC-MS analysis.

Dried-down extracts were resuspended in 25 µL HPLC-grade water, and 1 µL was analysed using hydrophilic interaction chromatography coupled to tandem mass spectrometry analysis operated in the selected reaction monitoring mode (LC–SRM–MS). Analytical instruments used included a Nexera X2 (Shimadzu) liquid chromatography system with a XBridge BEH amide 2.1 × 100 mm, 2.5-µm column (Waters) and a QTRAP 6500 hybrid triple quadrupole/linear ion trap mass spectrometer (SCIEX) equipped with an electrospray ion source. Raw LC–SRM–MS data were acquired with Analyst 1.6.2 (SCIEX) and peak areas of LC–SRM–MS traces for each metabolite were integrated using MultiQuant 1.1 software (SCIEX).

2.5.3.2 LC-MS Glasgow Polyomics

Cells were seeded onto 6-well plates at a density of 200,000/well 48hrs prior to extraction. On the day of extraction, the plates were placed on ice and the media was removed carefully. The cells were washed with cold PBS before addition of 400 µL extraction buffer (chloroform/methanol/H₂O, 1:3:1 v/v/v at -20 °C). Plates were incubated at 4 °C for 1 hr with agitation then cell extracts were collected and centrifuged for 10 mins at 13,000 rpm at 4 °C and supernatant was used for LC-MS analysis.

Hydrophilic interaction liquid chromatography (HILIC) was carried out on a Dionex UltiMate 3000 RSLC system (Thermo Fisher) using a ZIC-pHILIC column (150 mm × 4.6 mm, 5 µm column, Merck Sequant). The column was maintained at 40°C and samples were eluted with a linear gradient (20 mM ammonium carbonate in water, A and acetonitrile, B) over 26 min at a flow rate of 0.3 mL/min. The injection volume was 10 µL and samples were maintained at 5°C prior to injection. For the MS analysis, a Thermo Orbitrap Fusion (Thermo Fisher) was operated in polarity switching mode and the MS settings were as follows: Resolution: 120,000; AGC: 2e5; m/z range: 70–1000; Sheath gas: 40; Auxiliary gas: 5; Sweep gas: 1; Probe temperature: 150°C; Capillary temperature: 325°C. Source voltage was +4.3 or -3.2 kV for positive and negative mode ionisation respectively. S-Lens RF level 60%. Fragmentation was performed with the following parameters: Collision energy: 60%; Stepped collision energy: 35%; Isolation window: 2; Dynamic exclusion after 1 time; Exclusion duration: 6 seconds; Exclude isotopes: true; Minimum intensity: 50000. The instrument was calibrated to standard operating parameters prior to sample run. To enhance calibration stability, lock-mass correction was also applied to each analytical run. Positive Mode Lock masses: Number of Lock Masses: 1 Lock Mass #1 (m/z): 144.9821 Negative Mode Lock masses: Number of Lock Masses: 1 Lock Mass #1 (m/z): 135.971.

Instrument .raw files were converted to positive and negative ionisation mode mzXML files. These files were then analysed using IDEOM, mzMatchISO and PiMP (Gloaguen 2017) with the FrAnK in-house fragmentation data analysis software.

2.5.3.3 LC-MS Imperial College London

Cells were seeded onto 6-well plates at a density of 200,000/well 48hrs prior to extraction. For ¹⁵N- or ¹³C-labeled glutamine tracing experiments, the media was changed for the appropriate media supplemented with 0.5 mM L-glutamine (13C5, 99%) or L-glutamine (15N2, 98%) and 0.5 mM unlabelled glutamine 24 hrs prior to metabolite extraction. On the day of extraction, the plates were placed on ice and the media was removed carefully. The cells were washed three times with cold PBS before the addition of 1 mL extraction buffer (acetonitrile/methanol/H₂O, 40:40:20 v/v/v at -20 °C). Cells were then scrapped and transferred into an Eppendorf vial. A 100 µL aliquot of the metabolite solution was then mixed with 100 µL of acetonitrile with 0.2 % acetic acid at -20°C, and centrifuged for 10 mins at 13,000 rpm at 4°C. The final concentration of 70% acetonitrile was compatible with the starting conditions of the HILIC chromatography. The supernatant was then transferred into an LC/MS V-shape vials and 4 µL was injected into the LC/MS.

Aqueous normal phase liquid chromatography was performed using an Agilent 1290 Infinity II LC system equipped with a binary pump, temperature-controlled auto-sampler (set at 4°C) and temperature-controlled column compartment (set at 25°C) containing a Cogent Diamond Hydride Type C silica column (150 mm × 2.1 mm; dead volume 315 µL). A flow rate of 0.4 mL/min was used. Elution of polar metabolites was carried out using solvent A consisting of deionized water (resistivity ~18 MΩ cm) and 0.2% acetic acid and solvent B

consisting of 0.2% acetic acid in acetonitrile. The following gradient was used: 0 min 85% B; 0-2 min 85% B; 3-5 min to 80% B; 6-7 min 75% B; 8-9 min 70% B; 10-11 min 50% B; 11.1-14 min 20% B; 14.1-25 min hold 20% B followed by a 5 min re-equilibration period at 85% B at a flow rate of 0.4 mL/min. Accurate mass spectrometry was carried out using an Agilent Accurate Mass 6545 QTOF apparatus. Dynamic mass axis calibration was achieved by continuous infusion, post-chromatography, of a reference mass solution using an isocratic pump connected to an ESI ionization source operated in the positive-ion mode. The nozzle voltage and fragmentor voltage were set at 2,000 V and 100 V, respectively. The nebulizer pressure was set at 50 psig, and the nitrogen drying gas flow rate was set at 5 L/min. The drying gas temperature was maintained at 300 °C. The MS acquisition rate was 1.5 spectra/sec, and m/z data ranging from 50-1,200 were stored. This instrument enabled accurate mass spectral measurements with an error of less than 5 parts-per-million (ppm), mass resolution ranging from 10,000-45,000 over the m/z range of 121-955 atomic mass units, and a 100,000-fold dynamic range with picomolar sensitivity. The data were collected in the centroid 4 GHz (extended dynamic range) mode. Detected m/z were deemed to be identified metabolites on the basis of unique accurate mass-retention time and MS/MS fragmentation identifiers for masses exhibiting the expected distribution of accompanying isotopomers. Typical variation in abundance for most of the metabolites remained between 5 and 10% under these experimental conditions.

For labelling experiments, the fractional enrichment for each metabolite was determined by dividing the peak height ion intensities of each labelled species by

the ion intensities of both labelled and unlabelled species using the software Agilent Profinder version B.8.0.00 service pack 3. For total metabolite levels, peak height ion intensities for each metabolite were determined using the software Agilent Profinder version B.8.0.00, and normalized to total protein levels measured via BCA assay following the manufacturer's instructions. Media metabolite levels were determined by subtracting the blank media peak height ion intensities for each metabolite to each sample's peak height ion intensities and dividing by the blank peak height ion intensities for each metabolite. Negative values represent net metabolite consumption from the media while positive values represent net secretion into the media.

2.6 Statistical Analysis

Data were analysed by *t*-test with or without FDR correction, 1-way or 2-way analysis of variance (ANOVA) followed by Dunnett's or Sidak's multiple comparisons test, or non-linear regression analysis, as indicated in the figure legends. Total metabolite levels and mRNA levels were normalised to control group. All bar charts represent mean \pm SEM for each group. Unless otherwise indicated, statistical analyses were performed using GraphPad Prism 6. FDR corrected *p*-values and fold change for each metabolic pathway in the metabolite enrichment analysis were performed using MetaboAnalyst 3.0 and values were plotted using R.

3 Identification and characterisation of metabolic vulnerabilities in *BRCA1* mutant breast cancer

Since *BRCA1* mutations are enriched in TNBC and basal-like breast cancer, we chose to investigate the effect of *BRCA1* mutations on metabolism in the previously described *BRCA1* mutant (c.2288delT, p.N723fsX13) TNBC SUM149 cell line, hereafter referred to as BRCA1-mutant¹⁷³, and its functionally restored *BRCA1* secondary mutant isogenic equivalent, hereafter referred to as BRCA1-restored¹⁷⁴. For each genotype (i.e. BRCA1-mutant and BRCA1-restored), three clones that were cultured separately were used across all experiments and consolidated under the relevant genotype unless specified otherwise. All BRCA1-mutant clones harbour the same frameshift mutation which leads to the introduction of an early stop codon, however, one clone expresses Cas9 while the other expresses Dox-inducible Cas9. On the other hand, the three BRCA1-restored clones harbour different mutations (1.1: 99-bp deletion, c.[2212del99]; 1.5: 95-bp deletion, c.[2150del95; 2288delT] ; 2.5: 80-bp deletion, c.[2288delT; 2293del80]) that restore the reading frame of the BRCA1-mutant parental cell line and lead to a functional BRCA1 protein¹⁷⁴. Of note, the secondary mutations lead to a loss of 33, 32, or 27 amino acids respectively that do not disrupt BRCA1 function.

3.1 Glycolytic capacity as well as glutamine and fatty acid dependencies are increased in BRCA1-mutant cells

As an initial step to investigate the changes in metabolism caused by manipulations in *BRCA1*, we first probed for changes in mitochondrial respiration and glycolysis using the Seahorse XFe96 Analyzer which allows real-time

measurements of OCR and ECAR. To investigate mitochondrial respiration, we measured OCR over time while manipulating the ETC with sequential injections of: ATP synthase inhibitor, oligomycin; oxidative phosphorylation uncoupler, FCCP; and complex I and III inhibitors, rotenone and antimycin A, respectively. Unlike previous studies^{91,93}, we did not observe any changes in basal or maximal respiration rate in BRCA1-mutant cells (Figure 3.1A). We took a similar approach to measure changes in glycolysis by measuring ECAR over time while manipulating cell metabolism with sequential injections of glucose, oligomycin, and glucose analogue, 2-DG, which cannot be metabolised. While basal glycolysis rate was similar between both genotypes after glucose injection, we observed a more pronounced increase in ECAR in BRCA1-mutant cells following oligomycin injection, which suggests an increased glycolytic capacity consistent with previous reports (Figure 3.1B)⁹³.

To further probe for metabolic differences, we examined the changes in dependency and capacity to the main metabolic substrates of the TCA cycle: glucose, glutamine, and fatty acid. We measured real-time OCR levels with the Seahorse XFe96 Analyzer and assessed the dependency of mitochondrial respiration to each of the substrates following inhibition with the relevant inhibitors (glucose: UK5099, glutamine: BPTES, fatty acid: etomoxir). While glucose dependency was unchanged, we observed increased glutamine and fatty acid dependency in BRCA1-mutant cells (Figure 3.1C-E).

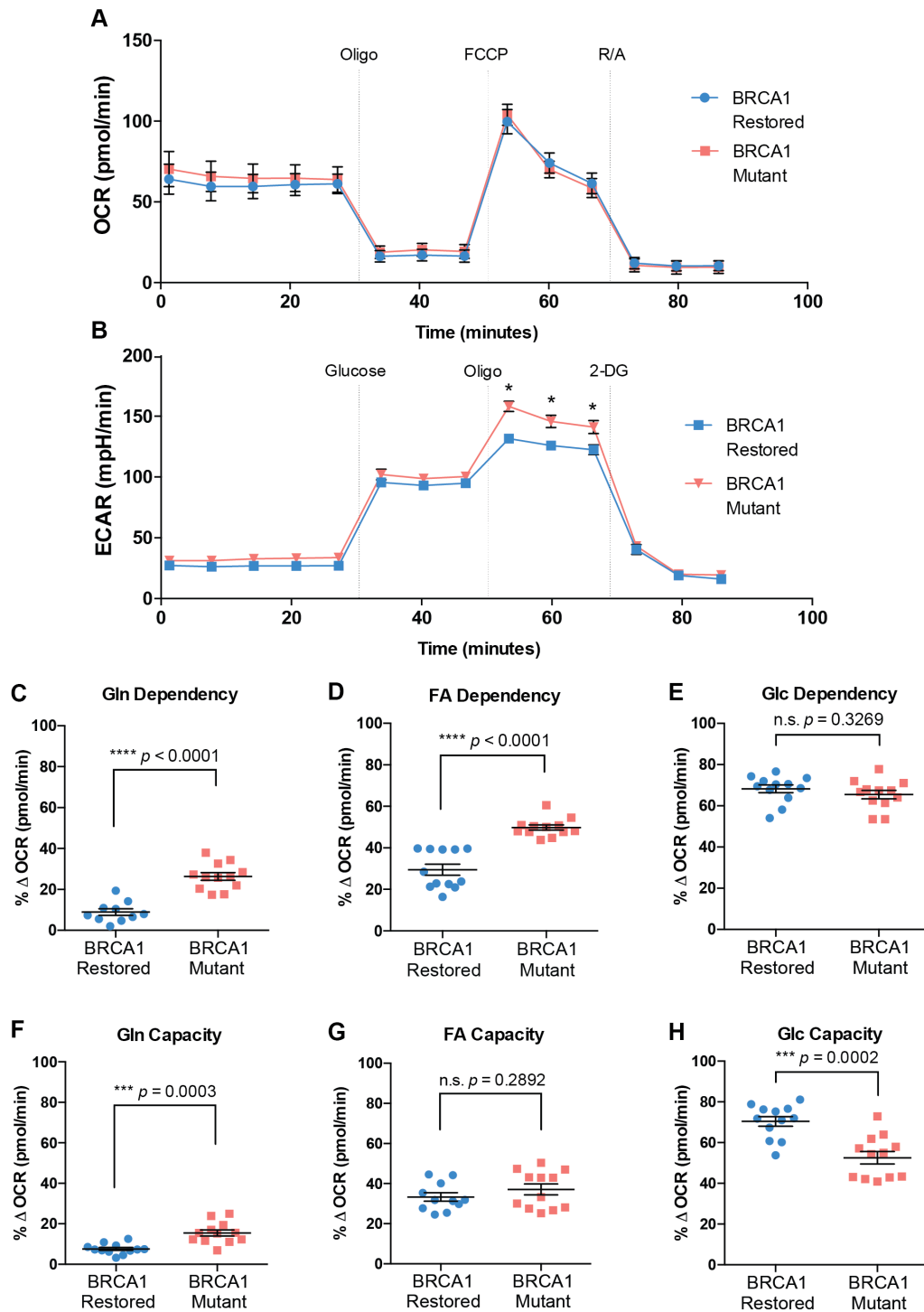


Figure 3.1 - BRCA1-mutant cells have increased glycolytic capacity as well as increased glutamine and fatty acid dependencies

(A) Oxygen consumption rate (OCR) of SUM149 BRCA1-restored (blue) or -mutant (red) cells measured over time using the Seahorse XFe96 Analyzer following injections of oligomycin

(oligo), FCCP, and rotenone/antimycin A (R/A) as indicated. Data is presented as mean \pm SEM (n = 6), and analysed by 2-way ANOVA and Sidak's multiple comparisons test.

(B) Extracellular acidification rate (ECAR) of SUM149 BRCA1-restored or -mutant cells measured over time using the Seahorse XFe96 Analyzer following injections of glucose, oligo, and 2-deoxy-D-glucose (2-DG) as indicated. Data is presented as mean \pm SEM (n = 6), and analysed by 2-way ANOVA and Sidak's multiple comparisons test (* $p < 0.0001$).

(C-H) Percentage change in OCR of SUM149 BRCA1-restored or -mutant cells following injections of relevant inhibitors used to determine (C) glutamine (Gln), (D) fatty acid (FA), or (E) glucose (Glc) dependency, or (F) Gln, (G) FA, or (H) Glc capacity using the Mito Fuel Flex test and the Seahorse XFe96 Analyzer according to the manufacturer's instructions. Data is presented as mean \pm SEM, and analysed by *t*-test.

Interestingly, glucose dependency was the highest of the three substrates suggesting that SUM149 cells rely mostly on glucose derivatives to support mitochondrial respiration, however, this was not affected by loss-of-function of BRCA1. Additionally, fatty acid capacity was unchanged between both genotypes, and there was a small, but significant, increase in glutamine capacity and a reduction in glucose capacity in BRCA1-mutant cells (Figure 3.1F-H). While these data support the hypothesis that BRCA1 plays a role in metabolism, they focus on glycolysis and mitochondrial respiration only and do not identify any specific metabolic vulnerabilities.

3.2 BRCA1-mutant cells have increased sensitivity to glutamine but not glucose deprivation

To test whether the metabolic changes observed lead to metabolic vulnerabilities, we measured cell proliferation following removal of specific nutrients from the cell culture media. Since glutamine was the only TCA cycle substrate to show increased dependency and capacity in BRCA1-mutant cells (Figure 3.1C and F), and its role in cancer metabolism is well established, we explored sensitivity to glutamine deprivation. The SUM149 cells are normally maintained under 1 mM

glutamine conditions. As such, we cultured BRCA1-mutant and BRCA1-restored cells for 5 days under decreasing concentrations of glutamine starting with 1 mM as the highest concentration. While glutamine deprivation led to reduced cell proliferation for both genotypes, the effect was more pronounced in BRCA1-mutant cells (Figure 3.2A). In line with this, we also observed an increase in glutamine uptake from the cell culture media in BRCA1-mutant cells (Figure 3.2B) paired with an overall reduction of intracellular glutamine (Figure 3.2C), which suggested an increase in downstream glutamine usage. Importantly, this differential sensitivity to nutrient removal was specific to glutamine since withdrawal of glucose from the media led to a sharp reduction in proliferation that was, however, equivalent across both genotypes (Figure 3.2D).

To confirm that the phenotype observed was due to changes in *BRCA1* mutation status and not an artefact resulting from the selection process used when generating the cell lines, we stably overexpressed HA-tagged wild-type BRCA1 (HA-BRCA1) in the BRCA1-mutant cells and tested the sensitivity to glutamine deprivation. As expected, cell lines expressing the HA-BRCA1 became more resistant to glutamine withdrawal as compared to their counterpart expressing the empty vector (Figure 3.2E and F). Additionally, using shRNA to repress *BRCA1* expression in BRCA1-restored cells also led to an increased sensitivity to glutamine deprivation, albeit to a lesser extent (Figure 3.2H and I). Finally, repression of *BRCA1* mRNA expression in luminal breast cancer MCF7 cells led to a similar effect as the one observed in SUM149 cells (Figure 3.2J and K),

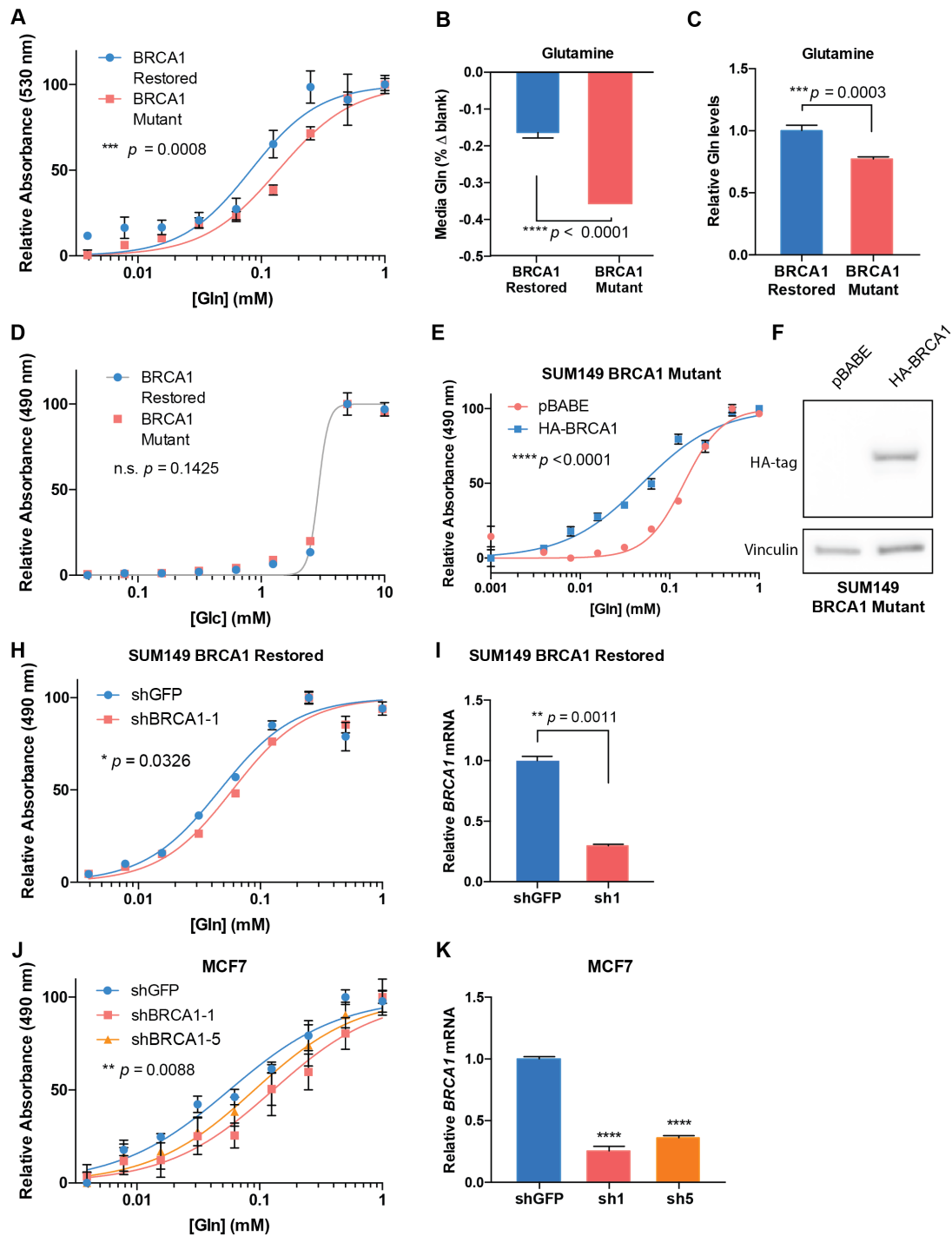


Figure 3.2 - BRCA1-mutant cells have increased sensitivity to glutamine, but not glucose deprivation

(A) Cell density of SUM149 BRCA1-restored (blue) or -mutant (red) cells grown for 5 days under indicated glutamine (Gln) concentrations and quantified using Sulforhodamine B staining. Data is presented as mean \pm SEM ($n = 6$), and analysed by non-linear regression.

(B-C) LC-MS quantification of SUM149 BRCA1-restored or -mutant Gln (B) cell culture media levels expressed as % change of blank media, or (C) relative intracellular levels. Data is presented as mean \pm SEM (n = 12), and analysed by *t*-test.

(D) Cell density of SUM149 BRCA1-restored or -mutant cells grown for 5 days under indicated glucose (Glc) concentrations and quantified using CellTiter 96® AQ_{ueous} One Solution according to the manufacturer's instructions. Data is presented as mean \pm SEM (n = 6), and analysed by non-linear regression.

(E) Cell density of SUM149 parental BRCA1-mutant cells stably overexpressing wild-type HA-BRCA1 construct (blue) or pBABE vector control (red) grown as in (A) and quantified and analysed as in (D).

(F) Immunoblot for HA and vinculin using lysates extracted from cells in (E).

(H) Cell density of SUM149 BRCA1-restored cells stably expressing shRNA against GFP (blue) or BRCA1 (red) grown and analysed as in (E).

(I) RT-qPCR quantification of *BRCA1* mRNA extracted from cells in (H). Data is presented as mean \pm SEM (n = 3), and analysed by *t*-test.

(J) Cell density of MCF7 cells stably expressing shRNA against GFP (blue) or BRCA1 (red and orange) grown and analysed as in (E).

(K) RT-qPCR quantification of *BRCA1* mRNA extracted from cells in (J). Data is presented as mean \pm SEM (n = 3), and analysed by Dunnett's test (**** $p < 0.0001$).

suggesting that the glutamine deprivation sensitivity phenotype is not specific to SUM149 cells.

3.3 BRCA1-mutant cells exhibit increased sensitivity to glutamine inhibitors

To further characterize the glutamine sensitivity phenotype, we investigated the changes in proliferation following treatment with increasing doses of the glutamine antagonist, DON, or the inhibitor BenSer, which blocks the main glutamine transporter SLC1A5. As expected, proliferation of cells from both genotypes was affected, however, similarly to glutamine deprivation, treatment with DON or BenSer led to a more rapid reduction in proliferation in the BRCA1-mutant cells (Figure 3.3A and B). Additionally, we tested whether transient inhibition of *BRCA1* expression with siRNA was enough to reproduce the sensitivity to DON. Indeed, BRCA1-restored cells treated with siRNA against *BRCA1* prior to

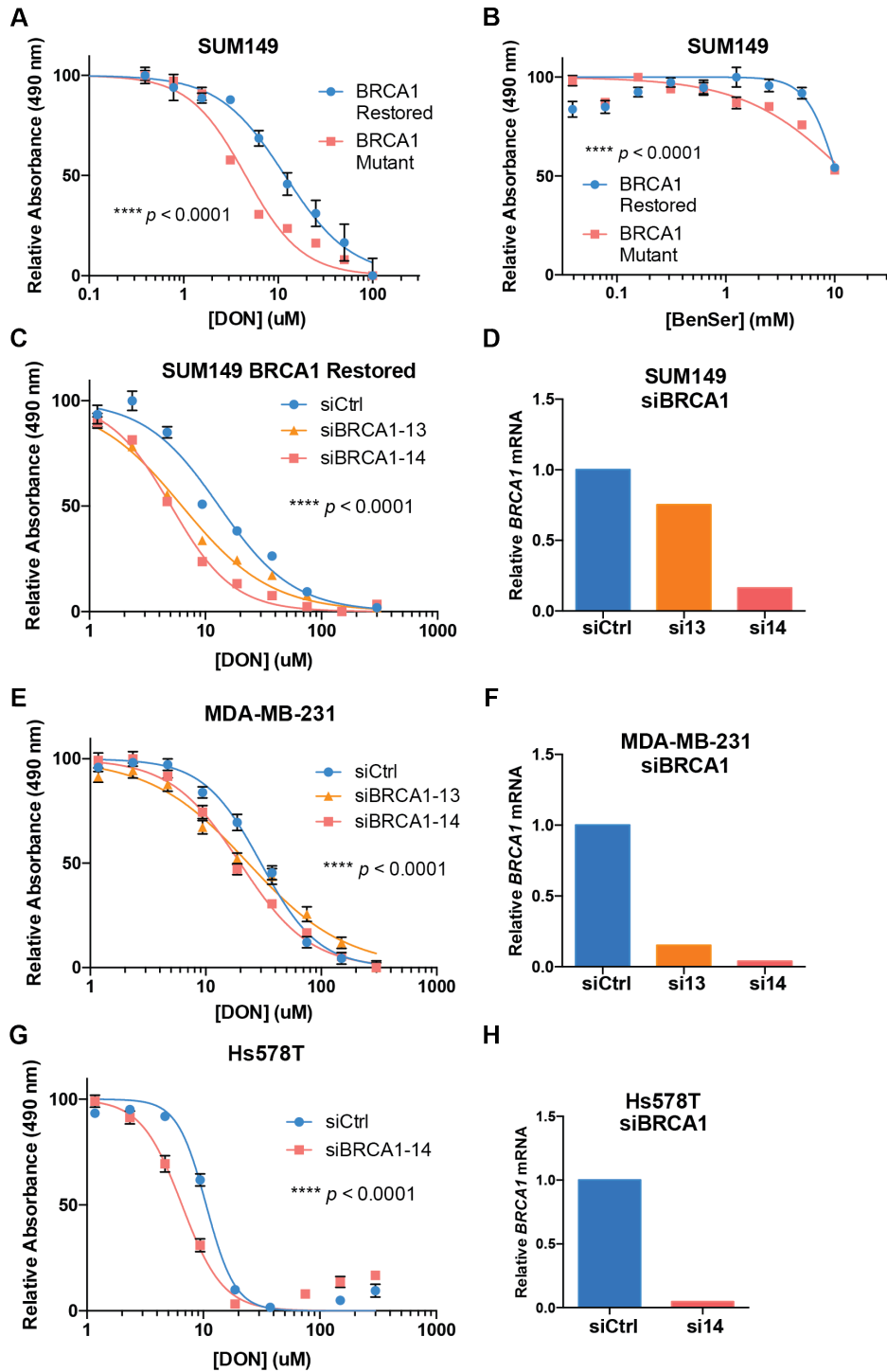


Figure 3.3 - BRCA1-mutant cells exhibit increased sensitivity to glutamine inhibitors

(A-B) Cell density of SUM149 BRCA1-restored (blue) or -mutant (red) cells grown for 5 days under indicated (A) DON or (B) BenSer concentrations and quantified using CellTiter 96® AQ_{ueous}

One Solution according to the manufacturer's instructions. Data is presented as mean \pm SEM (n = 6), and analysed by non-linear regression.

(C) Cell density of SUM149 BRCA1-restored cells grown for 3 days under indicated concentrations of DON 48 hrs following transient transfection with control siRNA (siCtrl, blue) or siRNA against *BRCA1* (red and orange), and quantified using CellTiter 96® AQ_{ueous} One Solution. Data are presented as mean \pm SEM (n = 6), and analysed by non-linear regression.

(D) RT-qPCR quantification of *BRCA1* mRNA extracted from cells in (C), (n = 1).

(E-G) Cell density and RT-qPCR quantification of *BRCA1* mRNA extracted from (E-F) MDA-MB-231 or (G-H) Hs578T cells grown and analysed as in (C-D).

treatment with DON over 3 days showed increase sensitivity to DON (Figure 3.3C and D). These findings were also reproduced in two other TNBC cell lines, MDA-MB-231 and Hs578T (Figure 3.3E-H).

3.4 Cell proliferation and clonogenic potential is increased in BRCA1-mutant cells and altered by glutamine withdrawal

The simplest explanation for an increase in nutrient consumption and sensitivity to withdrawal, is an increase in cell proliferation rate, which ultimately leads to a higher need for anabolic reactions. Although the phenotype observed in BRCA1-mutant cells appears to be specific to glutamine and not glucose, we decided to investigate the effect of BRCA1 loss-of-function on the proliferation rate. Interestingly, we found that BRCA1-mutant cells had a small but significant increase in cell proliferation over 4 days which was abrogated by withdrawal of glutamine (Figure 3.4A).

Next, we examined the proliferation and clonogenic potential of BRCA1-mutant cells using colony formation assays. After 12 days of incubation under normal glutamine (1 mM) conditions, we saw a marked increase in BRCA1-mutant cells total area and colony numbers, consistent with an increase in cell proliferation

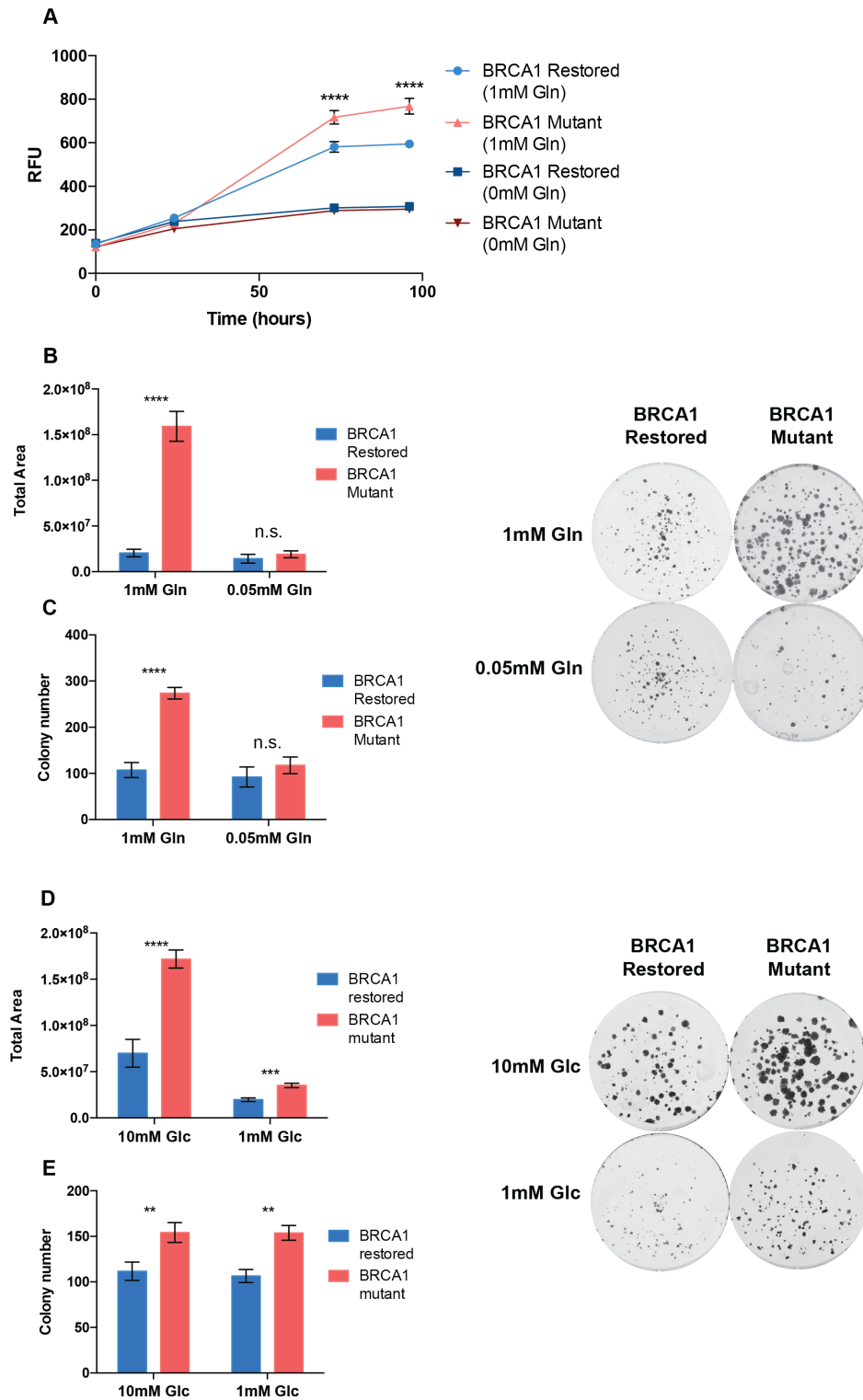


Figure 3.4 - Cell proliferation and clonogenic potential is increased in BRCA1-mutant cells and altered by glutamine withdrawal

(A) Cell density over 4 days of SUM149 BRCA1-restored (blue) or -mutant (red) cells grown under indicated glutamine concentrations and quantified using CyQUANT according to the

manufacturer's instructions. Data is presented as mean \pm SEM ($n = 6$), and analysed by 2-way ANOVA and Tukey's multiple comparisons test. RFU = relative fluorescence unit.

(B-C) Representative images and quantification of (B) total area and (C) colony number of SUM149 BRCA1-restored or -mutant cells grown for 12 days under indicated glutamine concentrations as part of a clonogenic assay and stained with crystal violet. Data is presented as mean \pm SEM ($n = 9$), and analysed by 2-way ANOVA and Sidak's multiple comparisons test.

(D-E) Same assay and analysis as in (B-C) but performed under indicated glucose concentrations.

(**** $p < 0.0001$; *** $p < 0.001$; ** $p < 0.01$; * $p < 0.05$)

as a result of BRCA1 mutation, while also suggesting an increase in clonogenic potential. On the other hand, cells grown under low glutamine (0.05 mM) conditions formed significantly less colonies and had lower total area measurements which were similar between both genotypes (Figure 3.4B and C). Using the same assay to investigate the role of glucose in proliferation and clonogenic potential, we observed a reduction in total area as a result of low glucose (1 mM) concentration, however, this reduction was proportional to the total area of cells grown under normal glucose (10 mM) conditions for both genotypes (Figure 3.4D). Moreover, while the number of colonies was higher in BRCA1-mutant cells, as seen previously, glucose withdrawal did not affect the number of colonies (Figure 3.4E). Together, these data suggest that while both glucose and glutamine are essential for cell proliferation, BRCA1-mutant cells appear to have a specific affinity for glutamine. Additionally, glutamine appears to be particularly important to sustain the increased clonogenic potential of BRCA1-mutant cells.

3.5 Glutamine deprivation-induced cell cycle arrest and cell death are more pronounced in BRCA1-mutant cells

To refine our understanding of how BRCA1 loss-of-function affects cell proliferation, we examined the effect of glutamine withdrawal on cell cycle and cell

viability following 48hrs incubation under low glutamine (0.1 mM) conditions. For cell cycle analysis, we measured the incorporation of BrdU in combination with PI staining to identify the cycling stage of the cells analysed. We found that low glutamine led to an increase of cells in G1 combined with a reduction of cells in S and G2 (Figure 3.5A and B). Taken together with the proliferation data presented earlier (Figure 3.4A), this suggests a blockage of cells in G1 under low glutamine.

While it is clear that glutamine withdrawal affects proliferation, we wanted to test whether the phenotype observed was due to a cytotoxic, as opposed to only a cytostatic effect. Therefore, we stained the cells with PI and the apoptosis marker Annexin V and used flow cytometry to separate the cells based on their staining profiles. We observed that low glutamine led to an increase of apoptotic cells (Q2) and a reduction in live cells (Q3) across both genotypes (Figure 3.6A and B). However, the changes observed were more pronounced in BRCA1-mutant compared to BRCA1-restored cells.

3.6 Chapter discussion

Consistent with previous reports, the data presented in this chapter clearly support the claims that BRCA1 is involved directly or indirectly in metabolic regulation. More specifically, BRCA1 loss-of-function leads to increased sensitivity to glutamine deprivation, which is expressed through reduced proliferation and increased cell death. Although BRCA1-mutant cells proliferate faster, our data suggests that this increased proliferation rate alone does not explain the higher glutamine consumption as glucose withdrawal causes similar changes in both

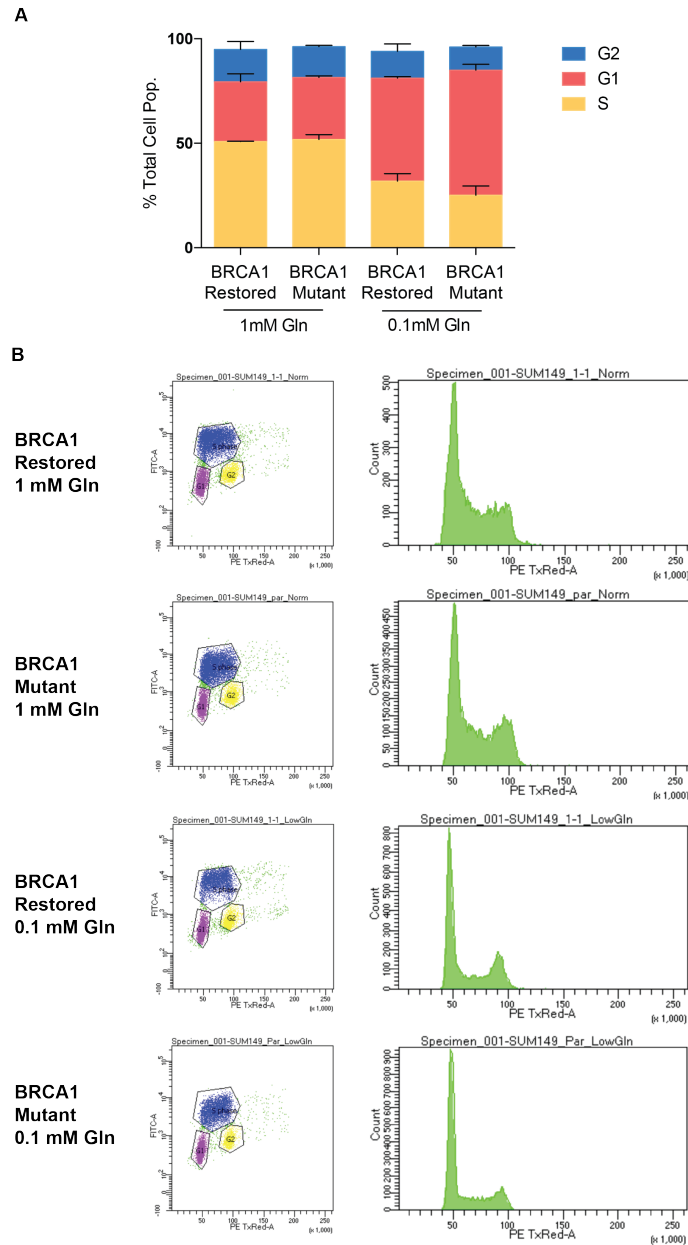


Figure 3.5 - Glutamine deprivation-induced cell cycle arrest is more pronounced in BRCA1-mutant cells

(A) Classification of cell cycle stage (G1: red, G2: blue, or S: yellow) of SUM149 BRCA1-restored or -mutant cell populations based on propidium iodide (PI) and BrdU co-staining measured by flow cytometry. Cells were grown under indicated glutamine (Gln) concentrations for 48 hours prior to the staining. Data is presented as mean \pm SEM ($n = 3$), and G1 fraction was analysed by 2-way ANOVA (Interaction: * $p = 0.0201$; Genotype: ** $p = 0.0082$; Treatment: **** $p < 0.0001$). (B) Representative images of flow cytometry scatter for each condition described in (A). Images demonstrate clustering of each group based on PI staining (PE TxRed-A) and BrdU staining (FITC-A).

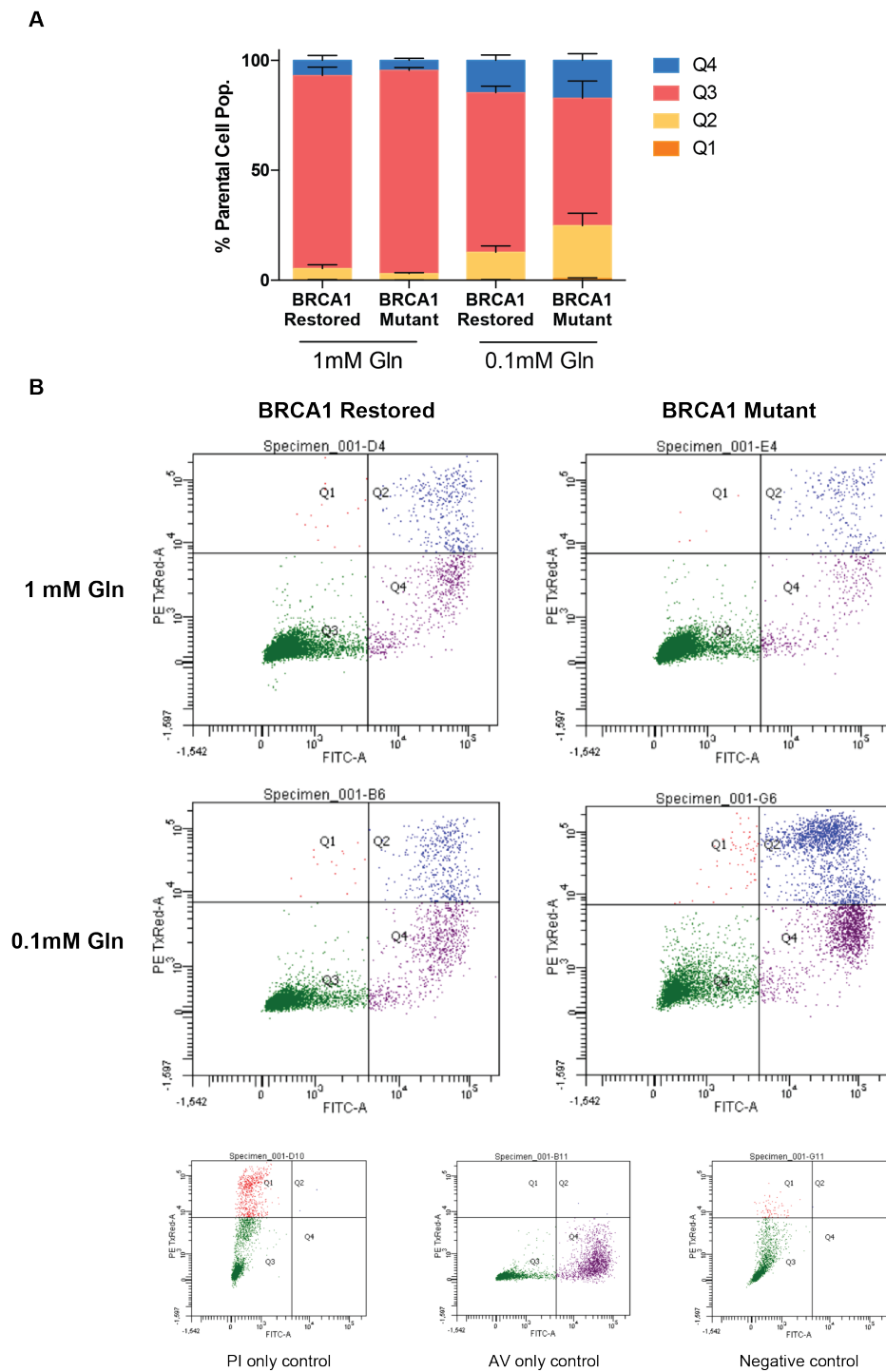


Figure 3.6 - Glutamine deprivation-induced apoptosis is more pronounced in BRCA1-mutant cells

(A) Classification of cell viability (Q1: necrotic, Q2: apoptotic, Q3: live, Q4: pre-apoptotic) of SUM149 BRCA1-restored or -mutant cell populations based on Annexin V (AV) and propidium iodine (PI) co-staining measured by flow cytometry. Cells were grown under indicated glutamine (Gln) concentrations for 48 hours prior to the staining. Data is presented as mean \pm SEM ($n =$

12), and Q2 fraction was analysed by 2-way ANOVA (Interaction: **** $p < 0.0001$; Genotype: **** $p < 0.0001$; Treatment: **** $p < 0.0001$).

(B) Representative images of flow cytometry scatter for each condition described in (A). Images demonstrate clustering of each group based on PI staining (PE TxRed-A) and AV staining (FITC-A). Bottom 3 panels represent staining controls: PI only, AV only, and unstained controls from left to right respectively.

genotypes. Of note, glucose and glutamine can be interchanged as main substrates of the TCA cycle and the dependency to both substrates is highly variable between cancer types. Therefore, multiple factors, both intrinsic and extrinsic, most likely dictate the metabolic needs of the cells. As such, cells grown at low density for a colony formation assay could potentially have different metabolic needs than cells grown under more confluent conditions. This could also explain why some of the metabolic changes that we observed are consistent with the literature, while others are conflicting. Nevertheless, the phenotype identified and characterised in this chapter provides a solid base to investigate the role of BRCA1 in metabolism further. Therefore, the next chapter will build onto the current phenotype and explore the potential roles of glutamine in breast cancer.

4 Exploration of the roles of glutamine in breast cancer and their importance in *BRCA1* mutant cells

As discussed in Chapter 3, *BRCA1*-mutant cells display increased glutamine consumption and sensitivity to glutamine deprivation, suggesting that reprogramming of glutamine metabolism is crucial for the tumour suppressor activity of *BRCA1* mutations. Glutamine is essential for a wide range of cell functions including synthesis of proteins, NEAA, GSH, GABA, and nucleotides, while also providing a fuel source for the TCA cycle. The data presented in this chapter explores the roles of glutamine in breast cancer and attempts to decipher which pathways are most important in *BRCA1*-mutant cells.

4.1 Glutaminolysis is similar between *BRCA1*-mutant and -restored cells

As a starting point to study the role of glutamine in *BRCA1*-mutant cells, we examined anaplerosis, the most well-described glutamine function in cancer. Briefly, anaplerosis is the process through which glutamine-derived carbons are used to refuel the TCA cycle via processing of glutamate into α KG. First, we set out to investigate whether there were changes in glutaminolysis. We measured the mRNA expression levels of the key enzymes of glutaminolysis, GLS1 and GDH1, and found no significant differences between the two genotypes (Figure 4.1A and B). Next, we tested whether inhibition of GLS1 could reproduce the glutamine deprivation sensitivity phenotype observed in *BRCA1*-mutant cells. Similarly for both genotypes, treatment with increasing doses of GLS1 inhibitors BPTES and CB-839 did not affect, or only mildly affected cell proliferation and survival when cells were grown over 5 days from approximately 10-70% confluency in 96-well

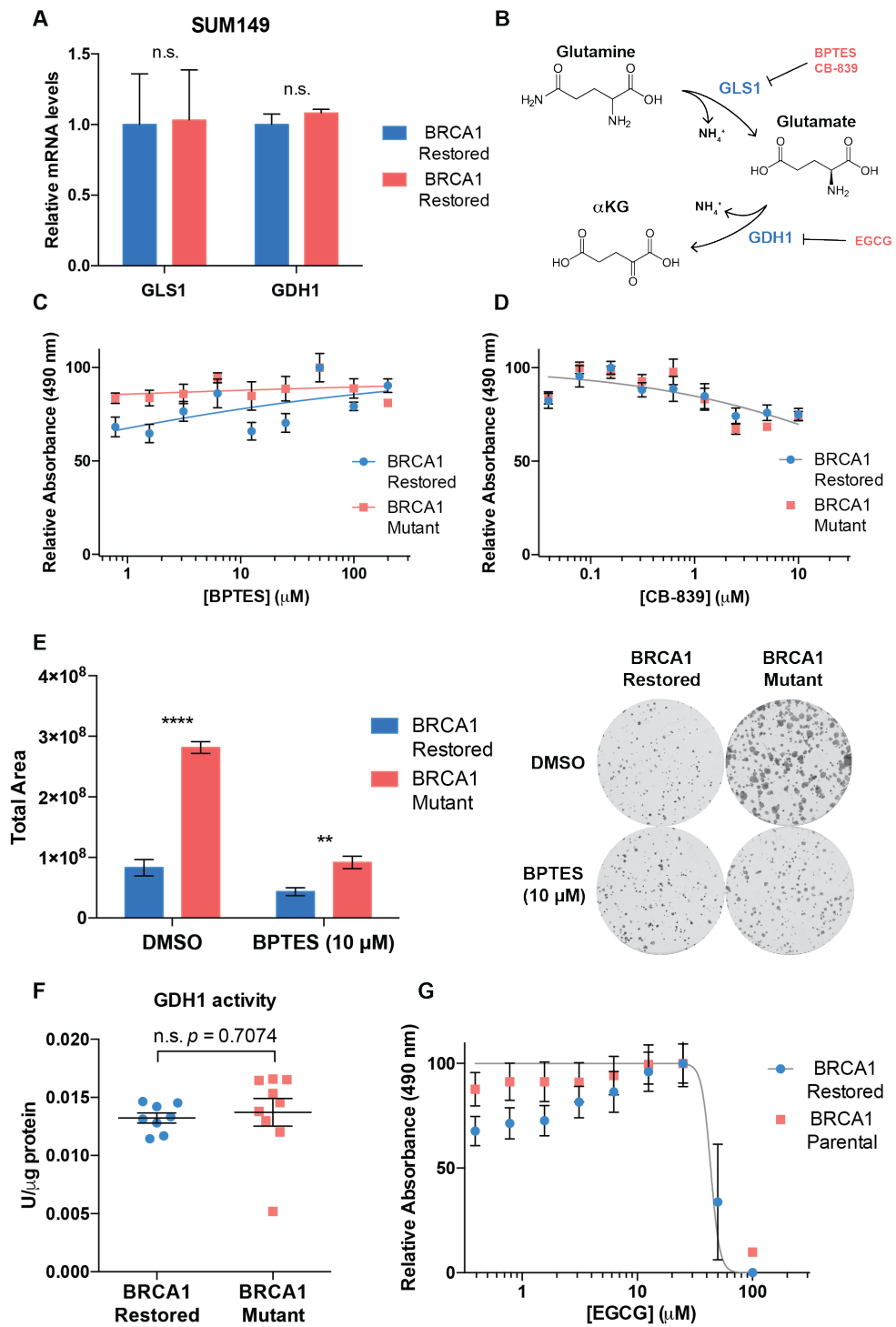


Figure 4.1 - Glutaminolysis is equivalent between BRCA1-mutant and restored cells

(A) RT-qPCR quantification of indicated mRNA extracted from SUM149 BRCA1-restored (blue) or -mutant (red) cells. Data is presented as mean \pm SEM ($n = 6$), and analysed by *t*-test with FDR correction ($Q = 1\%$).

(B) Schematic representation of glutamine processing through glutaminolysis with relevant enzymes (blue) and inhibitors (red) indicated.

(C-D) Cell density of SUM149 BRCA1-restored or -mutant cells grown for 5 days under indicated (C) BPTES or (D) CB-839 concentrations and quantified using CellTiter 96® AQueous One Solution according to the manufacturer's instructions. Data is presented as mean \pm SEM (n = 6), and analysed by non-linear regression.

(E) Representative images and quantification of total area of SUM149 BRCA1-restored or -mutant cells grown for 12 days under 10 μ M BPTES or DMSO control as part of a clonogenic assay and stained with crystal violet. Data is presented as mean \pm SEM (n = 9), and analysed by 2-way ANOVA and Sidak's multiple comparisons test.

(F) GDH1 activity in SUM149 BRCA1-restored or -mutant lysates measured via Glutamate Dehydrogenase Activity Assay Kit following manufacturer's instructions and normalised to total amount of protein. Data was analysed by *t*-test.

(G) Cell density of SUM149 BRCA1-restored or -mutant cells grown for 5 days under indicated EGCG concentrations in pyruvate-free media and quantified and analysed as in (C). (**** $p < 0.0001$; *** $p < 0.001$; ** $p < 0.01$; * $p < 0.05$)

plates (Figure 4.1B-D). However, in clonogenic assays where 1,000 cells/well were seeded in 6-well plates, 10 μ M BPTES treatment lead to a reduction in total area similar to glutamine deprivation, albeit to a lesser extent (Figure 3.4B and 4.1E). Finally, we examined the role of GDH1 in BRCA1-mutant cells. The enzymatic activity of GDH1 was unchanged between the two genotypes (Figure 4.1F), and cells were equally sensitive to GDH1 inhibitor EGCG (Figure 4.1G). Of note, although SUM149 cells are normally grown in pyruvate-containing media, EGCG dose response curves were performed in the absence of pyruvate as cells did not respond to the drug treatment in the presence of pyruvate. While manipulations of the canonical glutaminolysis pathway affected the growth of SUM149 cells, there were no clear differences between BRCA1-mutant and their restored counterparts.

4.2 BRCA1-mutant cells display increased glutamine-derived TCA cycle intermediates

To further characterise glutaminolysis and anaplerosis in our model, we measured the total levels of glutaminolysis and TCA cycle derivatives using an LC-

MS approach. While there were no changes in α KG and a non-significant increase in glutamate, TCA cycle derivatives, succinate, malate, and fumarate were all significantly increased in BRCA1-mutant cells (Figure 4.2A). Interestingly, there was also a small decrease in citrate. These data are consistent with an increase in glutamine consumption and suggest that BRCA1-mutant cells use α KG for the oxidative part of the TCA cycle rather than for reductive carboxylation. To test this hypothesis and examine the role of glutamine in the TCA cycle further, we measured the incorporation of ^{13}C -labelled glutamine into downstream derivatives. Consistent with our previous observations, there were no changes in the fractional enrichment of ^{13}C -labelled glutamate and α KG while there were small, but significant, increases in the M+4 fraction of succinate, malate, and fumarate (Figure 4.2B). Importantly, we could not detect any M+3 species for succinate, malate, and fumarate confirming an absence of reductive carboxylation in both genotypes. Additionally, we could not detect M+2 species for these same metabolites, or M+3 species for glutamate and α KG suggesting that the labelled carbons do not cycle twice through the TCA cycle, but rather exit altogether at some point along the way (Figure 4.2B). Taken together, these observations are consistent with an increase in glutamine consumption in the BRCA1-mutant cells but do not show specific differences in the processing of glutamine. Therefore, we hypothesised that other glutamine processing pathways might explain the difference in glutamine deprivation sensitivity and consumption.

4.3 GSH levels and sensitivity to oxidative stress are equivalent in BRCA1-mutant and -restored cells

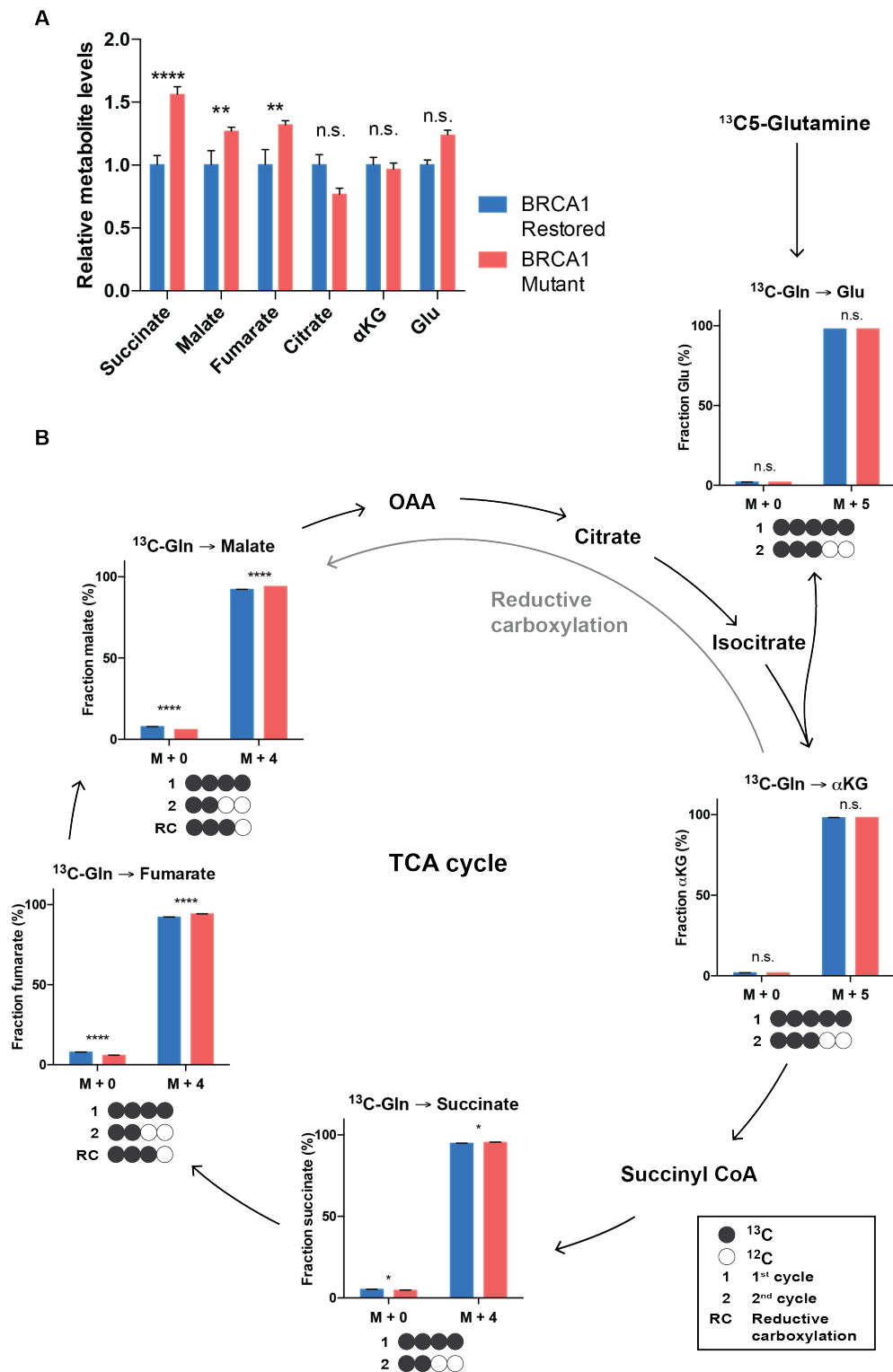


Figure 4.2 - TCA cycle intermediates are increased in BRCA1-mutant cells

(A) Total normalised intracellular metabolite levels of SUM149 BRCA1-restored (blue) or -mutant (red) cells as measured by LC-MS. Data is presented as mean \pm SEM ($n = 12$), and analysed by t -test with FDR correction ($Q = 1\%$).

(B) Fractional enrichment of detected glutamine derivatives extracted from SUM149 BRCA1-restored or -mutant cells and measured by LC-MS following 24-hour incubation with $^{13}\text{C}_5$ -labelled glutamine. Only detected species are included for each metabolite. Data is presented as part of a TCA cycle schematic describing which metabolite species results from different glutamine processing. Data is presented as mean \pm SEM (n = 4), and analysed by 2-way ANOVA and Sidak's multiple comparisons test. (**** $p < 0.0001$; *** $p < 0.001$; ** $p < 0.01$; * $p < 0.05$)

Although glutamine is incorporated in the TCA cycle, and we observed changes in TCA cycle derivatives in BRCA1-mutant cells, we hypothesised that the glutamine deprivation sensitivity could originate from alternative uses of glutamine. The first derivative of glutamine, glutamate is one of the key component in the synthesis of GSH, an important antioxidant that regulates ROS levels. We thought that blockage of GSH synthesis could explain the accumulation of glutamate upstream and the subsequent diversion of glutamate derivatives into the TCA cycle. Therefore, we measured GSH levels and explored sensitivity to ROS in our model.

Firstly, GSH levels were similar between BRCA1-mutant and -restored cells (Figure 4.3A). Additionally, the mRNA expression levels of the GSH synthesis rate-limiting enzyme GCLC and downstream enzyme GSH synthetase (GSS) were equivalent (Figure 4.3B and C). The expression levels of GSH peroxidase 1 (GPX1) and GSH reductase (GSR), responsible for the GSH-GSSG recycling were also equivalent between the two genotypes (Figure 4.3B and C). Finally, both genotypes were equally sensitive to inhibition of GCLC with L-BSO (Figure 4.3D), and to inhibition with sulfasalazine of the cystine-glutamate transporter xCT which is essential to import cysteine, the rate-limiting reagent in GSH synthesis (Figure 4.3E). Together, these data suggested that there were no differences in GSH synthesis.

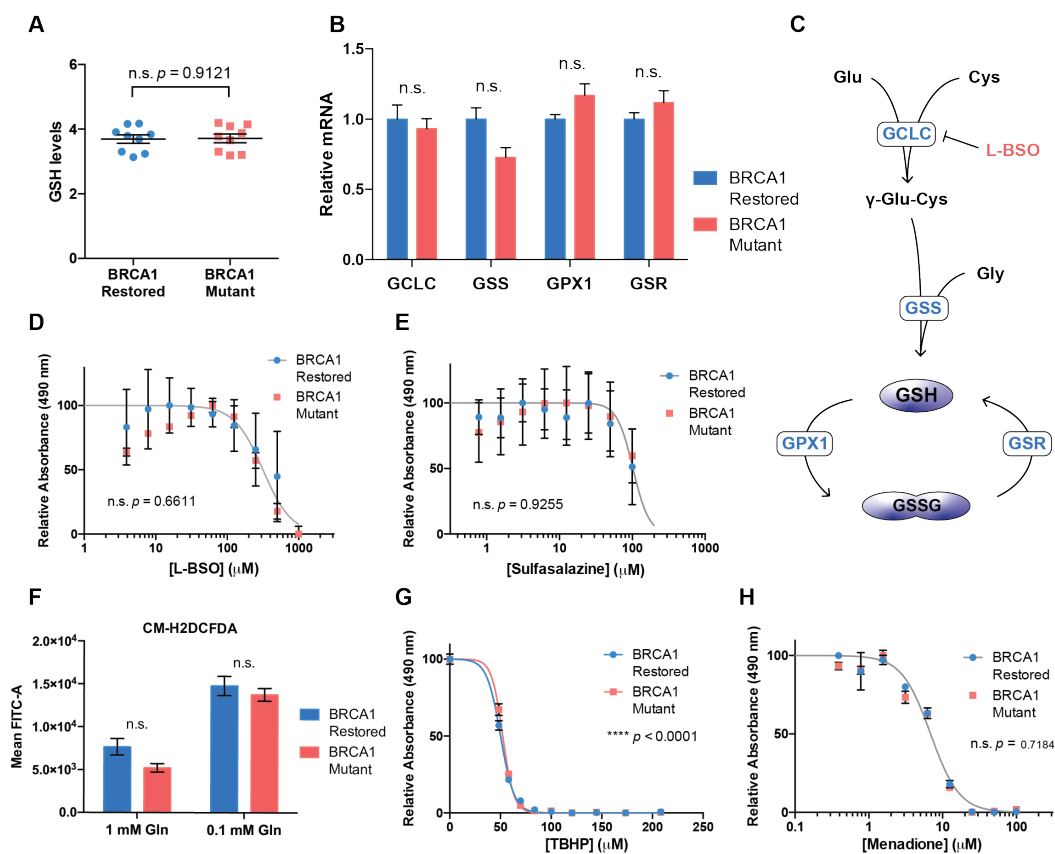


Figure 4.3 - GSH levels and sensitivity to oxidative stress are equivalent in BRCA1-mutant and -restored cells

(A) Total GSH levels in SUM149 BRCA1-restored (blue) or -mutant (red) lysates measured using GSH-Glo™ Glutathione Assay following the manufacturer's instructions. Data was analysed by *t*-test.

(B) RT-qPCR quantification of indicated mRNA extracted from SUM149 BRCA1-restored or -mutant cells. Data is presented as mean \pm SEM ($n = 9$), and analysed by *t*-test with FDR correction ($Q = 1\%$).

(C) Schematic representation of GSH synthesis and recycling with relevant enzymes (blue) and inhibitors (red) indicated.

(D-E) Cell density of SUM149 BRCA1-restored or -mutant cells grown for 5 days under indicated (D) L-BSO or (E) sulfasalazine concentrations and quantified using CellTiter 96® AQueous One Solution according to the manufacturer's instructions. Data is presented as mean \pm SEM ($n = 6$), and analysed by non-linear regression.

(F) General ROS levels in SUM149 BRCA1-restored or -mutant cells measured with the CM-H2DCFDA fluorescent probe using flow cytometry following 48-hour incubation under indicated glutamine concentrations. Data is presented as mean \pm SEM ($n = 6$), and analysed by 2-way ANOVA and Sidak's multiple comparisons test.

(G-H) Cell density of SUM149 BRCA1-restored or -mutant cells grown for 24 hours under indicated (G) TBHP or (H) Menadione concentrations and quantified and analysed as in (D). (**** $p < 0.0001$; *** $p < 0.001$; ** $p < 0.01$; * $p < 0.05$)

Since the major role of GSH is to detoxify ROS, we hypothesised that there are no differences in ROS levels between the two genotypes. To further rule out a role for ROS in the glutamine deprivation sensitivity phenotype that we observed, we measured the sensitivity to different oxidising agents. Interestingly, cells grown for 48 hours under low glutamine (0.1 mM) displayed higher ROS levels than controls, however, this increase was equivalent in both genotypes (Figure 4.3F). Additionally, both genotypes were similarly sensitive to treatment with TBHP or endogenous ROS inducer Menadione (Figure 4.3G and H).

4.4 Glutamine synthetase regulation is independent of BRCA1

Apart from its role in anaplerosis and GSH synthesis, many other functions of glutamine do not require any processing into downstream metabolites. In fact, the amide group of glutamine can be donated for asparagine or nucleotide synthesis, resulting in glutamate as a by-product. Previous reports have demonstrated that cancer cells with high requirements in glutamine could upregulate GS in order to produce more glutamine to use in purine synthesis¹⁴⁰. Therefore, we investigated the role of GS in BRCA1-mutant cells. Interestingly, we observed that BRCA1-mutant cells showed a reduction in GS protein as well as *GLUL* mRNA levels, the gene encoding GS (Figure 4.4A and B). However, overexpression of BRCA1-WT in SUM149 BRCA1-mutant cells did not rescue the expression levels of GS or *GLUL* (Figure 4.4C and D). Similarly, downregulation of *BRCA1* mRNA via shRNA in MCF7 cells did not affect GS levels (Figure 4.4E and F). Therefore, changes in GS expression could not explain the increased glutamine

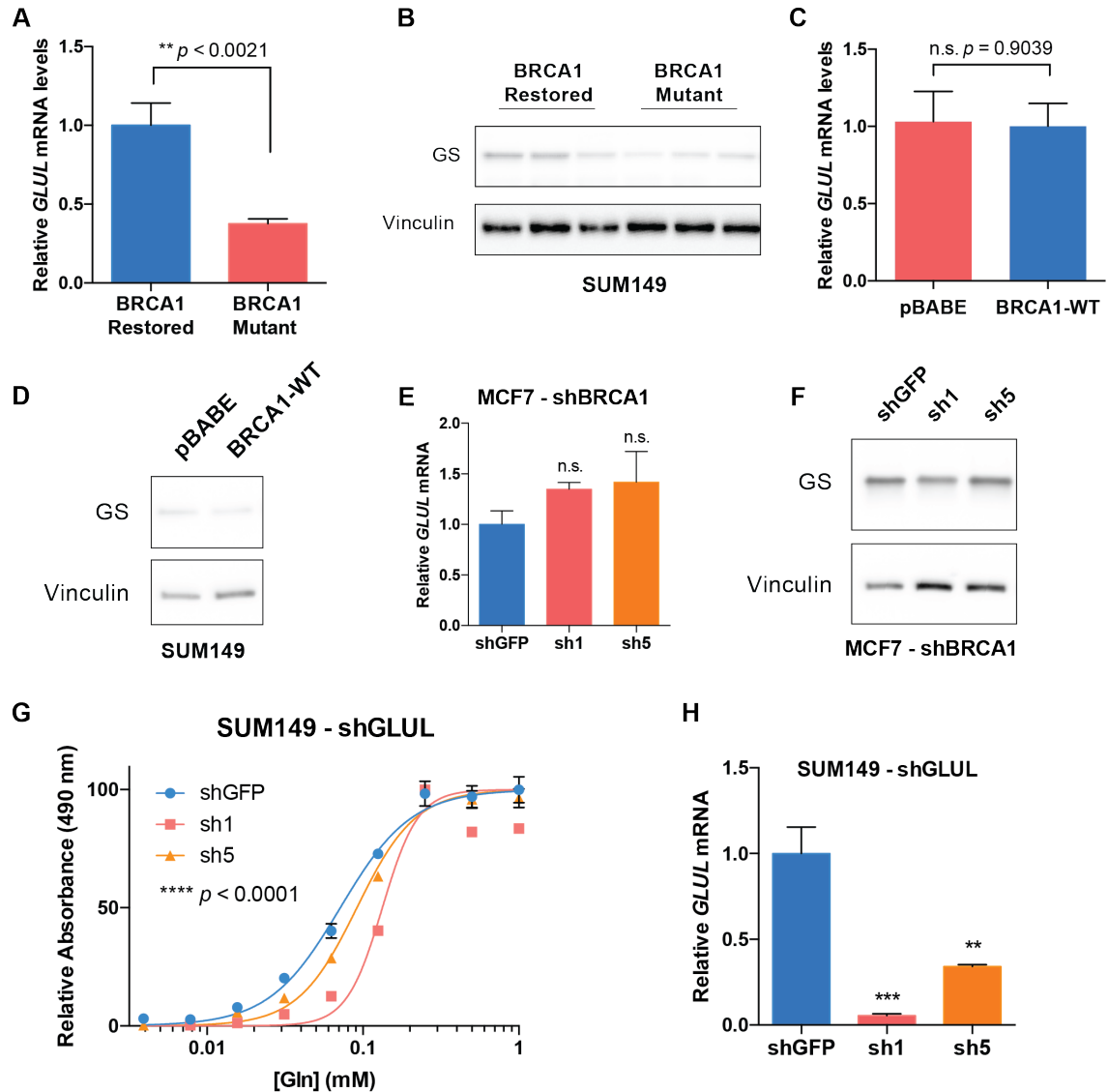


Figure 4.4 - Glutamine synthetase regulation is independent of BRCA1

(A) RT-qPCR quantification of *GLUL* mRNA extracted from SUM149 BRCA1-restored (blue) or mutant (red) cells. Data is presented as mean \pm SEM ($n = 4$), and analysed by *t*-test.

(B) Immunoblot for GS and vinculin using lysates extracted from cells in (A). The 3 lanes for each genotype represent lysates from individual clones cultured separately.

(C) RT-qPCR quantification of *GLUL* mRNA extracted from SUM149 BRCA1-mutant cells stably overexpressing wild-type HA-BRCA1 construct (blue) or pBABE vector levels (red). Data is presented as mean \pm SEM ($n = 4$), and analysed by *t*-test.

(D) Immunoblot for GS and vinculin using lysates extracted from cells in (C).

(E) RT-qPCR quantification of *GLUL* mRNA extracted from MCF7 cells stably expressing shRNA against GFP (blue) or BRCA1 (red and orange). Data is presented as mean \pm SEM ($n = 4$), and analysed by 1-way ANOVA and Dunnett's test.

(F) Immunoblot for GS and vinculin using lysates extracted from cells in (E).

(G) Cell density of SUM149 BRCA1-restored cells stably expressing shRNA against GFP (blue) or *GLUL* (red and orange) grown for 5 days under indicated glutamine concentrations and

quantified using CellTiter 96® AQ_{ueous} One Solution according to the manufacturer's instructions. Data is presented as mean ± SEM (n = 6), and analysed by non-linear regression.

(H) RT-qPCR quantification of *GLUL* mRNA extracted from cells in (G) and analysed as in (E).

(**** $p < 0.0001$; *** $p < 0.001$; ** $p < 0.01$; * $p < 0.05$)

consumption observed in BRCA1-mutant cells. Of note, downregulation of *GLUL* mRNA in BRCA1-restored cells led to increased sensitivity to glutamine deprivation (Figure 4.4G and H), suggesting that synthesis of glutamine through the GS reaction happens in these cells. However, our data suggested that this effect is most likely independent of *BRCA1* mutation status.

4.5 BRCA1-mutant cells process glutamine through the GABA shunt to produce aspartate more efficiently

To investigate the role of glutamine in BRCA1-mutant cells from a broader perspective, we measured changes in a wider panel of metabolites involved in different metabolic pathways. Metabolic pathway enrichment analysis using the MetaboAnalyst software, showed an enrichment in nitrogen-related pathways (Figure 4.5A). More specifically, aspartate, glutamate, purines and pyrimidines metabolism, as well as ammonia recycling were among the most enriched pathways in BRCA1-mutant cells (Figure 4.5A). Consistently, glutamate and aspartate were the metabolites with the highest fold change increase in BRCA1-mutant versus -restored cells (Figure 4.5B).

In a separate experiment, we observed that aspartate was the only upregulated amino acid among the ones that we could detect while cysteine, phenylalanine, tyrosine, serine, leucine, valine, and histidine were significantly

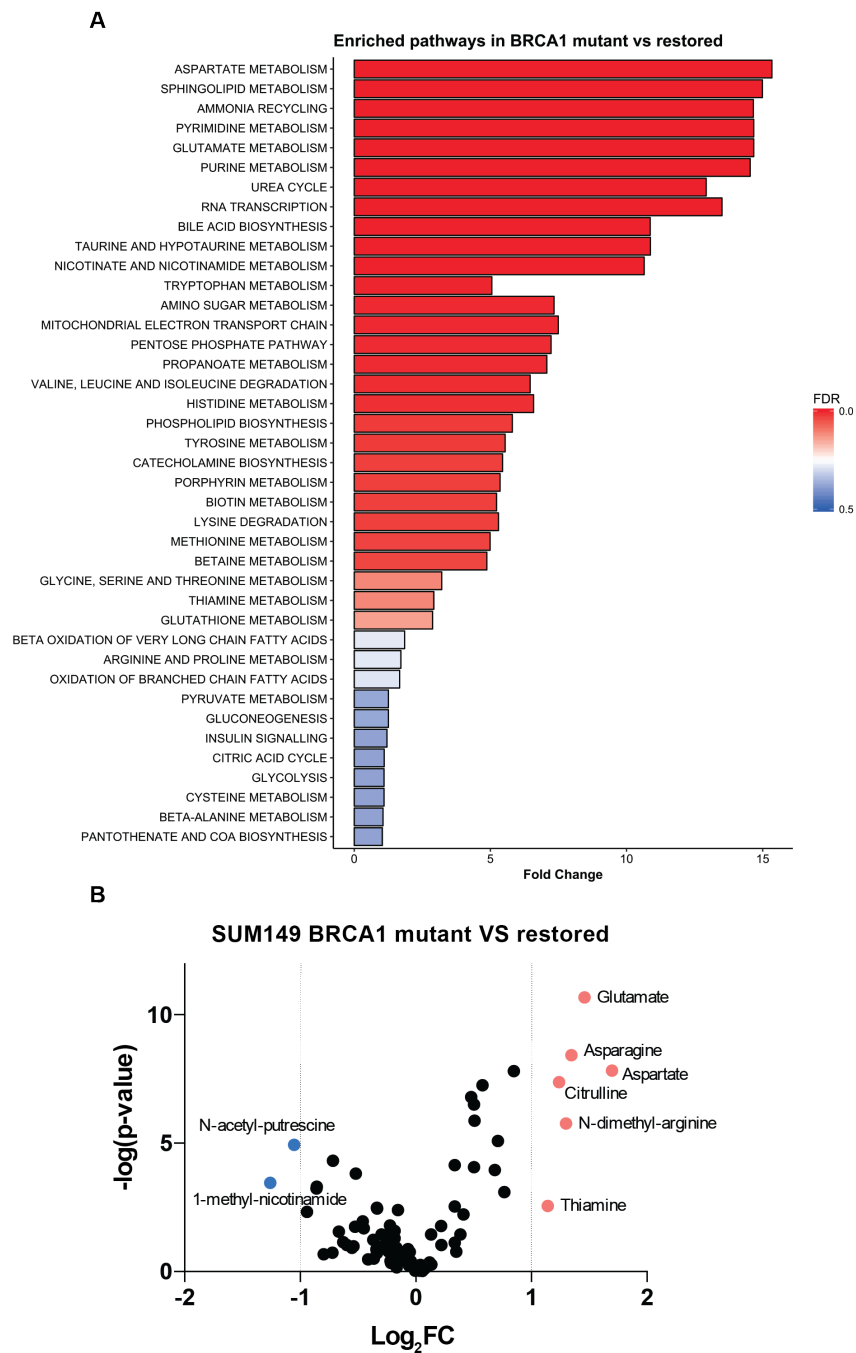


Figure 4.5 - BRCA1-mutant cells show enrichment of changes in nitrogen-related pathways

(A) Metabolite enrichment analysis performed with MetaboAnalyst 3.0 based on a panel of metabolites measured by LC-MS. Metabolic pathways are classified based on fold change and FDR corrected p -value.

(B) Volcano plot based on the same panel of metabolites as in (A). Metabolites with Log_2 fold change greater than 1 (red) or less than -1 (blue) are coloured and labelled accordingly.

lower (Figure 4.2A and 4.6A). This suggests that BRCA1-mutant cells pool resources in order to maintain high intracellular aspartate levels at the expense of the production of other amino acids. Additionally, there was a small but significant increase in ^{13}C -glutamine-derived carbon incorporation in aspartate in the BRCA1-mutant cells (Figure 4.6B). Of note, close to 100% of the carbons in aspartate detected in both genotypes were derived from glutamine (Figure 4.6B).

To examine more specifically the nitrogen processing in BRCA1-mutant cells, we measured the incorporation of isotopically labelled $^{15}\text{N}_2$ -glutamine in downstream metabolites. Interestingly, only 4 downstream metabolites (aspartate, glutamate, alanine, and GABA) reached fractional enrichment above 20% and were labelled as quickly as 4 hours after the addition of labelled glutamine to the media. Additionally, for each of those four metabolites, there was an increase in the M+1 fraction and consistent decrease in the unlabelled fraction in the BRCA1-mutant cells (Figure 4.6C-F). This suggests that BRCA1-mutant cells process nitrogen derived from glutamine more efficiently than BRCA1-restored counterparts.

More specifically, while glutamate is the first downstream metabolite of glutamine and should be almost 100% labelled, we found that only around 50% of glutamate was nitrogen labelled, suggesting that transamination reactions contribute to the regulation of the glutamate pool. Additionally, we observed labelling of GABA suggesting that glutamine-derived glutamate is processed through the GABA shunt and can replenish the TCA cycle via succinate (Figure

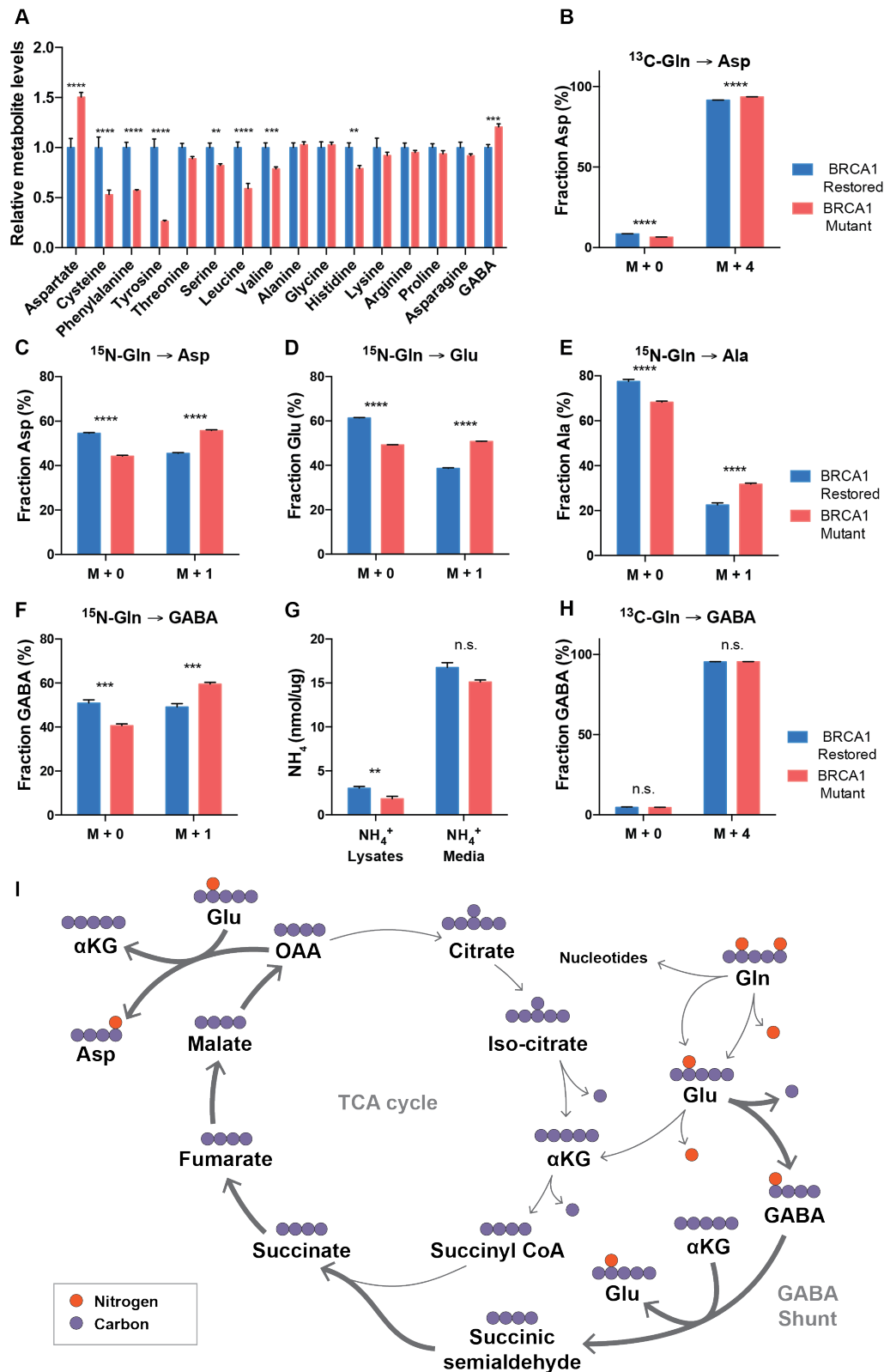


Figure 4.6 - BRCA1-mutant cells process glutamine through the GABA shunt to maintain high intracellular aspartate

(A) Total normalised intracellular metabolite levels of SUM149 BRCA1-restored (blue) or -mutant (red) cells as measured by LC-MS. Data is presented as mean \pm SEM ($n = 12$), and analysed by t -test with FDR correction ($Q = 1\%$).

(B) Fractional enrichment of ^{13}C -glutamine-derived aspartate in SUM149 BRCA1-restored or -mutant cells following 24-hour incubation with labelled glutamine. Data is presented as mean \pm SEM ($n = 4$), and analysed by 2-way ANOVA and Sidak's multiple comparisons test.

(C-F) Fractional enrichment of ^{15}N -glutamine-derived (C) aspartate (Asp), (D) glutamate (Glu), (E) alanine (Ala), or (F) γ -aminobutyric acid (GABA) in SUM149 BRCA1-restored or -mutant cells following 24-hour incubation with labelled glutamine. Data was analysed as in (B).

(G) Ammonia (NH_4^+) levels in lysates and cell culture media of SUM149 BRCA1-restored and -mutant cells measured with the Abcam Ammonia Assay Kit. Data is presented as mean \pm SEM ($n = 9$), and analysed by t -test with FDR correction ($Q = 1\%$).

(H) Fractional enrichment of ^{13}C -glutamine-derived GABA in SUM149 BRCA1-restored or -mutant cells following 24-hour incubation with labelled glutamine. Data was analysed as in (B).

(I) Schematic representation of the metabolic rewiring occurring in BRCA1-mutant cells as compared to BRCA1-restored counterparts. Orange spheres represent nitrogen and purple spheres represent carbons. Thicker arrows represent increased flux through those pathways.

Oxaloacetate (OAA), α -ketoglutarate (αKG).

(**** $p < 0.0001$; *** $p < 0.001$; ** $p < 0.01$; * $p < 0.05$)

4.6A and F), which explains the high succinate levels observed in BRCA1-mutant cells (Figure 4.2A). Through transamination of GABA into succinic semialdehyde, the amine group is recycled into glutamate or alanine which explains the higher fractional enrichment of M+1 species for both of these metabolites (Figure 4.6D and E). Since this pathway promotes a more efficient nitrogen processing, it leads to less release of ammonia intracellularly with no changes in the cell culture media (Figure 4.6G). Aspartate is synthesised via transamination of OAA with nitrogen coming from glutamate or alanine, therefore higher fractional enrichment of glutamate and alanine also leads to higher ^{15}N -labelled aspartate (Figure 4.6C). Of note, ^{13}C -glutamine derived carbons were also incorporated into GABA but similarly for both genotypes (Figure 4.6H). In summary, our data pointed to BRCA1-mutant cells using the GABA shunt to process glutamine more efficiently and increase the incorporation of glutamine-derived nitrogen into aspartate, in order to maintain high intracellular aspartate levels (Figure 4.6I).

Finally, we tested whether these metabolic changes were also observed in other breast cancer cell lines. As expected, there were variations in the metabolic changes induced by siRNA against *BRCA1* in different cell lines. However, we saw consistent increases in total aspartate and GABA levels in MDA-MB-468, SUM149 *BRCA1*-restored, and T47D cells following siRNA-mediated knockdown of *BRCA1* expression (Figure 4.7A-F). Additionally, there was an overall increase in TCA cycle metabolites succinate, fumarate, and malate although the changes were not consistent for all 3 metabolites across all cell lines.

4.6 Chapter discussion

The data presented in this chapter demonstrate that *BRCA1* loss-of-function leads to changes in glutamine incorporation providing a more efficient nitrogen processing through the GABA shunt and supporting the synthesis of high intracellular aspartate levels. These data are consistent with glutamine being the main nitrogen source in many cancer types^{99,133}. Additionally, aspartate has also been described as an important metabolite for cancer progression and is used for synthesis of proteins, NEAA, N-acetyl-aspartate, and nucleotides^{122,124}. Interestingly, glutamine and aspartate share similar and complementary functions particularly for nucleotide synthesis. Therefore, the metabolic changes observed in our model are consistent with a need for glutamine and aspartate.

Based on our data, it appears that aspartate is the key metabolite derived from glutamine, however, glutamine itself donates its amide group for nucleotide

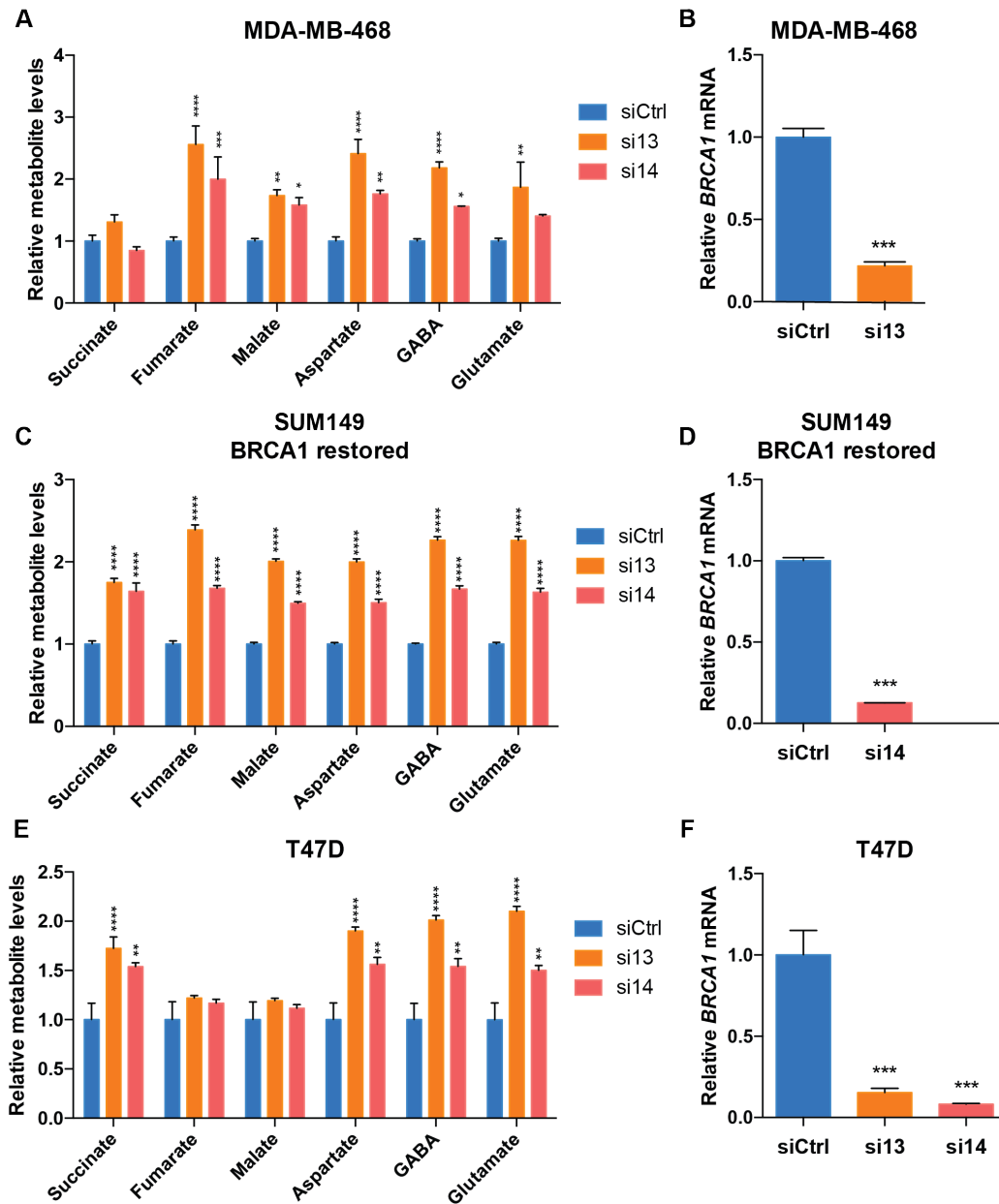


Figure 4.7 - BRCA1 loss-of-function leads to consistent increase in aspartate and GABA across different cell lines

(A-F) LC-MS measurements of total normalised intracellular metabolite levels of (A) MDA-MB-468, (C) SUM149 BRCA1-restored, and (E) T47D cells transiently transfected with siCtrl (blue) or siRNA against *BRCA1* (red and orange) 48 hours prior to metabolite extraction. Data is presented as mean \pm SEM ($n = 4$), and analysed by 2-way ANOVA and Dunnett's multiple comparisons test. (B), (D), and (F) RT-qPCR quantification of *BRCA1* mRNA extracted from same cells as in (A), (C), and (E) respectively. Data was analysed by (B) and (D) *t*-test, and (F) one-way ANOVA and Dunnett's multiple comparisons test.

(**** $p < 0.0001$; *** $p < 0.001$; ** $p < 0.01$; * $p < 0.05$)

synthesis generating glutamate in the process. In some context, this is the main function of glutamine and the resulting glutamate is exported out of the cells while GS is used to synthesise glutamine *de novo*¹⁴⁰. In our model, however, the downstream incorporation of glutamate into the TCA cycle to synthesise aspartate also appears to be important for cell survival. In line with this, we do not observe any reductive carboxylation of α KG but rather increases in the oxidative side of the TCA cycle. Overall, both glutamine-derived amide directly, as well as amine group from aspartate appear to be important.

Although BRCA1 loss-of-function leads to changes in glutamine processing, extrinsic factors most likely also dictate the needs for glutamine. This could explain the difference in sensitivity to BPTES of cells in clonogenic assays versus grown at higher confluency. Interestingly, the study of GLS inhibitors in clinical trials have led to variable results, suggesting that there is more to glutamine metabolism than we understand¹⁷⁵. As described above, glutamate is produced when glutamine is used for nucleotide or asparagine synthesis which could replace the need for GLS. Additionally, we observed variations in metabolic changes caused by *BRCA1* downregulation in different cell lines, and we saw an increase in glutamine deprivation sensitivity following downregulation of *GLUL*. Since glutamine plays a role in a variety of essential cell biology functions, it is important to distinguish between these potential confounding variables and the changes induced by *BRCA1* mutation.

5 Mechanistic investigation of the links between *BRCA1* mutation and increased glutamine consumption

The work presented in previous chapters of this thesis has defined the metabolic phenotype of *BRCA1*-mutant cells and highlighted a specific need for glutamine. In particular, I focused on the processing of glutamine through the GABA shunt to sustain high intracellular aspartate levels. The role of glutamine has been explored extensively in a variety of cancer types, however, there is no clear link between functions of *BRCA1* and glutamine consumption. In this chapter, we examine different functions of *BRCA1* and how they could relate directly or indirectly with the increased glutamine consumption and high aspartate levels found in *BRCA1*-mutant cells. Since *BRCA1* plays a broad role in cell biology, we anticipate that there could be a few non-mutually exclusive explanations for the metabolic changes observed.

5.1 Sensitivity to glutamine deprivation is independent of HR DNA repair potential

The most well described role of *BRCA1* in cell biology is regulation of DNA repair, more specifically HR. HR involves multiple complexes of proteins which, when deregulated or mutated, can also lead to the BRCAness phenotype^{57,176}. As such, we investigated whether the metabolic changes observed in *BRCA1*-mutant cells could be linked to the BRCAness phenotype or HR defects. Using the same SUM149 *BRCA1*-restored model described previously, we stably downregulated the expression of *BRCA2* mRNA using shRNA to disrupt HR without affecting *BRCA1* function. Interestingly, unlike loss-of-function of *BRCA1*, *BRCA2* silencing

did not affect sensitivity to glutamine deprivation or treatment with DON (Figure 5.1A-C). Additionally, we took advantage of HR-deficient cancer resistance mechanisms to look at whether restoring HR in a *BRCA1* mutant context could rescue the glutamine deprivation sensitivity. Although the exact mechanism is still under investigation, mutations or loss-of-functions of Rev7 and 53BP1 have been shown to restore HR function in cells with *BRCA1* mutations^{177,178}. Therefore, we tested whether SUM149 *BRCA1*-mutant cells lacking Rev7 and 53BP1 became more resistant to glutamine deprivation as a result of restoring HR function. Interestingly, although the growth rate was slower for both cell lines, the sensitivity to glutamine deprivation in clonogenic assay was equivalent across both Rev7 and 53BP1 knock-out *BRCA1*-mutant cells while the *BRCA1*-restored cells showed a smaller reduction in total area as a result of low glutamine concentrations (Figure 5.1D). Together, these data suggest that the metabolic phenotype observed in *BRCA1*-mutant cells is a result of HR-independent functions of *BRCA1*.

Next, we tested whether low glutamine conditions led to increased cell death as a result of increased DNA damage. While 8 Gray of ionising radiation led to an increase in γ H2AX and P-Chk1 (S345) 24 hours following treatment, culturing cells under 0.1 mM glutamine for 48 hours did not exacerbate DNA damage, based on the aforementioned markers (Figure 5.1E). There was, however, a clear increase in apoptotic cells within the same treatment time frame (Figure 3.7A-B). Interestingly, however, treatment with 8 Gray of ionising radiation led to increased sensitivity to glutamine deprivation in *BRCA1*-mutant cells, while there were no significant changes in the sensitivity of *BRCA1*-restored cells (Figure 5.1F).

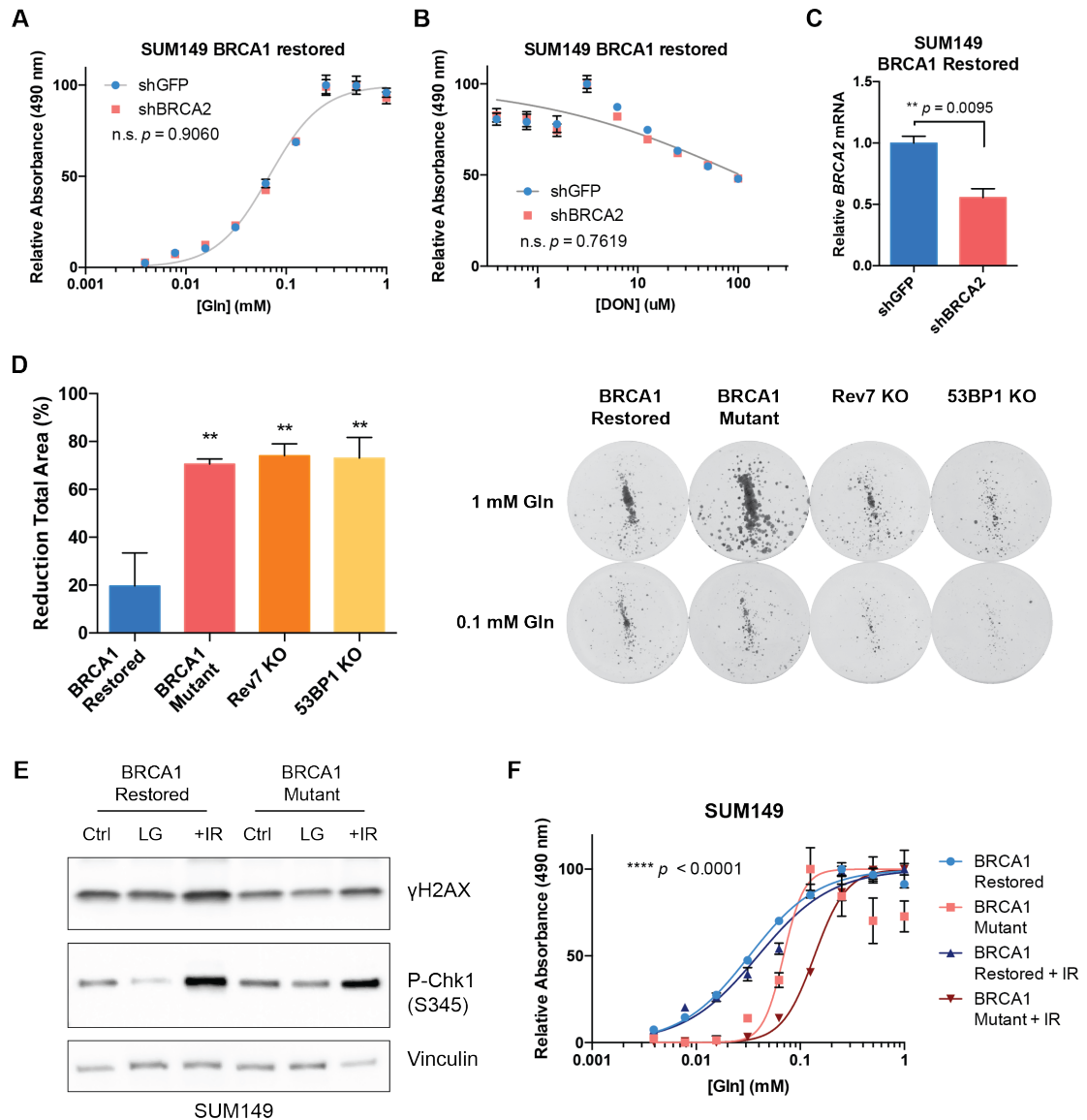


Figure 5.1 - Sensitivity to glutamine deprivation is independent of HR DNA repair potential

(A-B) Cell density of SUM149 BRCA1-restored cells stably expressing shRNA against GFP (blue) or BRCA2 (red) grown for 5 days under indicated (A) glutamine or (B) DON concentrations and quantified using CellTiter 96® AQ_{UEOUS} One Solution according to the manufacturer's instructions. Data is presented as mean \pm SEM ($n = 6$), and analysed by non-linear regression.

(C) RT-qPCR quantification of *BRCA2* mRNA extracted from cells in (A-B). Data is presented as mean \pm SEM ($n = 3$), and analysed by *t*-test.

(D) Representative images and quantification of % reduction in total area of SUM149 BRCA1-restored (blue), BRCA1-mutant (red), BRCA1-mutant Rev7 KO (orange), or BRCA1-mutant 53BP1 KO (yellow) cells grown for 12 days under indicated glutamine concentrations as part of a clonogenic assay and stained with crystal violet. Data is presented as mean \pm SEM ($n = 3$), and analysed by 1-way ANOVA and Dunnett's multiple comparisons test.

(E) Immunoblot for γ H2AX, P-Chk1 (S345), and vinculin using lysates extracted from BRCA1-restored or -mutant cells grown for 48 hrs under 1 mM (Ctrl) or 0.1 mM glutamine (LG), or treated with 8 Gray of ionising radiation 24 hrs prior to extraction (+IR).

(F) Cell density of SUM149 BRCA1-restored or -mutant cells grown for 5 days under indicated glutamine concentrations following treatment with 8 Gray of ionising radiation (+IR) or not and quantified using CellTiter 96® AQ_{ueous} One Solution according to the manufacturer's instructions. Data is presented as mean \pm SEM (n = 6), and analysed by non-linear regression.

(**** $p < 0.0001$; *** $p < 0.001$; ** $p < 0.01$; * $p < 0.05$)

5.2 High *TWIST1* mRNA expression does not drive the increased glutamine deprivation sensitivity phenotype

Another well described function of BRCA1 in cancer cells is its role in cancer progression and EMT. More specifically, BRCA1 has been shown to regulate a number of EMT related transcription factors^{76,77}. Consistently, we found a 5 to 10-fold increase in *TWIST1* mRNA expression and an increase in *FOXC2*, although there were no changes in *FOXC1* mRNA levels (Figure 5.2A). In line with this, we found higher expression of EMT markers and increased migration rate in BRCA1-mutant cells (Figure 5.2B and C). The morphology of BRCA1-mutant cells also appears more mesenchymal when compared to BRCA1-restored counterparts (data not shown). Of note, low glutamine conditions (0.1 mM) led to a reduction in cell migration across both genotypes (Figure 5.2C). Since the mesenchymal phenotype observed in BRCA1-mutant cells appears to be driven by high *TWIST1* expression levels, we investigated whether downregulating *TWIST1* mRNA could rescue the sensitivity to glutamine deprivation. Surprisingly, downregulation of *TWIST1* in BRCA1-mutant cells with high *TWIST1* levels did not affect sensitivity to glutamine deprivation while in BRCA1-restored cells with low *TWIST1* levels, further reducing *TWIST1* levels made the cells more sensitive to glutamine deprivation (Figure 5.2D and E). Together, these data show that while glutamine is essential for migration, the increased *TWIST1* expression and associated

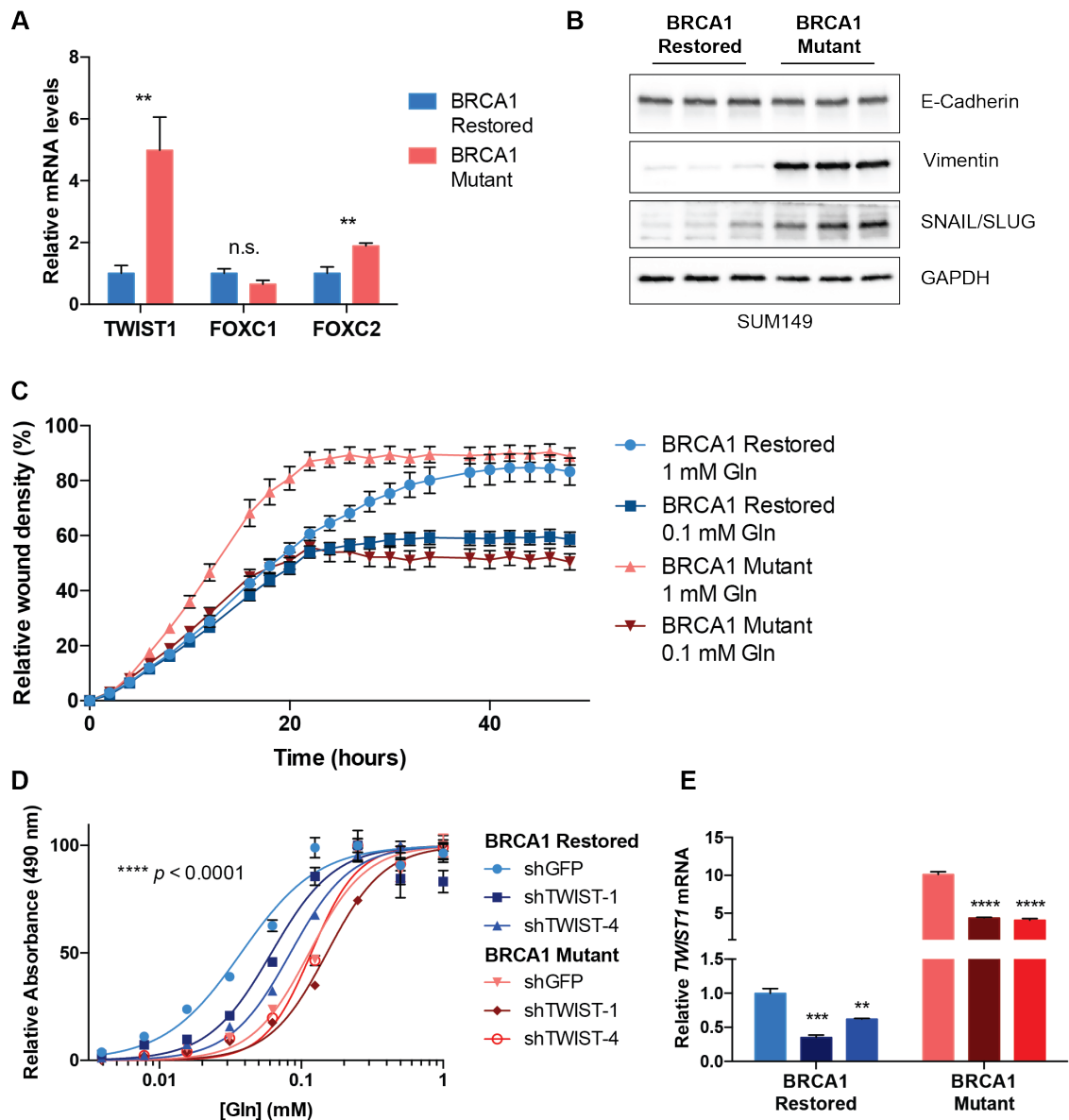


Figure 5.2 - High TWIST1 mRNA expression does not drive the increased glutamine deprivation sensitivity phenotype

(A) RT-qPCR quantification of indicated mRNA extracted from BRCA1-restored (blue) or -mutant (red) cells. Data is presented as mean \pm SEM ($n = 6$), and analysed by multiple t -test with FDR correction ($Q = 1\%$).

(B) Immunoblot for E-cadherin, vimentin, SNAIL/SLUG, and GAPDH using lysates extracted from BRCA1-restored or -mutant cells. The 3 lanes for each genotype represent lysates from individual clones cultured separately.

(C) Relative wound density of BRCA1-restored and mutant cells measured over time under indicated glutamine conditions using an IncuCyte, following a scratch assay performed using the Essen 96-well WoundMaker® after 24 hr incubation under indicated glutamine conditions.

(D) Cell density of SUM149 BRCA1-restored (blue) or -mutant (red) cells stably expressing shRNA against GFP or TWIST grown for 5 days under indicated glutamine concentrations and

quantified using CellTiter 96® AQueous One Solution according to the manufacturer's instructions. Data is presented as mean ± SEM (n = 6), and analysed by non-linear regression.

(E) RT-qPCR quantification of *TWIST1* mRNA extracted from cells in (D). Data is presented as mean ± SEM (n = 3), and analysed by 2-way ANOVA and Dunnett's multiple comparisons test. (**** $p < 0.0001$; *** $p < 0.001$; ** $p < 0.01$; * $p < 0.05$)

mesenchymal phenotype do not explain the increased sensitivity to glutamine deprivation observed in BRCA1-mutant cells.

5.3 BRCA1 mutation leads to a purine conserving phenotype

BRCA1 has been suggested to interact and potentially regulate a number of important transcription factors and oncogenes. One of them, c-Myc, has been shown to regulate glutaminolysis and dictate glutamine dependency^{83,139,179}. c-Myc is also an important regulator of key nucleotide synthesis and polyamine synthesis enzymes^{180,181}. Interestingly, we did not see an increase in *MYC* mRNA expression in BRCA1-mutant cells, in fact, we observed a small decrease that was not significant (Figure 5.3A). Additionally, we did not observe mRNA changes in enzymes transcriptionally regulated by c-Myc, including *GLS1*, suggesting no changes in c-Myc activity levels (Figures 4.1A and 5.3A). However, out of the identified metabolites detected in our LC-MS analyses, most of the compounds with nucleic bases showed significantly lower total levels in BRCA1-mutant cells (Figure 5.3B). Consistently, we also observed more intake from the media of nucleotide precursor hypoxanthine and a reduction in secretion of guanine into the media (Figure 5.3C). While we could not detect all the nucleotide related metabolites in our experiments, together, these data suggest a nucleotide conserving mechanism that could be explained by a reduction in synthesis or an increase in usage. In line with this, we could rescue the glutamine sensitivity

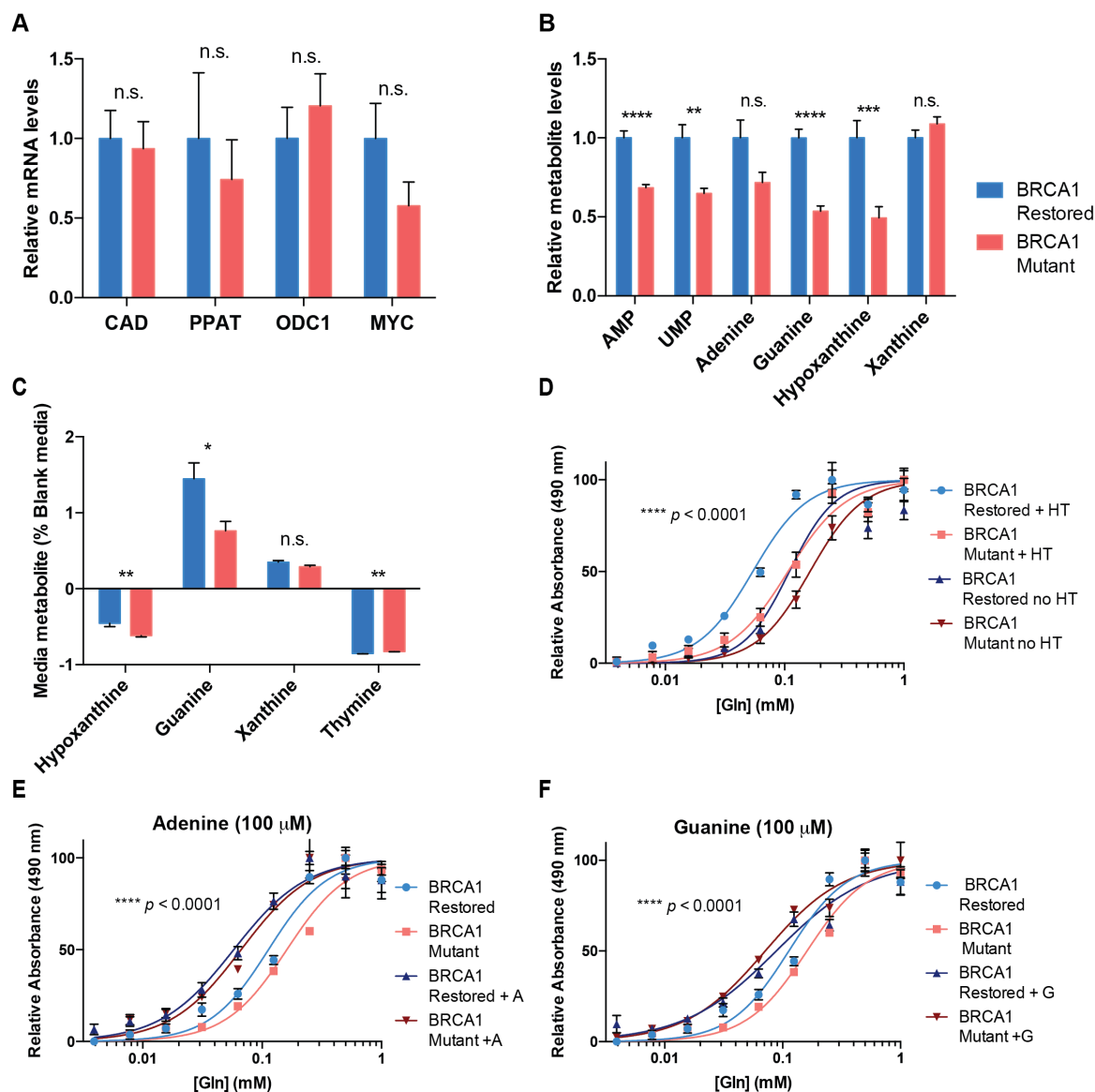


Figure 5.3 - BRCA1 mutation leads to a purine conserving phenotype.

(A) RT-qPCR quantification of indicated mRNA extracted from BRCA1-restored (blue) or -mutant (red) cells. Data is presented as mean \pm SEM (CAD and ODC1: $n = 9$; PPAT and MYC: $n = 5$), and analysed by multiple t -tests with FDR correction ($Q = 1\%$).

(B) Total normalised intracellular metabolite levels of SUM149 BRCA1-restored or -mutant cells as measured by LC-MS. Data is presented as mean \pm SEM (AMP, UMP, and xanthine: $n = 9$; adenine, guanine, and hypoxanthine: $n = 12$), and analysed by t -test with FDR correction ($Q = 1\%$).

(C) LC-MS quantification of SUM149 BRCA1-restored or -mutant cell culture media metabolite levels expressed as % change of blank media. Data is presented as mean \pm SEM ($n = 9$), and analysed by multiple t -tests with FDR correction ($Q = 1\%$).

(D) Cell density of SUM149 BRCA1-restored or -mutant cells grown for 5 days under indicated glutamine concentrations in the presence or absence of hypoxanthine and thymidine (HT) and quantified using CellTiter 96[®] AQ_{ueous} One Solution according to the manufacturer's instructions. Data is presented as mean \pm SEM ($n = 6$), and analysed by non-linear regression.

(E-F) Cell density of SUM149 BRCA1-restored or -mutant cells grown for 5 days under indicated glutamine concentrations supplemented or not with (E) 100 μ M adenine (A), or (F) 100 μ M guanine (G) the absence of hypoxanthine and thymidine, and quantified and analysed as in (D). (**** $p < 0.0001$; *** $p < 0.001$; ** $p < 0.01$; * $p < 0.05$)

phenotype by supplementing cell culture media with purine bases (Figure 5.3E-F). Of note, the Ham's F12 cell culture media used to grow SUM149 cells contains purine precursor hypoxanthine as well as thymidine. We observed that removal of hypoxanthine and thymidine from the cell culture media made the cells more sensitive to glutamine deprivation (Figure 5.3D).

5.4 BRCA1 loss-of-function increases GAD1 protein, but not mRNA levels.

In addition to transcriptional regulation, BRCA1 has also been shown to affect post-translational modifications or protein expression levels in different contexts. Since we observed an overactive GABA shunt in BRCA1-mutant cells (Figure 4.6), we investigated GAD1, the rate-limiting enzyme involved in the synthesis of GABA. Interestingly, we observed higher GAD1 protein expression in BRCA1-mutant cells (Figure 5.4A). Additionally, shRNA repression of *BRCA1* mRNA in MCF7 cells led to increase in GAD1 protein expression, while overexpression of wild-type HA-BRCA1 in SUM149 parental *BRCA1* mutant cells abolished GAD1 protein expression levels (Figure 5.4B and C). Importantly, we did not observe any changes in *GAD1* mRNA levels or in 4-aminobutyrate aminotransferase (*ABAT*) and aldehyde dehydrogenase 5 family member A1 (*ALDH5A1*) expression, the genes encoding the other two enzymes of the GABA shunt (Figure 5.4D).

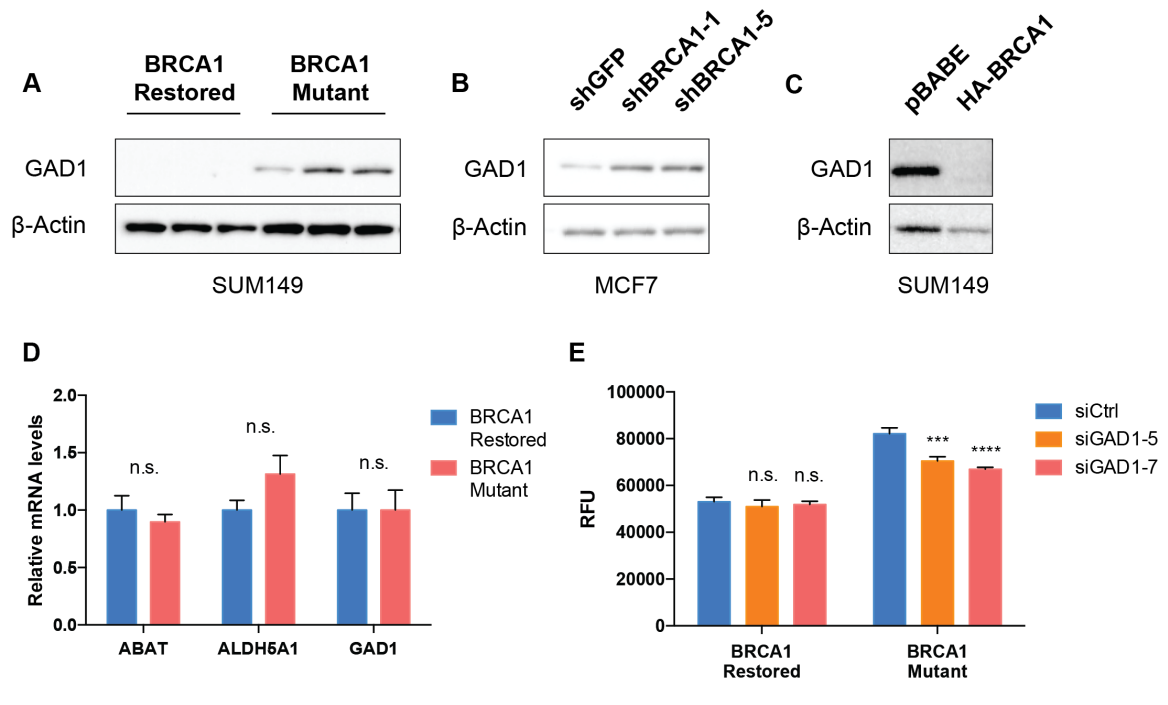


Figure 5.4 - BRCA1 loss-of-function increases GAD1 protein, but not mRNA levels.

(A-C) Immunoblot for GAD1 and β -actin using lysates extracted from: (A) BRCA1-restored or -mutant cells, the 3 lanes for each genotype represent lysates from individual clones cultured separately; (B) MCF7 cells stably transfected with the indicated shRNA; (C) SUM149 parental BRCA1-mutant cells stably overexpressing wild-type HA-BRCA1 construct or pBABE vector control as indicated.

(D) RT-qPCR quantification of indicated mRNA extracted from BRCA1-restored (blue) or -mutant (red) cells. Data is presented as mean \pm SEM ($n = 9$), and analysed by multiple t -tests with FDR correction ($Q = 1\%$).

(E) Cell density of SUM149 BRCA1-restored or -mutant cells grown for 5 days following treatment with siCtrl (blue) or siGAD1 (orange and red) and quantified using CyQuant according to the manufacturer's instructions. Data is presented as mean \pm SEM ($n = 6$), and analysed by 2-way ANOVA and Tukey's multiple comparisons test. RFU = relative fluorescence unit.

(**** $p < 0.0001$; *** $p < 0.001$; ** $p < 0.01$; * $p < 0.05$)

Finally, we observed a metabolic vulnerability to repression of GAD1 mRNA in the BRCA1-mutant cells that was not present in BRCA1-restored cells. Indeed, repression of GAD1 in BRCA1-mutant cells led to a reduction in proliferation while BRCA1-restored cells which already proliferate slower were not affected (Figure

5.4E). This suggests that BRCA1-mutant cells rely on the GABA shunt, at least in part, to support their proliferation.

5.5 Chapter discussion

As discussed previously, BRCA1 plays a broad role in cell biology, and cell metabolism is dependent on multiple intrinsic and extrinsic factors. Therefore, while BRCA1 may be important to regulate metabolism in certain contexts, that may not be true across all conditions. Accordingly, the data presented here provides one example of BRCA1 metabolic regulation that is not mutually exclusive with previously published data. Since glutamine is important for multiple cell functions, it is possible that related pathways use it for alternative purposes. For example, while BRCA1 regulates EMT, and glutamine is essential for certain EMT functions, the links between glutamine usage and EMT or glutamine usage and BRCA1 appear to be unrelated.

Our results suggest that BRCA1 regulates GAD1 protein stability/expression. The increase in GABA shunt activity and potentially related increase in glutamine consumption give BRCA1-mutant cells an increased proliferation potential or survival advantage, unveiling a novel metabolic vulnerability. While some reports suggest that GABA signalling can increase proliferation or metastasis in some context^{158,182,183}, our data supports the hypothesis that downstream metabolites processed through the GABA shunt are important for cancer growth.

De novo nucleotide synthesis is a metabolically demanding process that involves multiple feeder pathways and uses glutamine as the main source of nitrogen. Interestingly, processing of glutamine through the GABA shunt provides a more efficient nitrogen usage. We could not detect all nucleotide derivatives in our experiments, therefore it is difficult to assess whether specific steps involving aspartate or glutamine are particularly affected in *BRCA1* mutant cells. However, it is well known that nucleotides and aspartate are essential for cancer cells. Therefore, using the GABA shunt to produce these substrates more efficiently could provide *BRCA1* mutant cells with a survival advantage.

Additionally, our observations are consistent with an HR-independent role of *BRCA1* in metabolic regulation in this context. Of note, the increased sensitivity to glutamine deprivation following exposure to ionising radiation could also be explained by a reduced pool of nucleotides in the *BRCA1*-mutant cells as a result of increased consumption. Importantly, under normal glutamine conditions, enhanced burden in DSBs as a result of HR defects would only lead to a marginal increase in nucleotide pools which is insignificant compared to the nucleotides needed to replicate the whole genome.

6 Discussion

In line with the renewed interest in cancer metabolism, the role of important tumour suppressors such as BRCA1 in modulating metabolism are starting to emerge. However, more mechanistic work investigating those potential links could improve our understanding of cancer metabolism and lead to more precise and effective treatments. In this thesis, I demonstrate that metabolic rewiring induced by BRCA1 loss-of-function results in enhanced sensitivity to glutamine deprivation. Since glutamine is involved in multiple metabolic pathways, further investigation is needed to refine our understanding of the links between glutamine and BRCA1. The data presented here provides a solid base to explore those potential links, more specifically related to nitrogen-processing pathways, GABA shunt, aspartate synthesis, and nucleotides.

6.1 Microenvironment influences metabolic rewiring and homeostasis

Historically, cancer has been defined as a genetic disease driven by intrinsic cell modifications that lead to unregulated cell growth. However, in the last few decades, the importance of the microenvironment on cancer progression has become a key research interest. The microenvironment includes non-cancerous stromal and immune cells which can impact the survival of cancer cells through secretion of growth factors, nutrients, or cytokines, among other molecules¹⁸⁴⁻¹⁸⁶. Due to the high plasticity of metabolic rewiring, metabolic status of cells is dependent on the nutrients found in the microenvironment. Nutrient availability varies significantly between different tissues and is also affected by systemic

factors¹³⁰, which can provide selective pressures on cell metabolism. More specifically, circulating metabolite levels can differ from local microenvironments providing a specific niche for cancer cells. Since our work was performed in cell line models grown *in vitro*, the impact of the microenvironment was mitigated to a certain extent and the focus was more on intrinsic metabolic changes. While, secreted metabolites and consumption from the media can influence cell growth, more thorough investigation of external factors would complement the work presented here.

Since the discovery of the importance of glutamine in cancer, the variability of glutamine usage between cancer types or cancer models has been extensively explored. While most cancer cell line models grown *in vitro* require glutamine, the deprivation sensitivity is highly variable, and some cells can grow in the absence of glutamine altogether¹³³. Additionally, the sensitivity of the same cell lines implanted *in vivo* does not necessarily correlate with the *in vitro* sensitivity, suggesting effects caused by the microenvironment. This has been hypothesised to be a result of high glutamine concentrations (2-4 mM) in cell culture media, however, glutamine is also the most abundant amino acid in circulation and is equivalently concentrated in the tumour environment^{129,130}. Of note, the SUM149 cells grow in 1 mM glutamine which is within the range of physiological tumour glutamine concentrations. In some context, it has been shown that high cystine concentration in the media dictates the increased glutamine need as import of cystine is paired with export of glutamate through the xCT transporter^{137,187}. However, in our model, both genotypes were equivalently sensitive to xCT transporter inhibition and there

were no changes in GSH synthesis or ROS sensitivity. Additionally, glutamate was incorporated into downstream metabolites rather than being excreted in exchange for cystine. However, it is still possible that other nutrients in the tumour environment might influence the need for glutamine.

While we did not explore the sensitivity of SUM149 cells *in vivo* directly, it is clear that some tumours require glutamine *in vivo* which is why GLS inhibitors are being explored as treatments in clinical trials^{133,175}. Interestingly, many studies focus on glutamine functions that are interchangeable with glucose such as anaplerosis while our work focuses on nitrogen processing. It is widely accepted that glutamine is the key nitrogen donor in cancer, therefore glutamine is most likely important as a nitrogen donor *in vivo*. Accordingly, the increased sensitivity to glutamine deprivation in BRCA1-mutant cells was specific to glutamine while glucose sensitivity was equivalent between both genotypes. Therefore, the concept of cells using glucose or glutamine interchangeably to replenish the TCA cycle depending on the media concentration does not fit with our results.

Interestingly, growing the same cells at low density (1,000/well in 6-well plate) or “normal” density (5,000/well in 96-well plate) affected the response of cells to glutaminase inhibitor BTPES. Consistent with the discussion above, different growth conditions most likely affect cell metabolism and therefore usage of glutamine in different contexts. Of note, glutamine deprivation affects both colony number and overall total area while glucose withdrawal and BPTES inhibition only affect total area. Additionally, glutamine deprivation affects cells in both low and

normal density settings, suggesting alternative processing of glutamine or GLS-independent cell growth. Overall, changes in the microenvironment and external factors lead to variability in glutamine usage/dependency. However, our results point to specific aspects of glutamine functions that are relevant in the context of BRCA1 loss-of-function. It would be interesting to investigate whether these intrinsic changes are sustained in the presence of external metabolic pressures.

6.2 Glutamine is essential for various cell functions

As mentioned previously, glutamine is used across a broad range of metabolic functions including anaplerosis and synthesis of proteins, GSH, GABA, NEAA, and nucleotides¹³¹⁻¹³³. Therefore, withdrawal of glutamine from cell culture media affects a wide range of signalling and metabolic pathways. We observed an increased sensitivity to glutamine deprivation in BRCA1-mutant cells, however, both genotypes are sensitive to glutamine deprivation overall. This suggests that glutamine is essential for at least some functions that are equivalent between cells from both genotypes. To understand the changes driven by BRCA1 loss-of-function specifically, we focused our attention on changes that were more pronounced or only present in one genotype. Interestingly, it is possible that increased glutamine consumption in BRCA1-mutant cells happens through the same glutamine processing pathway being enhanced, or through alternative glutamine processing altogether, both of which are not mutually exclusive.

Looking at glutamine deprivation sensitivity and cell density/survival as a readout, we get a broad overview of whether glutamine is essential and to what

extent. However, it does not provide a clear breakdown of which aspects of glutamine are key. Interestingly, when examining GSH synthesis or ROS sensitivity, as well as migration rate, we found that glutamine is essential for each of these processes to a similar extent across both genotypes. Of note, BRCA1 modulates EMT and affects glutamine usage, however, based on our results, the changes in glutamine processing observed in BRCA1-mutant cells do not appear to be driven by EMT-related mechanisms. Therefore, the link between EMT and glutamine is most likely independent of BRCA1. Overall, deciphering which aspects of glutamine can explain the difference between BRCA1-mutant and -restored cells requires more precise investigation than looking at cell density/survival, cell cycle, or apoptosis.

Metabolic analyses can provide a more precise tool to investigate the use of specific metabolites. Our results identified the use of the GABA shunt for more efficient processing of glutamine-derived nitrogen in *BRCA1* mutant cells, resulting in the increased production of aspartate. Importantly, glutamine is still being used for functions that are common between both genotypes to a similar extent. Our data suggests, that the excess glutamine consumed by *BRCA1* mutant cells is redirected into the GABA shunt. It is also possible that some common pathways are upregulated in *BRCA1* mutant cells. However, the fractional enrichment of ^{15}N -labelled glutamate, GABA, and aspartate indicates an alternative processing pathway that is increased in *BRCA1* mutant cells and could explain the difference that we observed in glutamine deprivation sensitivity. In fact, we hypothesise that increases in GAD1 protein levels caused by BRCA1 loss-of-function drives the

increase use of the GABA shunt. Subsequently, this allows the cells a more efficient use of glutamine and more efficient production of downstream intermediates essential to support faster cell proliferation or adaptation to stress. As such, *BRCA1* mutant cells rely on the GABA shunt to maintain a higher proliferation rate than their *BRCA1* restored counterparts, and therefore have a metabolic vulnerability to GABA shunt inhibition. Analysis of metabolite levels following manipulations of the GABA shunt would confirm the importance of those changes in driving the glutamine deprivation sensitivity phenotype observed in *BRCA1* mutant cells.

Due to its role as the main inhibitory neurotransmitter in mammalian neurons, GABA synthesis has been extensively studied¹⁵². Regulation of glutamate and GABA levels in the brain is a complex process that involves multiple cell types and compartments at a tissue level. Recently, the role of GABA in cancer has started to be explored following the discovery of GABA shunt enzymes being expressed in cancer¹⁸². While some reports suggest that GABA acts on certain GABA receptors to stimulate cell proliferation or promote metastasis to the brain, other reports suggest that GABA provides inhibitory effects on cancer growth^{158,183,188}. The data presented here show a correlation between cell proliferation and GABA levels. However, based on our metabolic analysis, we hypothesise that downstream metabolites are more important for cell proliferation than GABA itself. More investigation is essential to test this hypothesis. Of note, GABA can be used as a source of carbons and nitrogen, therefore it is essential to

separate GABA signalling from the usage of GABA as a metabolic substrate when performing GABA supplementation experiments.

As mentioned previously, glutamine deprivation leads to changes in both genotypes that were more pronounced in *BRCA1*-mutant cells. This is the case with the cell cycle analysis, apoptosis assay, as well as proliferation assays. Interestingly, we also observed changes that only occurred in *BRCA1*-mutant cells such as increased sensitivity to glutamine deprivation following IR, or treatment that rescued the difference between both genotypes without rescuing the full effect, such as nucleotide supplementation rescuing the glutamine deprivation sensitivity difference. These changes appear to be more specific to the role of *BRCA1* in glutamine regulation. More specifically, both results could be explained by the nucleotide conserving phenotype that we observed in *BRCA1* mutant cells. Since *de novo* nucleotide synthesis is a metabolically demanding process, we hypothesised that it acts as the rate-limiting factor for proliferative capacity. Therefore, an overactive GABA shunt could provide more nucleotides for proliferation and DNA repair. Additionally, *BRCA1* mutant cells would rely on this metabolic rewiring and more efficient consumption of glutamine for proliferation.

6.3 Role of aspartate and glutamine in nucleotide synthesis

Our metabolic analyses demonstrate that *BRCA1* mutant cells upregulate the production of aspartate using glutamine-derived nitrogen and carbons at the expense of other amino acids. This suggests an important role for aspartate in the *BRCA1* mutant cells. However, it does not mean that glutamine itself is less

important. In fact, both glutamine and aspartate are important for synthesis of nucleotides and other NEAAs. Since glutamine deprivation affects both glutamine and aspartate levels, it is hard to differentiate between both metabolites given our current data and more investigation is needed to evaluate this question.

Interestingly, previous studies have demonstrated that glutamine is essential for nucleotide synthesis in glioblastoma. In this context, GS was used to synthesise glutamine *de novo* and excess glutamate did not enter the TCA cycle¹⁴⁰. We cannot confirm or rule out whether there is an increase in glutamine usage for nucleotide synthesis in BRCA1 loss-of-function cells, however, it is clear that upregulation of aspartate is important in *BRCA1* mutant breast cancer unlike glioblastoma.

Using the LC-MS approaches described in this thesis, we were not able to detect all relevant nucleotides and derivatives, therefore it is more challenging to decipher which aspects of nucleotide synthesis are affected by BRCA1 loss-of-function. Nucleotide synthesis is a complex and metabolically demanding process through which glutamine and aspartate are needed for different reactions. More thorough analysis of nucleotides and derivatives would allow to differentiate between the roles of glutamine and aspartate. However, negative feedback regulation of nucleotide further complicates this analysis as the cell attempts to maintain equivalent nucleotide levels. Therefore, blocking the synthesis of one nucleic base would affect the levels of all of them to a certain extent.

Unlike signalling pathways, metabolic pathways are not only regulated by expression levels and activity of enzymes but also through allosteric regulation. Therefore, the amounts of substrates on either side of the reaction are important. This complicates the idea of rate-limiting reactions or enzymes which should be considered as funnels rather than gates. In our experiments, we could rescue the glutamine deprivation phenotype with nucleotides, suggesting that this is an important function of glutamine and/or aspartate. However, due to allosteric regulation, supporting one downstream use of glutamine or aspartate has the potential to allow more of the amino acid to be used for other reactions. Therefore, supporting one downstream branch of a metabolic pathway could support the whole pathway to a certain extent. Overall, more investigation is needed to refine the role of aspartate and glutamine in *BRCA1* mutant breast cancer.

6.4 BRCA1 in metabolic rewiring and tumour progression

One of the key questions in cancer biology is what factors are involved in cancer progression. We know that mutations in key tumour suppressors or oncogenes can lead to cancer development by activating essential pathways, however, in certain context those mutations can be present in cells that are non-cancerous. Additionally, extrinsic factors in the microenvironment provide evolutionary pressures necessary for cancer progression. This means that the analysis of the mutational landscape of a tumour cannot consistently predict the outcome, but rather, most likely reflects the history of its progression. Mutations that previously provided a survival advantage in a past cell environment are still present but are not essential for survival anymore. Those “passenger” mutations

are then difficult to differentiate from “driver” mutations essential for survival in the current tumour niche.

Given the increased cancer risk associated with *BRCA1* germline mutations, the role of *BRCA1* has been extensively explored in tumour progression. While *BRCA1* is important for HR across all cell/tissue types, a key research focus is to understand why *BRCA1* germline mutations mostly lead to predisposition to breast and ovarian cancer specifically, and to a much lesser extent to other cancers. Some hypotheses have been postulated based on the role of *BRCA1* in DNA repair and DDR, however, recent evidence have also demonstrated that *BRCA1* can regulate cell fate and cancer stemness through different mechanisms⁷⁴. While DNA repair is an essential cell function, regulating cancer cell stemness and cell fate has broader implications and leads to changes in cell physiology that rely on interactions with the microenvironment. Interestingly, it is widely accepted that different tissue types provide different microenvironments, with nutrients and metabolism being an important aspect¹³⁰. Therefore, the combination of *BRCA1* mutations within a specific metabolic environment could explain the tissue specific predisposition to certain cancers.

As discussed in the introduction, manipulating the expression or mutation status of *BRCA1* leads to broad metabolic changes across different cancers/cell types. While some reports have demonstrated that *BRCA1* directly regulates certain metabolic enzymes or transcription factors, *BRCA1* could also play a more modulatory role on important cell functions which subsequently affect metabolic

needs. We observed that *BRCA1* mutant cells express high GAD1 protein levels which could, at least in part, explain the glutamine deprivation sensitivity and metabolic rewiring observed in our models. However, more investigation is needed to determine whether *BRCA1* regulates GAD1 expression directly. One potential explanation is that *BRCA1* regulates the ubiquitination of GAD1 through its E3 ubiquitin ligase activity and therefore regulates the stability/degradation of GAD1. However, based on the previous literature, *BRCA1* could also play a role in direct or modulatory role in many other aspects of metabolism. As such, some of the previously described general metabolic changes were consistent with our results, while others were not^{91,93}. We also observed increased dependency to fatty acids as a substrate for mitochondrial respiration, and increased glycolytic capacity in *BRCA1*-mutant cells. Together, these results suggest that the role of *BRCA1* in metabolism is variable and context dependent. Since glutamine deprivation is a metabolic vulnerability in *BRCA1* mutant cells in our models, it provides a strong justification to investigate glutamine downstream pathways more specifically. As with mutation profiles, the metabolic changes occurring in cancer cells are most likely not all essential at any one point, but rather specific to certain contexts within the tumour history. Therefore, while *BRCA1* manipulations lead to diverse metabolic changes, we focused our research on the role of glutamine.

The main SUM149 cell line model that we used is a unique model where tumour cells have developed with a *BRCA1* mutation over multiple cell divisions and in which the *BRCA1* reading frame was restored. It differs from models where *BRCA1* mRNA is repressed in the context of tumours growing with wild-type

BRCA1, and it also differs from models where wild-type *BRCA1* is overexpressed since the restored *BRCA1* is still under physiological regulation. Importantly, we could still replicate our findings in different cell line models that expressed wild-type *BRCA1* by downregulating its expression. However, as expected, we observed variability in the glutamine deprivation sensitivity of different cell lines, as well as variability in the metabolic rewiring induced by downregulation of *BRCA1*.

Therefore, other factors apart from *BRCA1* mutation status alone are probably needed to explain the metabolic changes that we observed in our model. Our results explore one link between *BRCA1* and metabolism, however, given the cancer heterogeneity across cancer types and even within individual tumours, more work is needed to investigate in which contexts this metabolic regulation is essential.

6.5 The importance of cancer metabolism in clinical treatment

Although glutamine is a NEAA in normal cells, it is widely accepted that it becomes essential in certain cancer subtypes and has been described as conditionally essential. Therefore, clinical treatments where glutamine usage could be blocked or manipulated to prevent tumour growth have started to be explored^{103,175}. However, while it is clear that glutamine is essential in certain contexts, its exact roles and relevant context is still not fully understood. A better understanding of the downstream use of glutamine into appropriate metabolic pathways would provide a more solid foundation to explore how manipulating glutamine could lead to better clinical outcomes. For example, one of the more promising drugs in clinical trials to block the use of glutamine in cancer cells is the

GLS1 inhibitor CB-839¹⁸⁹. There are currently six ongoing clinical trials for CB-839 in patients with advanced solid tumours or colorectal cancer. Refining the patient population or therapeutic approach with a more thorough understanding of glutamine metabolism could accelerate the approval of CB-839 and other glutamine related drugs and lead to more targeted approaches.

Importantly, as discussed before, inhibition of GLS1 is not equivalent to complete glutamine deprivation. Interestingly, other drugs such as glutamine antagonist, DON, can affect every aspect of glutamine processing. However, early clinical trials with DON have shown high toxicity and side effects¹⁹⁰. Therefore, more precise targeting of downstream uses of glutamine within certain contexts could lead to more efficient treatments with fewer side effects. Additionally, it is important to distinguish between the multiple functions of glutamine, as GLS1 inhibition does not prevent nucleotide synthesis from glutamine. In fact, GLS1 inhibition does not completely block the production of glutamate as it can be produced from alternative reactions using glutamine. However, blocking glutamate production altogether might be toxic to cells. Therefore, understanding which metabolic pathways of glutamine usage are essential in different context/environment could lead to better treatments.

With the improvements in our understanding of cancer biology and the increase in resulting targeted therapies, an interesting concept that has emerged is the idea of synthetic lethality. Briefly, synthetic lethality describes a situation through which molecular changes in cancer cells render them sensitive to an

otherwise non-lethal treatment/condition in normal cells. The most well-known example is the use of PARP inhibitors for the treatment of *BRCA1/2* mutant cancers which is now clinically approved^{61,191}. Interestingly, this concept can easily be applied to metabolic vulnerabilities. In fact, metabolic rewiring that occurs in cancer often results from changes in metabolic needs between normal and cancerous cells. Therefore, identifying key metabolic vulnerabilities in different contexts could provide synthetic lethal interactions with metabolism. In fact, multiple examples reviewed in Luengo *et al.* have started to emerge from the recent studies of cancer metabolism¹⁰³. One example is the use of mitochondrial complex I inhibitor metformin which is used for the management of type 2 diabetes. Surprisingly, inhibition of mitochondrial respiration with metformin is not toxic to normal cells, however, it leads to complete tumour regression in some breast cancer patients and promising results in various mouse cancer models^{103,192,193}. Interestingly, a number of commonly used chemotherapeutic drugs such as 6-mercaptopurine, 6-thioguanine, and 5-fluorouracil are part of a drug class called antimetabolites. As their name suggests, these metabolite analogues block the synthesis of certain metabolites such as nucleotides¹⁰³. While their mechanism of action is broad and leads to side effects, it demonstrates that targeting cells based on their metabolic changes is a promising approach. Another example where metabolic understanding can lead to improved treatment is with PI3K inhibitors. Although, *PIK3CA* and *PTEN* mutations lead to overactive PI3K in many cancers, PI3K inhibitors have failed in the clinic due to PI3K inhibitor-induced insulin feedback. Interestingly, pharmacological inhibition or dietary intervention such as ketogenic diet suppresses insulin feedback and results in efficient PI3K

inhibition¹⁹⁴. Unlike with the ketogenic diet, removing all glutamine from the diet could be very challenging and might not prove to be a successful intervention, however, it opens the door to noticing how changes in lifestyle could improve cancer prognosis.

Since the discovery of tumour suppressor genes and oncogenes, combined with the development of Alfred Knudson's "two-hit" hypothesis¹⁹⁵, cancer has mostly been defined as a genetic disease. However, we are confronted regularly by epidemiological studies that provide evidence of a more complex story. While one could argue that environmental factors lead to mutations in those key tumour suppressor genes or oncogenes, the variability observed from different geographical regions or patient groups suggests that other factors underlie the development of cancer^{196,197}. As discussed above, there is an increasing amount of research focused on understanding how the tumour microenvironment, which is itself affected by systemic changes, might modulate cancer growth. Therefore, systemic changes in metabolism as a result of diet, physical activity, stress, or environmental stimuli are most likely affecting cancer progression. More research in understanding the impact of lifestyle changes on cancer metabolism could provide more efficient cancer treatments.

6.6 Conclusion

The data presented in this thesis demonstrate a role for BRCA1 in modulating sensitivity to glutamine deprivation. More specifically, *BRCA1* mutant cells process glutamine more efficiently through the GABA shunt and upregulate the production

of aspartate and other downstream metabolites to support increased cell proliferation. We hypothesise that this is, at least in part, driven by high GAD1 protein expression due to loss-of-function of BRCA1. More research is needed to confirm the metabolic phenotype observed and investigate the link between GAD1 and BRCA1. However, the work presented here provides a solid base to further investigate the role of BRCA1 in glutamine metabolism and potentially improve treatments in *BRCA1* mutant cancers.

7 References

- 1 Collaborators, G. B. D. C. o. D. Global, regional, and national age-sex-specific mortality for 282 causes of death in 195 countries and territories, 1980-2017: a systematic analysis for the Global Burden of Disease Study 2017. *Lancet* **392**, 1736-1788, doi:10.1016/S0140-6736(18)32203-7 (2018).
- 2 Dagenais, G. R. *et al.* Variations in common diseases, hospital admissions, and deaths in middle-aged adults in 21 countries from five continents (PURE): a prospective cohort study. *Lancet*, doi:10.1016/S0140-6736(19)32007-0 (2019).
- 3 Yusuf, S. *et al.* Modifiable risk factors, cardiovascular disease, and mortality in 155 722 individuals from 21 high-income, middle-income, and low-income countries (PURE): a prospective cohort study. *Lancet*, doi:10.1016/S0140-6736(19)32008-2 (2019).
- 4 Vrinten, C. *et al.* What do people fear about cancer? A systematic review and meta-synthesis of cancer fears in the general population. *Psychooncology* **26**, 1070-1079, doi:10.1002/pon.4287 (2017).
- 5 Bray, F. *et al.* Global cancer statistics 2018: GLOBOCAN estimates of incidence and mortality worldwide for 36 cancers in 185 countries. *CA Cancer J Clin* **68**, 394-424, doi:10.3322/caac.21492 (2018).
- 6 Onitilo, A. A., Engel, J. M., Greenlee, R. T. & Mukesh, B. N. Breast cancer subtypes based on ER/PR and Her2 expression: comparison of clinicopathologic features and survival. *Clin Med Res* **7**, 4-13, doi:10.3121/cm.2009.825 (2009).
- 7 Perou, C. M. *et al.* Molecular portraits of human breast tumours. *Nature* **406**, 747-752, doi:10.1038/35021093 (2000).
- 8 Prat, A. *et al.* Clinical implications of the intrinsic molecular subtypes of breast cancer. *Breast* **24 Suppl 2**, S26-35, doi:10.1016/j.breast.2015.07.008 (2015).
- 9 Prat, A., Parker, J. S., Fan, C. & Perou, C. M. PAM50 assay and the three-gene model for identifying the major and clinically relevant molecular subtypes of breast cancer. *Breast Cancer Res Treat* **135**, 301-306, doi:10.1007/s10549-012-2143-0 (2012).
- 10 Prat, A. *et al.* Genomic analyses across six cancer types identify basal-like breast cancer as a unique molecular entity. *Sci Rep* **3**, 3544, doi:10.1038/srep03544 (2013).
- 11 Harbeck, N. & Gnant, M. Breast cancer. *Lancet* **389**, 1134-1150, doi:10.1016/S0140-6736(16)31891-8 (2017).

- 12 McDonald, E. S., Clark, A. S., Tchou, J., Zhang, P. & Freedman, G. M. Clinical Diagnosis and Management of Breast Cancer. *J Nucl Med* **57 Suppl 1**, 9S-16S, doi:10.2967/jnumed.115.157834 (2016).
- 13 Miller, W. R. Aromatase inhibitors: mechanism of action and role in the treatment of breast cancer. *Semin Oncol* **30**, 3-11 (2003).
- 14 Yu, F. L. & Bender, W. A proposed mechanism of tamoxifen in breast cancer prevention. *Cancer Detect Prev* **26**, 370-375 (2002).
- 15 Atchley, D. P. *et al.* Clinical and pathologic characteristics of patients with BRCA-positive and BRCA-negative breast cancer. *J Clin Oncol* **26**, 4282-4288, doi:10.1200/JCO.2008.16.6231 (2008).
- 16 Foulkes, W. D. *et al.* Germline BRCA1 mutations and a basal epithelial phenotype in breast cancer. *J Natl Cancer Inst* **95**, 1482-1485 (2003).
- 17 Antoniou, A. C. *et al.* Breast and ovarian cancer risks to carriers of the BRCA1 5382insC and 185delAG and BRCA2 6174delT mutations: a combined analysis of 22 population based studies. *J Med Genet* **42**, 602-603, doi:10.1136/jmg.2004.024133 (2005).
- 18 King, M. C., Marks, J. H., Mandell, J. B. & New York Breast Cancer Study, G. Breast and ovarian cancer risks due to inherited mutations in BRCA1 and BRCA2. *Science* **302**, 643-646, doi:10.1126/science.1088759 (2003).
- 19 Hall, J. M. *et al.* Linkage of early-onset familial breast cancer to chromosome 17q21. *Science* **250**, 1684-1689, doi:10.1126/science.2270482 (1990).
- 20 Miki, Y. *et al.* A strong candidate for the breast and ovarian cancer susceptibility gene BRCA1. *Science* **266**, 66-71, doi:10.1126/science.7545954 (1994).
- 21 Wooster, R. *et al.* Identification of the breast cancer susceptibility gene BRCA2. *Nature* **378**, 789-792, doi:10.1038/378789a0 (1995).
- 22 Wooster, R. *et al.* Localization of a breast cancer susceptibility gene, BRCA2, to chromosome 13q12-13. *Science* **265**, 2088-2090, doi:10.1126/science.8091231 (1994).
- 23 Risch, H. A. *et al.* Prevalence and penetrance of germline BRCA1 and BRCA2 mutations in a population series of 649 women with ovarian cancer. *Am J Hum Genet* **68**, 700-710, doi:10.1086/318787 (2001).
- 24 Narod, S. A. & Foulkes, W. D. BRCA1 and BRCA2: 1994 and beyond. *Nat Rev Cancer* **4**, 665-676, doi:10.1038/nrc1431 (2004).

- 25 de Bock, G. H. *et al.* A family history of breast cancer will not predict female early onset breast cancer in a population-based setting. *BMC Cancer* **8**, 203, doi:10.1186/1471-2407-8-203 (2008).
- 26 Cicenás, J. *et al.* KRAS, TP53, CDKN2A, SMAD4, BRCA1, and BRCA2 Mutations in Pancreatic Cancer. *Cancers (Basel)* **9**, doi:10.3390/cancers9050042 (2017).
- 27 Futreal, P. A. *et al.* BRCA1 mutations in primary breast and ovarian carcinomas. *Science* **266**, 120-122 (1994).
- 28 Janatova, M., Zikan, M., Dundr, P., Matous, B. & Pohlreich, P. Novel somatic mutations in the BRCA1 gene in sporadic breast tumors. *Hum Mutat* **25**, 319, doi:10.1002/humu.9308 (2005).
- 29 Scully, R., Panday, A., Elango, R. & Willis, N. A. DNA double-strand break repair-pathway choice in somatic mammalian cells. *Nat Rev Mol Cell Biol*, doi:10.1038/s41580-019-0152-0 (2019).
- 30 Paques, F. & Haber, J. E. Multiple pathways of recombination induced by double-strand breaks in *Saccharomyces cerevisiae*. *Microbiol Mol Biol Rev* **63**, 349-404 (1999).
- 31 Rothkamm, K., Kruger, I., Thompson, L. H. & Lobrich, M. Pathways of DNA double-strand break repair during the mammalian cell cycle. *Mol Cell Biol* **23**, 5706-5715 (2003).
- 32 Sung, P. & Klein, H. Mechanism of homologous recombination: mediators and helicases take on regulatory functions. *Nat Rev Mol Cell Biol* **7**, 739-750, doi:10.1038/nrm2008 (2006).
- 33 Pannunzio, N. R., Watanabe, G. & Lieber, M. R. Nonhomologous DNA end-joining for repair of DNA double-strand breaks. *J Biol Chem* **293**, 10512-10523, doi:10.1074/jbc.TM117.000374 (2018).
- 34 Ferguson, D. O. *et al.* The nonhomologous end-joining pathway of DNA repair is required for genomic stability and the suppression of translocations. *Proc Natl Acad Sci U S A* **97**, 6630-6633, doi:10.1073/pnas.110152897 (2000).
- 35 Moynahan, M. E., Chiu, J. W., Koller, B. H. & Jasin, M. Brca1 controls homology-directed DNA repair. *Mol Cell* **4**, 511-518 (1999).
- 36 Scully, R. *et al.* Association of BRCA1 with Rad51 in mitotic and meiotic cells. *Cell* **88**, 265-275 (1997).
- 37 Roy, R., Chun, J. & Powell, S. N. BRCA1 and BRCA2: different roles in a common pathway of genome protection. *Nat Rev Cancer* **12**, 68-78, doi:10.1038/nrc3181 (2011).

- 38 Yuan, S. S. *et al.* BRCA2 is required for ionizing radiation-induced assembly of Rad51 complex in vivo. *Cancer Res* **59**, 3547-3551 (1999).
- 39 Shahid, T. *et al.* Structure and mechanism of action of the BRCA2 breast cancer tumor suppressor. *Nat Struct Mol Biol* **21**, 962-968, doi:10.1038/nsmb.2899 (2014).
- 40 Sullivan, M. R. & Bernstein, K. A. RAD-ical New Insights into RAD51 Regulation. *Genes (Basel)* **9**, doi:10.3390/genes9120629 (2018).
- 41 Fradet-Turcotte, A., Sitz, J., Grapton, D. & Orthwein, A. BRCA2 functions: from DNA repair to replication fork stabilization. *Endocr Relat Cancer* **23**, T1-T17, doi:10.1530/ERC-16-0297 (2016).
- 42 Clark, S. L., Rodriguez, A. M., Snyder, R. R., Hankins, G. D. & Boehning, D. Structure-Function Of The Tumor Suppressor BRCA1. *Comput Struct Biotechnol J* **1**, doi:10.5936/csbj.201204005 (2012).
- 43 Liang, Y. *et al.* Structural analysis of BRCA1 reveals modification hotspot. *Sci Adv* **3**, e1701386, doi:10.1126/sciadv.1701386 (2017).
- 44 Hoa, N. N. *et al.* BRCA1 and CtIP Are Both Required to Recruit Dna2 at Double-Strand Breaks in Homologous Recombination. *PLoS One* **10**, e0124495, doi:10.1371/journal.pone.0124495 (2015).
- 45 Yu, X., Fu, S., Lai, M., Baer, R. & Chen, J. BRCA1 ubiquitinates its phosphorylation-dependent binding partner CtIP. *Genes Dev* **20**, 1721-1726, doi:10.1101/gad.1431006 (2006).
- 46 Daley, J. M. & Sung, P. 53BP1, BRCA1, and the choice between recombination and end joining at DNA double-strand breaks. *Mol Cell Biol* **34**, 1380-1388, doi:10.1128/MCB.01639-13 (2014).
- 47 Densham, R. M. & Morris, J. R. Moving Mountains-The BRCA1 Promotion of DNA Resection. *Front Mol Biosci* **6**, 79, doi:10.3389/fmolb.2019.00079 (2019).
- 48 Sivanand, S. *et al.* Nuclear Acetyl-CoA Production by ACLY Promotes Homologous Recombination. *Mol Cell* **67**, 252-265 e256, doi:10.1016/j.molcel.2017.06.008 (2017).
- 49 Liao, H., Ji, F., Helleday, T. & Ying, S. Mechanisms for stalled replication fork stabilization: new targets for synthetic lethality strategies in cancer treatments. *EMBO Rep* **19**, doi:10.15252/embr.201846263 (2018).
- 50 Cortez, D. Preventing replication fork collapse to maintain genome integrity. *DNA Repair (Amst)* **32**, 149-157, doi:10.1016/j.dnarep.2015.04.026 (2015).

- 51 Ying, S. *et al.* DNA-PKcs and PARP1 Bind to Unresected Stalled DNA Replication Forks Where They Recruit XRCC1 to Mediate Repair. *Cancer Res* **76**, 1078-1088, doi:10.1158/0008-5472.CAN-15-0608 (2016).
- 52 Maffia, A., Ranise, C. & Sabbioneda, S. From R-Loops to G-Quadruplexes: Emerging New Threats for the Replication Fork. *Int J Mol Sci* **21**, doi:10.3390/ijms21041506 (2020).
- 53 Garcia-Muse, T. & Aguilera, A. Transcription-replication conflicts: how they occur and how they are resolved. *Nat Rev Mol Cell Biol* **17**, 553-563, doi:10.1038/nrm.2016.88 (2016).
- 54 Schlacher, K. *et al.* Double-strand break repair-independent role for BRCA2 in blocking stalled replication fork degradation by MRE11. *Cell* **145**, 529-542, doi:10.1016/j.cell.2011.03.041 (2011).
- 55 Schlacher, K., Wu, H. & Jasin, M. A distinct replication fork protection pathway connects Fanconi anemia tumor suppressors to RAD51-BRCA1/2. *Cancer Cell* **22**, 106-116, doi:10.1016/j.ccr.2012.05.015 (2012).
- 56 Ying, S., Hamdy, F. C. & Helleday, T. Mre11-dependent degradation of stalled DNA replication forks is prevented by BRCA2 and PARP1. *Cancer Res* **72**, 2814-2821, doi:10.1158/0008-5472.CAN-11-3417 (2012).
- 57 Lord, C. J. & Ashworth, A. BRCAness revisited. *Nat Rev Cancer* **16**, 110-120, doi:10.1038/nrc.2015.21 (2016).
- 58 Hopkins, T. A. *et al.* Mechanistic Dissection of PARP1 Trapping and the Impact on In Vivo Tolerability and Efficacy of PARP Inhibitors. *Mol Cancer Res* **13**, 1465-1477, doi:10.1158/1541-7786.MCR-15-0191-T (2015).
- 59 Murai, J. *et al.* Trapping of PARP1 and PARP2 by Clinical PARP Inhibitors. *Cancer Res* **72**, 5588-5599, doi:10.1158/0008-5472.CAN-12-2753 (2012).
- 60 Ray Chaudhuri, A. *et al.* Replication fork stability confers chemoresistance in BRCA-deficient cells. *Nature* **535**, 382-387, doi:10.1038/nature18325 (2016).
- 61 Jiang, X., Li, W., Li, X., Bai, H. & Zhang, Z. Current status and future prospects of PARP inhibitor clinical trials in ovarian cancer. *Cancer Manag Res* **11**, 4371-4390, doi:10.2147/CMAR.S200524 (2019).
- 62 Bouwman, P. & Jonkers, J. The effects of deregulated DNA damage signalling on cancer chemotherapy response and resistance. *Nat Rev Cancer* **12**, 587-598, doi:10.1038/nrc3342 (2012).
- 63 Quinet, A. *et al.* PRIMPOL-Mediated Adaptive Response Suppresses Replication Fork Reversal in BRCA-Deficient Cells. *Mol Cell* **77**, 461-474 e469, doi:10.1016/j.molcel.2019.10.008 (2020).

- 64 Wang, Q., Zhang, H., Fishel, R. & Greene, M. I. BRCA1 and cell signaling. *Oncogene* **19**, 6152-6158, doi:10.1038/sj.onc.1203974 (2000).
- 65 Deng, C. X. BRCA1: cell cycle checkpoint, genetic instability, DNA damage response and cancer evolution. *Nucleic Acids Res* **34**, 1416-1426, doi:10.1093/nar/gkl010 (2006).
- 66 Wu, J., Lu, L. Y. & Yu, X. The role of BRCA1 in DNA damage response. *Protein Cell* **1**, 117-123, doi:10.1007/s13238-010-0010-5 (2010).
- 67 Jackson, S. P. & Bartek, J. The DNA-damage response in human biology and disease. *Nature* **461**, 1071-1078, doi:10.1038/nature08467 (2009).
- 68 Haber, D. BRCA1: an emerging role in the cellular response to DNA damage. *Lancet* **355**, 2090-2091, doi:10.1016/S0140-6736(00)02371-0 (2000).
- 69 Shaltiel, I. A., Krenning, L., Bruinsma, W. & Medema, R. H. The same, only different - DNA damage checkpoints and their reversal throughout the cell cycle. *J Cell Sci* **128**, 607-620, doi:10.1242/jcs.163766 (2015).
- 70 Hartwell, L. H. & Weinert, T. A. Checkpoints: controls that ensure the order of cell cycle events. *Science* **246**, 629-634, doi:10.1126/science.2683079 (1989).
- 71 Shiloh, Y. & Ziv, Y. The ATM protein kinase: regulating the cellular response to genotoxic stress, and more. *Nat Rev Mol Cell Biol* **14**, 197-210 (2013).
- 72 Yarden, R. I., Pardo-Reoyo, S., Sgagias, M., Cowan, K. H. & Brody, L. C. BRCA1 regulates the G2/M checkpoint by activating Chk1 kinase upon DNA damage. *Nat Genet* **30**, 285-289, doi:10.1038/ng837 (2002).
- 73 Yu, X. & Chen, J. DNA damage-induced cell cycle checkpoint control requires CtlP, a phosphorylation-dependent binding partner of BRCA1 C-terminal domains. *Mol Cell Biol* **24**, 9478-9486, doi:10.1128/MCB.24.21.9478-9486.2004 (2004).
- 74 Gorodetska, I., Kozeretska, I. & Dubrovskaya, A. BRCA Genes: The Role in Genome Stability, Cancer Stemness and Therapy Resistance. *J Cancer* **10**, 2109-2127, doi:10.7150/jca.30410 (2019).
- 75 Mullan, P. B., Quinn, J. E. & Harkin, D. P. The role of BRCA1 in transcriptional regulation and cell cycle control. *Oncogene* **25**, 5854-5863, doi:10.1038/sj.onc.1209872 (2006).
- 76 Bai, F. *et al.* BRCA1 suppresses epithelial-to-mesenchymal transition and stem cell dedifferentiation during mammary and tumor development. *Cancer Res* **74**, 6161-6172, doi:10.1158/0008-5472.CAN-14-1119 (2014).

- 77 Tkocz, D. *et al.* BRCA1 and GATA3 corepress FOXC1 to inhibit the pathogenesis of basal-like breast cancers. *Oncogene* **31**, 3667-3678, doi:10.1038/onc.2011.531 (2012).
- 78 Dongre, A. & Weinberg, R. A. New insights into the mechanisms of epithelial-mesenchymal transition and implications for cancer. *Nat Rev Mol Cell Biol* **20**, 69-84, doi:10.1038/s41580-018-0080-4 (2019).
- 79 Kim, H., Lin, Q. & Yun, Z. BRCA1 regulates the cancer stem cell fate of breast cancer cells in the context of hypoxia and histone deacetylase inhibitors. *Sci Rep* **9**, 9702, doi:10.1038/s41598-019-46210-y (2019).
- 80 Liu, S. *et al.* BRCA1 regulates human mammary stem/progenitor cell fate. *Proc Natl Acad Sci U S A* **105**, 1680-1685, doi:10.1073/pnas.0711613105 (2008).
- 81 Buckley, N. E. *et al.* BRCA1 is a key regulator of breast differentiation through activation of Notch signalling with implications for anti-endocrine treatment of breast cancers. *Nucleic Acids Res* **41**, 8601-8614, doi:10.1093/nar/gkt626 (2013).
- 82 Starita, L. M. & Parvin, J. D. The multiple nuclear functions of BRCA1: transcription, ubiquitination and DNA repair. *Curr Opin Cell Biol* **15**, 345-350, doi:10.1016/s0955-0674(03)00042-5 (2003).
- 83 Wang, Q., Zhang, H., Kajino, K. & Greene, M. I. BRCA1 binds c-Myc and inhibits its transcriptional and transforming activity in cells. *Oncogene* **17**, 1939-1948, doi:10.1038/sj.onc.1202403 (1998).
- 84 Zhang, H. *et al.* BRCA1 physically associates with p53 and stimulates its transcriptional activity. *Oncogene* **16**, 1713-1721, doi:10.1038/sj.onc.1201932 (1998).
- 85 Zheng, L., Annab, L. A., Afshari, C. A., Lee, W. H. & Boyer, T. G. BRCA1 mediates ligand-independent transcriptional repression of the estrogen receptor. *Proc Natl Acad Sci U S A* **98**, 9587-9592, doi:10.1073/pnas.171174298 (2001).
- 86 Gao, B. *et al.* Constitutive activation of JAK-STAT3 signaling by BRCA1 in human prostate cancer cells. *FEBS Lett* **488**, 179-184, doi:10.1016/s0014-5793(00)02430-3 (2001).
- 87 Ouchi, T., Lee, S. W., Ouchi, M., Aaronson, S. A. & Horvath, C. M. Collaboration of signal transducer and activator of transcription 1 (STAT1) and BRCA1 in differential regulation of IFN-gamma target genes. *Proc Natl Acad Sci U S A* **97**, 5208-5213, doi:10.1073/pnas.080469697 (2000).
- 88 Stefansson, O. A. & Esteller, M. BRCA1 as a tumor suppressor linked to the regulation of epigenetic states: keeping oncomiRs under control. *Breast Cancer Res* **14**, 304, doi:10.1186/bcr3119 (2012).

- 89 Ye, Q. *et al.* BRCA1-induced large-scale chromatin unfolding and allele-specific effects of cancer-predisposing mutations. *J Cell Biol* **155**, 911-921, doi:10.1083/jcb.200108049 (2001).
- 90 Zhang, X. *et al.* BRCA1 mutations attenuate super-enhancer function and chromatin looping in haploinsufficient human breast epithelial cells. *Breast Cancer Res* **21**, 51, doi:10.1186/s13058-019-1132-1 (2019).
- 91 Cuyas, E. *et al.* Germline BRCA1 mutation reprograms breast epithelial cell metabolism towards mitochondrial-dependent biosynthesis: evidence for metformin-based "starvation" strategies in BRCA1 carriers. *Oncotarget* **7**, 52974-52992, doi:10.18632/oncotarget.9732 (2016).
- 92 Gorrini, C. *et al.* BRCA1 interacts with Nrf2 to regulate antioxidant signaling and cell survival. *J Exp Med* **210**, 1529-1544, doi:10.1084/jem.20121337 (2013).
- 93 Privat, M. *et al.* BRCA1 induces major energetic metabolism reprogramming in breast cancer cells. *PLoS One* **9**, e102438, doi:10.1371/journal.pone.0102438 (2014).
- 94 Warburg, O. On the origin of cancer cells. *Science* **123**, 309-314 (1956).
- 95 Warburg, O., Wind, F. & Negelein, E. The Metabolism of Tumors in the Body. *J Gen Physiol* **8**, 519-530 (1927).
- 96 Vander Heiden, M. G., Cantley, L. C. & Thompson, C. B. Understanding the Warburg effect: the metabolic requirements of cell proliferation. *Science* **324**, 1029-1033, doi:10.1126/science.1160809 (2009).
- 97 Koppenol, W. H., Bounds, P. L. & Dang, C. V. Otto Warburg's contributions to current concepts of cancer metabolism. *Nat Rev Cancer* **11**, 325-337, doi:10.1038/nrc3038 (2011).
- 98 Fu, Y. *et al.* The reverse Warburg effect is likely to be an Achilles' heel of cancer that can be exploited for cancer therapy. *Oncotarget* **8**, 57813-57825, doi:10.18632/oncotarget.18175 (2017).
- 99 Pavlova, N. N. & Thompson, C. B. The Emerging Hallmarks of Cancer Metabolism. *Cell Metab* **23**, 27-47, doi:10.1016/j.cmet.2015.12.006 (2016).
- 100 Vander Heiden, M. G. & DeBerardinis, R. J. Understanding the Intersections between Metabolism and Cancer Biology. *Cell* **168**, 657-669, doi:10.1016/j.cell.2016.12.039 (2017).
- 101 Davidson, S. M. *et al.* Environment Impacts the Metabolic Dependencies of Ras-Driven Non-Small Cell Lung Cancer. *Cell Metab* **23**, 517-528, doi:10.1016/j.cmet.2016.01.007 (2016).

- 102 Possemato, R. *et al.* Functional genomics reveal that the serine synthesis pathway is essential in breast cancer. *Nature* **476**, 346-350, doi:10.1038/nature10350 (2011).
- 103 Luengo, A., Gui, D. Y. & Vander Heiden, M. G. Targeting Metabolism for Cancer Therapy. *Cell Chem Biol* **24**, 1161-1180, doi:10.1016/j.chembiol.2017.08.028 (2017).
- 104 Mullarky, E. *et al.* Identification of a small molecule inhibitor of 3-phosphoglycerate dehydrogenase to target serine biosynthesis in cancers. *Proc Natl Acad Sci U S A* **113**, 1778-1783, doi:10.1073/pnas.1521548113 (2016).
- 105 Pacold, M. E. *et al.* A PHGDH inhibitor reveals coordination of serine synthesis and one-carbon unit fate. *Nat Chem Biol* **12**, 452-458, doi:10.1038/nchembio.2070 (2016).
- 106 Chen, J. *et al.* Phosphoglycerate dehydrogenase is dispensable for breast tumor maintenance and growth. *Oncotarget* **4**, 2502-2511, doi:10.18632/oncotarget.1540 (2013).
- 107 Tateishi, K. *et al.* Extreme Vulnerability of IDH1 Mutant Cancers to NAD⁺ Depletion. *Cancer Cell* **28**, 773-784, doi:10.1016/j.ccell.2015.11.006 (2015).
- 108 Turcan, S. *et al.* Efficient induction of differentiation and growth inhibition in IDH1 mutant glioma cells by the DNMT Inhibitor Decitabine. *Oncotarget* **4**, 1729-1736, doi:10.18632/oncotarget.1412 (2013).
- 109 Alberts, B. *Molecular Biology of the Cell*. (CRC Press, 2017).
- 110 Liu, Y. *et al.* Metabolic reprogramming results in abnormal glycolysis in gastric cancer: a review. *Onco Targets Ther* **12**, 1195-1204, doi:10.2147/OTT.S189687 (2019).
- 111 Zdravlevic, M., Marchiq, I., de Padua, M. M. C., Parks, S. K. & Pouyssegur, J. Metabolic Plasticity in Cancers-Distinct Role of Glycolytic Enzymes GPI, LDHs or Membrane Transporters MCTs. *Front Oncol* **7**, 313, doi:10.3389/fonc.2017.00313 (2017).
- 112 Stein, L. R. & Imai, S. The dynamic regulation of NAD metabolism in mitochondria. *Trends Endocrinol Metab* **23**, 420-428, doi:10.1016/j.tem.2012.06.005 (2012).
- 113 Anderson, N. M., Mucka, P., Kern, J. G. & Feng, H. The emerging role and targetability of the TCA cycle in cancer metabolism. *Protein Cell* **9**, 216-237, doi:10.1007/s13238-017-0451-1 (2018).
- 114 Labuschagne, C. F., Cheung, E. C., Blagih, J., Domart, M. C. & Vousden, K. H. Cell Clustering Promotes a Metabolic Switch that Supports Metastatic Colonization. *Cell Metab*, doi:10.1016/j.cmet.2019.07.014 (2019).

- 115 Jiang, L. *et al.* Reductive carboxylation supports redox homeostasis during anchorage-independent growth. *Nature* **532**, 255-258, doi:10.1038/nature17393 (2016).
- 116 Hanse, E. A. *et al.* Cytosolic malate dehydrogenase activity helps support glycolysis in actively proliferating cells and cancer. *Oncogene* **36**, 3915-3924, doi:10.1038/onc.2017.36 (2017).
- 117 Ernster, L. & Schatz, G. Mitochondria: a historical review. *J Cell Biol* **91**, 227s-255s, doi:10.1083/jcb.91.3.227s (1981).
- 118 Vyas, S., Zaganjor, E. & Haigis, M. C. Mitochondria and Cancer. *Cell* **166**, 555-566, doi:10.1016/j.cell.2016.07.002 (2016).
- 119 Solaini, G., Sgarbi, G. & Baracca, A. Oxidative phosphorylation in cancer cells. *Biochim Biophys Acta* **1807**, 534-542, doi:10.1016/j.bbabi.2010.09.003 (2011).
- 120 Ashton, T. M., McKenna, W. G., Kunz-Schughart, L. A. & Higgins, G. S. Oxidative Phosphorylation as an Emerging Target in Cancer Therapy. *Clin Cancer Res* **24**, 2482-2490, doi:10.1158/1078-0432.CCR-17-3070 (2018).
- 121 Schleyer, M., Schmidt, B. & Neupert, W. Requirement of a membrane potential for the posttranslational transfer of proteins into mitochondria. *Eur J Biochem* **125**, 109-116, doi:10.1111/j.1432-1033.1982.tb06657.x (1982).
- 122 Sullivan, L. B. *et al.* Supporting Aspartate Biosynthesis Is an Essential Function of Respiration in Proliferating Cells. *Cell* **162**, 552-563, doi:10.1016/j.cell.2015.07.017 (2015).
- 123 Gui, D. Y. *et al.* Environment Dictates Dependence on Mitochondrial Complex I for NAD⁺ and Aspartate Production and Determines Cancer Cell Sensitivity to Metformin. *Cell Metab* **24**, 716-727, doi:10.1016/j.cmet.2016.09.006 (2016).
- 124 Birsoy, K. *et al.* An Essential Role of the Mitochondrial Electron Transport Chain in Cell Proliferation Is to Enable Aspartate Synthesis. *Cell* **162**, 540-551, doi:10.1016/j.cell.2015.07.016 (2015).
- 125 Patra, K. C. & Hay, N. The pentose phosphate pathway and cancer. *Trends Biochem Sci* **39**, 347-354, doi:10.1016/j.tibs.2014.06.005 (2014).
- 126 Jiang, P., Du, W. & Wu, M. Regulation of the pentose phosphate pathway in cancer. *Protein Cell* **5**, 592-602, doi:10.1007/s13238-014-0082-8 (2014).
- 127 Boros, L. G. *et al.* Inhibition of the oxidative and nonoxidative pentose phosphate pathways by somatostatin: a possible mechanism of antitumor action. *Med Hypotheses* **50**, 501-506, doi:10.1016/s0306-9877(98)90271-7 (1998).

- 128 Boros, L. G. *et al.* Nonoxidative pentose phosphate pathways and their direct role in ribose synthesis in tumors: is cancer a disease of cellular glucose metabolism? *Med Hypotheses* **50**, 55-59, doi:10.1016/s0306-9877(98)90178-5 (1998).
- 129 Bhutia, Y. D. & Ganapathy, V. Glutamine transporters in mammalian cells and their functions in physiology and cancer. *Biochim Biophys Acta* **1863**, 2531-2539, doi:10.1016/j.bbamcr.2015.12.017 (2016).
- 130 Sullivan, M. R. *et al.* Quantification of microenvironmental metabolites in murine cancers reveals determinants of tumor nutrient availability. *Elife* **8**, doi:10.7554/eLife.44235 (2019).
- 131 Bott, A. J., Maimouni, S. & Zong, W. X. The Pleiotropic Effects of Glutamine Metabolism in Cancer. *Cancers (Basel)* **11**, doi:10.3390/cancers11060770 (2019).
- 132 DeBerardinis, R. J. & Cheng, T. Q's next: the diverse functions of glutamine in metabolism, cell biology and cancer. *Oncogene* **29**, 313-324, doi:10.1038/onc.2009.358 (2010).
- 133 Cluntun, A. A., Lukey, M. J., Cerione, R. A. & Locasale, J. W. Glutamine Metabolism in Cancer: Understanding the Heterogeneity. *Trends Cancer* **3**, 169-180, doi:10.1016/j.trecan.2017.01.005 (2017).
- 134 van Geldermalsen, M. *et al.* ASCT2/SLC1A5 controls glutamine uptake and tumour growth in triple-negative basal-like breast cancer. *Oncogene* **35**, 3201-3208, doi:10.1038/onc.2015.381 (2016).
- 135 Reynolds, M. R. *et al.* Control of glutamine metabolism by the tumor suppressor Rb. *Oncogene* **33**, 556-566, doi:10.1038/onc.2012.635 (2014).
- 136 Nicklin, P. *et al.* Bidirectional transport of amino acids regulates mTOR and autophagy. *Cell* **136**, 521-534, doi:10.1016/j.cell.2008.11.044 (2009).
- 137 Timmerman, L. A. *et al.* Glutamine sensitivity analysis identifies the xCT antiporter as a common triple-negative breast tumor therapeutic target. *Cancer Cell* **24**, 450-465, doi:10.1016/j.ccr.2013.08.020 (2013).
- 138 Spinelli, J. B. *et al.* Metabolic recycling of ammonia via glutamate dehydrogenase supports breast cancer biomass. *Science* **358**, 941-946, doi:10.1126/science.aam9305 (2017).
- 139 Li, J. *et al.* miR-145 inhibits glutamine metabolism through c-myc/GLS1 pathways in ovarian cancer cells. *Cell Biol Int* **43**, 921-930, doi:10.1002/cbin.11182 (2019).
- 140 Tardito, S. *et al.* Glutamine synthetase activity fuels nucleotide biosynthesis and supports growth of glutamine-restricted glioblastoma. *Nat Cell Biol* **17**, 1556-1568, doi:10.1038/ncb3272 (2015).

- 141 Hakvoort, T. B. *et al.* Pivotal role of glutamine synthetase in ammonia detoxification. *Hepatology* **65**, 281-293, doi:10.1002/hep.28852 (2017).
- 142 Castegna, A. & Menga, A. Glutamine Synthetase: Localization Dictates Outcome. *Genes (Basel)* **9**, doi:10.3390/genes9020108 (2018).
- 143 Kung, H. N., Marks, J. R. & Chi, J. T. Glutamine synthetase is a genetic determinant of cell type-specific glutamine independence in breast epithelia. *PLoS Genet* **7**, e1002229, doi:10.1371/journal.pgen.1002229 (2011).
- 144 Altman, B. J., Stine, Z. E. & Dang, C. V. From Krebs to clinic: glutamine metabolism to cancer therapy. *Nat Rev Cancer* **16**, 749, doi:10.1038/nrc.2016.114 (2016).
- 145 Panieri, E. & Santoro, M. M. ROS homeostasis and metabolism: a dangerous liason in cancer cells. *Cell Death Dis* **7**, e2253, doi:10.1038/cddis.2016.105 (2016).
- 146 Alleman, R. J., Katunga, L. A., Nelson, M. A., Brown, D. A. & Anderson, E. J. The "Goldilocks Zone" from a redox perspective-Adaptive vs. deleterious responses to oxidative stress in striated muscle. *Front Physiol* **5**, 358, doi:10.3389/fphys.2014.00358 (2014).
- 147 Schieber, M. & Chandel, N. S. ROS function in redox signaling and oxidative stress. *Curr Biol* **24**, R453-462, doi:10.1016/j.cub.2014.03.034 (2014).
- 148 Lu, S. C. Regulation of glutathione synthesis. *Mol Aspects Med* **30**, 42-59, doi:10.1016/j.mam.2008.05.005 (2009).
- 149 Yang, M. & Vousden, K. H. Serine and one-carbon metabolism in cancer. *Nat Rev Cancer* **16**, 650-662, doi:10.1038/nrc.2016.81 (2016).
- 150 Gu, Y. *et al.* mTORC2 Regulates Amino Acid Metabolism in Cancer by Phosphorylation of the Cystine-Glutamate Antiporter xCT. *Mol Cell* **67**, 128-138 e127, doi:10.1016/j.molcel.2017.05.030 (2017).
- 151 Shanware, N. P., Mullen, A. R., DeBerardinis, R. J. & Abraham, R. T. Glutamine: pleiotropic roles in tumor growth and stress resistance. *J Mol Med (Berl)* **89**, 229-236, doi:10.1007/s00109-011-0731-9 (2011).
- 152 Florey, E. GABA: history and perspectives. *Can J Physiol Pharmacol* **69**, 1049-1056, doi:10.1139/y91-156 (1991).
- 153 Soltani, N. *et al.* GABA exerts protective and regenerative effects on islet beta cells and reverses diabetes. *Proc Natl Acad Sci U S A* **108**, 11692-11697, doi:10.1073/pnas.1102715108 (2011).
- 154 Bown, A. W. & Shelp, B. J. The Metabolism and Functions of [gamma]-Aminobutyric Acid. *Plant Physiol* **115**, 1-5, doi:10.1104/pp.115.1.1 (1997).

- 155 Ramesh, S. A. *et al.* GABA signalling modulates plant growth by directly regulating the activity of plant-specific anion transporters. *Nat Commun* **6**, 7879, doi:10.1038/ncomms8879 (2015).
- 156 Gao, Y. *et al.* Glutamate Decarboxylase 65 Signals through the Androgen Receptor to Promote Castration Resistance in Prostate Cancer. *Cancer Res* **79**, 4638-4649, doi:10.1158/0008-5472.CAN-19-0700 (2019).
- 157 Zhang, X. *et al.* Expression of gamma-aminobutyric acid receptors on neoplastic growth and prediction of prognosis in non-small cell lung cancer. *J Transl Med* **11**, 102, doi:10.1186/1479-5876-11-102 (2013).
- 158 Neman, J. *et al.* Human breast cancer metastases to the brain display GABAergic properties in the neural niche. *Proc Natl Acad Sci U S A* **111**, 984-989, doi:10.1073/pnas.1322098111 (2014).
- 159 Ippolito, J. E. & Piwnicka-Worms, D. A fluorescence-coupled assay for gamma aminobutyric acid (GABA) reveals metabolic stress-induced modulation of GABA content in neuroendocrine cancer. *PLoS One* **9**, e88667, doi:10.1371/journal.pone.0088667 (2014).
- 160 Hujber, Z. *et al.* GABA, glutamine, glutamate oxidation and succinic semialdehyde dehydrogenase expression in human gliomas. *J Exp Clin Cancer Res* **37**, 271, doi:10.1186/s13046-018-0946-5 (2018).
- 161 Yogeeswari, P., Sriram, D. & Vaigundaragavendran, J. The GABA shunt: an attractive and potential therapeutic target in the treatment of epileptic disorders. *Curr Drug Metab* **6**, 127-139, doi:10.2174/1389200053586073 (2005).
- 162 Lane, A. N. & Fan, T. W. Regulation of mammalian nucleotide metabolism and biosynthesis. *Nucleic Acids Res* **43**, 2466-2485, doi:10.1093/nar/gkv047 (2015).
- 163 Villa, E., Ali, E. S., Sahu, U. & Ben-Sahra, I. Cancer Cells Tune the Signaling Pathways to Empower de Novo Synthesis of Nucleotides. *Cancers (Basel)* **11**, doi:10.3390/cancers11050688 (2019).
- 164 Bae, I. *et al.* BRCA1 induces antioxidant gene expression and resistance to oxidative stress. *Cancer Res* **64**, 7893-7909, doi:10.1158/0008-5472.CAN-04-1119 (2004).
- 165 Moreau, K. *et al.* BRCA1 affects lipid synthesis through its interaction with acetyl-CoA carboxylase. *J Biol Chem* **281**, 3172-3181, doi:10.1074/jbc.M504652200 (2006).
- 166 Vazquez-Arreguin, K. *et al.* BRCA1 through Its E3 Ligase Activity Regulates the Transcription Factor Oct1 and Carbohydrate Metabolism. *Mol Cancer Res* **16**, 439-452, doi:10.1158/1541-7786.MCR-17-0364 (2018).

- 167 Hong, R. *et al.* Preventing BRCA1/ZBRK1 repressor complex binding to the GOT2 promoter results in accelerated aspartate biosynthesis and promotion of cell proliferation. *Mol Oncol* **13**, 959-977, doi:10.1002/1878-0261.12466 (2019).
- 168 Cortez, D., Wang, Y., Qin, J. & Elledge, S. J. Requirement of ATM-dependent phosphorylation of brca1 in the DNA damage response to double-strand breaks. *Science* **286**, 1162-1166, doi:10.1126/science.286.5442.1162 (1999).
- 169 Morgenstern, J. P. & Land, H. Advanced mammalian gene transfer: high titre retroviral vectors with multiple drug selection markers and a complementary helper-free packaging cell line. *Nucleic Acids Res* **18**, 3587-3596, doi:10.1093/nar/18.12.3587 (1990).
- 170 Vichai, V. & Kirtikara, K. Sulforhodamine B colorimetric assay for cytotoxicity screening. *Nat Protoc* **1**, 1112-1116, doi:10.1038/nprot.2006.179 (2006).
- 171 Franken, N. A., Rodermond, H. M., Stap, J., Haveman, J. & van Bree, C. Clonogenic assay of cells in vitro. *Nat Protoc* **1**, 2315-2319, doi:10.1038/nprot.2006.339 (2006).
- 172 Livak, K. J. & Schmittgen, T. D. Analysis of relative gene expression data using real-time quantitative PCR and the 2(-Delta Delta C(T)) Method. *Methods* **25**, 402-408, doi:10.1006/meth.2001.1262 (2001).
- 173 Elstrodt, F. *et al.* BRCA1 mutation analysis of 41 human breast cancer cell lines reveals three new deleterious mutants. *Cancer Res* **66**, 41-45, doi:10.1158/0008-5472.CAN-05-2853 (2006).
- 174 Drean, A. *et al.* Modeling Therapy Resistance in BRCA1/2-Mutant Cancers. *Mol Cancer Ther*, doi:10.1158/1535-7163.MCT-17-0098 (2017).
- 175 Song, M., Kim, S. H., Im, C. Y. & Hwang, H. J. Recent Development of Small Molecule Glutaminase Inhibitors. *Curr Top Med Chem* **18**, 432-443, doi:10.2174/1568026618666180525100830 (2018).
- 176 Turner, N., Tutt, A. & Ashworth, A. Hallmarks of 'BRCAness' in sporadic cancers. *Nat Rev Cancer* **4**, 814-819, doi:10.1038/nrc1457 (2004).
- 177 Xu, G. *et al.* REV7 counteracts DNA double-strand break resection and affects PARP inhibition. *Nature* **521**, 541-544, doi:10.1038/nature14328 (2015).
- 178 Bunting, S. F. *et al.* 53BP1 inhibits homologous recombination in Brca1-deficient cells by blocking resection of DNA breaks. *Cell* **141**, 243-254, doi:10.1016/j.cell.2010.03.012 (2010).

- 179 Horiuchi, D. *et al.* MYC pathway activation in triple-negative breast cancer is synthetic lethal with CDK inhibition. *J Exp Med* **209**, 679-696, doi:10.1084/jem.20111512 (2012).
- 180 Bachmann, A. S. & Geerts, D. Polyamine synthesis as a target of MYC oncogenes. *J Biol Chem* **293**, 18757-18769, doi:10.1074/jbc.TM118.003336 (2018).
- 181 Liu, Y. C. *et al.* Global regulation of nucleotide biosynthetic genes by c-Myc. *PLoS One* **3**, e2722, doi:10.1371/journal.pone.0002722 (2008).
- 182 Abdul, M., McCray, S. D. & Hoosein, N. M. Expression of gamma-aminobutyric acid receptor (subtype A) in prostate cancer. *Acta Oncol* **47**, 1546-1550, doi:10.1080/02841860801961265 (2008).
- 183 Young, S. Z. & Bordey, A. GABA's control of stem and cancer cell proliferation in adult neural and peripheral niches. *Physiology (Bethesda)* **24**, 171-185, doi:10.1152/physiol.00002.2009 (2009).
- 184 Anastasiou, D. Tumour microenvironment factors shaping the cancer metabolism landscape. *Br J Cancer* **116**, 277-286, doi:10.1038/bjc.2016.412 (2017).
- 185 Binnewies, M. *et al.* Understanding the tumor immune microenvironment (TIME) for effective therapy. *Nat Med* **24**, 541-550, doi:10.1038/s41591-018-0014-x (2018).
- 186 Finicle, B. T., Jayashankar, V. & Edinger, A. L. Nutrient scavenging in cancer. *Nat Rev Cancer* **18**, 619-633, doi:10.1038/s41568-018-0048-x (2018).
- 187 Muir, A. *et al.* Environmental cystine drives glutamine anaplerosis and sensitizes cancer cells to glutaminase inhibition. *Elife* **6**, doi:10.7554/eLife.27713 (2017).
- 188 Shu, Q. *et al.* GABAB R/GSK-3beta/NF-kappaB signaling pathway regulates the proliferation of colorectal cancer cells. *Cancer Med* **5**, 1259-1267, doi:10.1002/cam4.686 (2016).
- 189 Xu, X. *et al.* Overview of the Development of Glutaminase Inhibitors: Achievements and Future Directions. *J Med Chem* **62**, 1096-1115, doi:10.1021/acs.jmedchem.8b00961 (2019).
- 190 Lemberg, K. M., Vornov, J. J., Rais, R. & Slusher, B. S. We're Not "DON" Yet: Optimal Dosing and Prodrug Delivery of 6-Diazo-5-oxo-L-norleucine. *Mol Cancer Ther* **17**, 1824-1832, doi:10.1158/1535-7163.MCT-17-1148 (2018).

- 191 Turk, A. A. & Wisinski, K. B. PARP inhibitors in breast cancer: Bringing synthetic lethality to the bedside. *Cancer* **124**, 2498-2506, doi:10.1002/cncr.31307 (2018).
- 192 Jiralerspong, S. *et al.* Metformin and pathologic complete responses to neoadjuvant chemotherapy in diabetic patients with breast cancer. *J Clin Oncol* **27**, 3297-3302, doi:10.1200/JCO.2009.19.6410 (2009).
- 193 Luengo, A., Sullivan, L. B. & Heiden, M. G. Understanding the complexity of metformin action: limiting mitochondrial respiration to improve cancer therapy. *BMC Biol* **12**, 82, doi:10.1186/s12915-014-0082-4 (2014).
- 194 Hopkins, B. D. *et al.* Suppression of insulin feedback enhances the efficacy of PI3K inhibitors. *Nature* **560**, 499-503, doi:10.1038/s41586-018-0343-4 (2018).
- 195 Knudson, A. G., Jr. Mutation and cancer: statistical study of retinoblastoma. *Proc Natl Acad Sci U S A* **68**, 820-823 (1971).
- 196 Arem, H. & Lofffield, E. Cancer Epidemiology: A Survey of Modifiable Risk Factors for Prevention and Survivorship. *Am J Lifestyle Med* **12**, 200-210, doi:10.1177/1559827617700600 (2018).
- 197 Torre, L. A., Siegel, R. L., Ward, E. M. & Jemal, A. Global Cancer Incidence and Mortality Rates and Trends--An Update. *Cancer Epidemiol Biomarkers Prev* **25**, 16-27, doi:10.1158/1055-9965.EPI-15-0578 (2016).